PAVEMENT SUBGRADE PERFORMANCE STUDY

Test Section 712

Subgrade AASHTO soil type A-7-5 at 20 percent gravimetric moisture content

by

Edel R. Cortez [1]

Subgrade Moisture Content	AASHTO Soil Type			
	A-2-4	A-4	A-6	A-7-5
M1	Optimum 10 % TS 701	Optimum 17 % TS 702	Optimum 16 % TS 709	Optimum 20 % TS 712
M2	12 % TS 707	19 % TS 704	19 % TS 708	21 % TS 710
M3	15 % TS 703	23 % TS 705	22% TS 706	25 % TS 711

[1] U.S. Army Cold Regions Research and Engineering Laboratory, 72 Lyme Road, Hanover, New Hampshire 03755, United States

EXECUTIVE SUMMARY

This report is one of a series of reports on the pooled-fund research project titled Subgrade Performance Study (SPR-2-208). The hypothesis for this study is that the failure criterion depends on the subgrade soil type and the in-situ moisture content. Current mechanistic design procedures incorporate the results from the AASHO Road Tests conducted in the late nineteen fifties. However, the AASHO Road Tests were all conducted on only one soil type (AASHTO type A-6). The tests results reflect the combined effect of traffic loads and seasonal variations. Applying failure criteria based on the AASHO Road Tests to other soil types, at different moisture contents and different climate introduces significant uncertainty.

In recent decades much progress has been achieved in computer and sensor technologies. Reliable measurements of in-situ stress and strain are now feasible and practical. The authors recognized the new opportunities brought by these technological advances to be able to develop more reliable pavement failure criteria that consider the effects of subgrade soil type and moisture condition.

Transportation agencies from nineteen US states are contributing to a research initiative that will develop the bases for new pavement failure criteria that is adequate for the most common subgrade soil types found in the United State at various soil moisture contents. As part of the research program, four subgrade soils were selected for testing in the Frost Effects Research Facility (FERF). Each subgrade soil was to be constructed at three moisture contents, with one at or near optimum density and moisture content. The test sections consisted of 75 mm of asphalt concrete, 229 mm of crushed base and 3 m of the test subgrade soil type at pre-determined moisture content. The current test section was named Test Section 712. The subgrade soil was classified as AASHTO type A-7-5, equivalent to a soil type MH in the Unified Soil Classification System. The as-built average subgrade soil gravimetric moisture content was 20.5 percent. According to laboratory modified Proctor tests this is the optimum moisture content for this soil. The maximum density was 1700 kg/m^3 (106.1 lb/ft^3).

Accelerated traffic was applied by means of a Heavy Vehicle Simulator (HVS). The traffic axial load was varied for each test window, ranging from 80 kN to 195.6 kN (18 to 44 kips). The load was applied through a dual truck tire assembly representing a half axle of a standard truck. Therefore, a 40-kN (9-kip) semi-axial load is equivalent to an 80 kN (18-kip) load applied with a complete truck axle. The tire pressure was kept constant at 689 kPa (100 psi).

The test section was built inside the FERF testing facility where soil moisture and temperature conditions were controlled and kept constant. The test section contained six test windows. Each effective test window was approximately 6.0 m long and 0.91 m wide. Additional length was provided at each end for acceleration and deceleration of the tire assembly. Loading was applied unidirectionally at an average speed of 12 km/hr. The test windows were subjected to approximately 600 load repetitions per hour. The HVS applied traffic 23 hours per day. The remaining hour was used for maintenance.

Stress, strain, and surface rut measurements were taken at various stages throughout the traffic testing. Stress and strain sensors were located at various depths in the base course and the subgrade. Permanent strain (while no traffic was occurring) and dynamic strain (during the passing of the tire assembly) were measured at continuous layers from the asphalt surface down to a depth of 1.52 m. This configuration provided a means to define a

2

distribution of deformations layer by layer. From these measurements, the midpoint strain was estimated for each layer. Adding the layer deformations and comparing to the rut depth measured at the pavement surface provided a way to calibrate the subsurface deformation measurements. Surface rutting was measured with a laser profilometer.

This report contains a description of the test section, construction, instrumentation, and pavement performance and mechanical response to accelerated traffic.

INTRODUCTION

As part of an international study on pavement subgrade performance, several full-scale test sections were constructed in the Frost Effects Research Facility (FERF) at the Cold Regions Research and Engineering Laboratory (CRREL) in Hanover, New Hampshire. CRREL is a component of the Engineers Research and Development Center (ERDC) which is the research and development division of the US Army Corps of Engineers. The tests were conducted indoors at approximately 20°C (68°F). Full-scale test sections were instrumented with stress cells, strain gages, moisture gages, and temperature sensors. The test sections were subjected to accelerated traffic loading using CRREL's Heavy Vehicle Simulator (HVS). Pavement failure was defined as 12.5 mm (0.5 in.) surface rut depth, or the development of asphalt cracks 9.5 mm (3/8 in.) wide. Surface rut depth measurements were taken periodically during the accelerated load tests. At the same time, subsurface stress and strain measurements were also taken. A detailed overview of the project can be found in Janoo et al (2001). The test sections consisted of a 76-mm (3 in.) asphalt concrete (AC) layer, a 229-mm (9 in.) crushed gravel base and 3 m (10 ft) of subgrade soil. All the test sections in this research project were alike in geometry, instrumentation, and materials, except for the subgrade soil type and moisture content. The test sections were constructed using several subgrade soil types conditioned at various moisture contents. For each test section, provisions were made to maintain the temperature and moisture content as constant as possible. The test matrix for this study is shown in the table below.

Table 1. Experimental test matrix.

Subgrade Moisture Content	AASHTO Soil Type			
	A-2-4	A-4	A-6	A-7-5
M1	Optimum 10 % TS 701	Optimum 17 % TS 702	Optimum 16 % TS 709	Optimum 20% TS 712
M2	12 % TS 707	19 % TS 704	19 % TS 708	21% TS 710 Borderline soil A-6 and A-7-6
M3	15 % TS 703	23 % TS 705	22% TS 706	25% TS 711

This reports deals with the construction, accelerated traffic testing, and pavement response of Test Section 712. As shown in Table 1, the subgrade soil in this test section was classified as AASHTO soil type A-7-5. The subgrade average as-built gravimetric moisture content was 20 percent. The laboratory CBR test results indicate that, at this moisture content, the subgrade soil had a CBR of 53 percent.

DESCRIPTION OF THE TEST SECTION

The pavement structure consisted of a 76-mm (3-in) hot mixed asphalt (HMA) layer, a 229-mm (9-in) crushed gravel base course, and 3 m (10 ft) of subgrade soil.

The test section was divided into six test windows. A test window is the area where traffic is applied. An effective test window was 0.91 m (3 ft) wide by 6.08 m (20 ft.) long, excluding acceleration and deceleration areas. The thickness and material properties for all test windows were designed to be constant, but the traffic load intensity was designed to vary from one test section to another.

Each test window was instrumented with embedded sensors to measure in-situ stress, strain, moisture and temperature at various locations within the pavement structure. Geokon® stress cells were embedded in the unbound base course and in the subgrade. εmu coils were installed in three stacks able to measure displacement between coil pairs in vertical, longitudinal and transverse directions. Vertical displacements were measured in ten layers to a depth of approximately 1.52 m (5 feet). Strains were calculated from the displacement measurements. Campbell Scientific® CS615 sensors were used to record volumetric soil moisture content in the base course and subgrade during the accelerated traffic period. Additionally, strings of thermocouples were used to record subgrade, base, asphalt and air temperatures.

The test section was built indoors where the temperature and soil moisture were controlled, and kept practically constant during the test period. The test basin where the test section was built consisted of 3 lateral concrete walls, a concrete floor and an access ramp also made of concrete. During construction, much care was applied to retain the soil moisture by covering the top soil layer with impermeable tarps. Later, the asphalt layer helped to contain the subgrade and base course moisture.

Ordinary construction equipment was used to build the test sections, but the quality control and quality assurance testing were more rigorous than those commonly used in regular construction.

Test Section 712 AASHTO A-7-5 subgrade soil at 20 percent (optimum) moisture content.

Y

W

S ← → N

E

B ←

Test Window 1	Test Window 4
Test Window 2	Test Window 5
Test Window 3	Test Window 6

A ↑   A ↑

South Wall

→ X

B ←

0.00

Z ↑

3.04 m   9.14 m   13.7 m   19.8 m   395 m

3.66m

Base 229 m thick   Pavement 76 mm thick

Subgrade

0.00

→ X

0.00

19.8 m
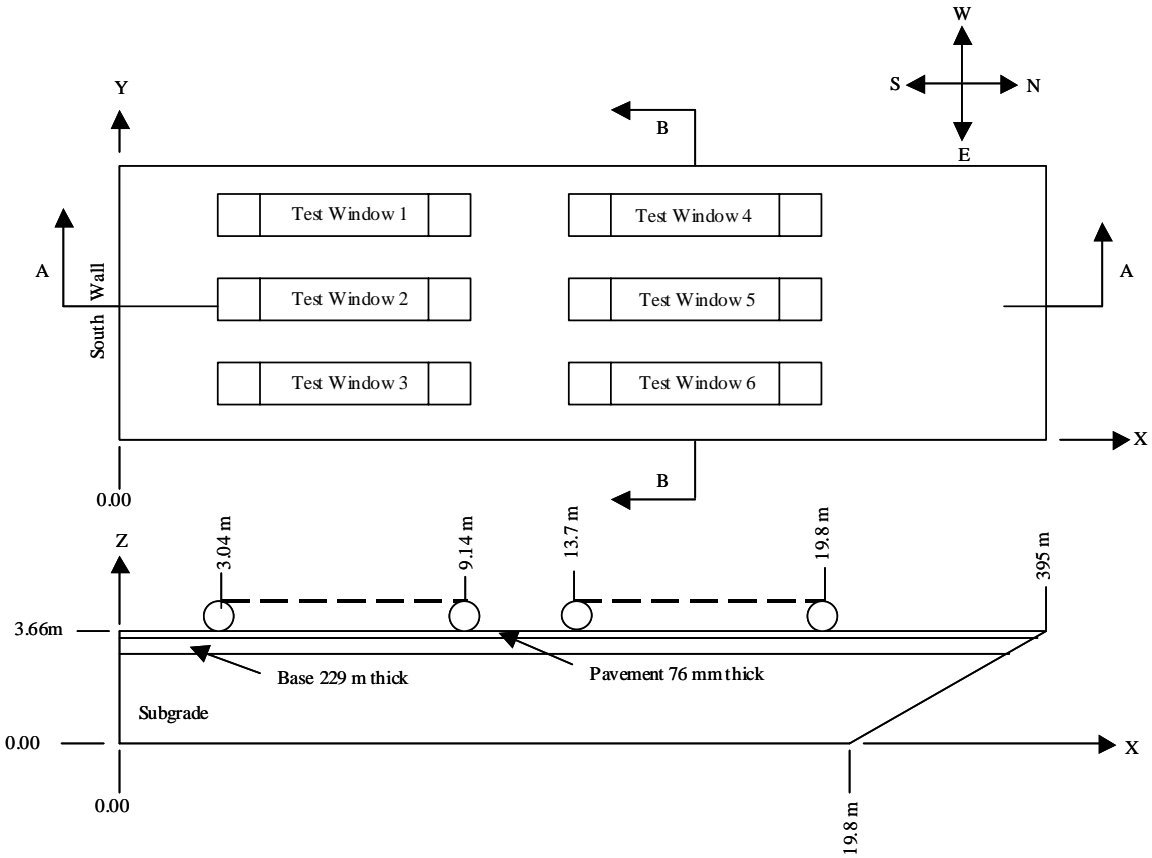
Figure 1 a. Plan view and longitudinal cross section of test section.

Asphalt 3"

Base course

0.076 m

0.23 m

Subgrade

3 m

6.36 m
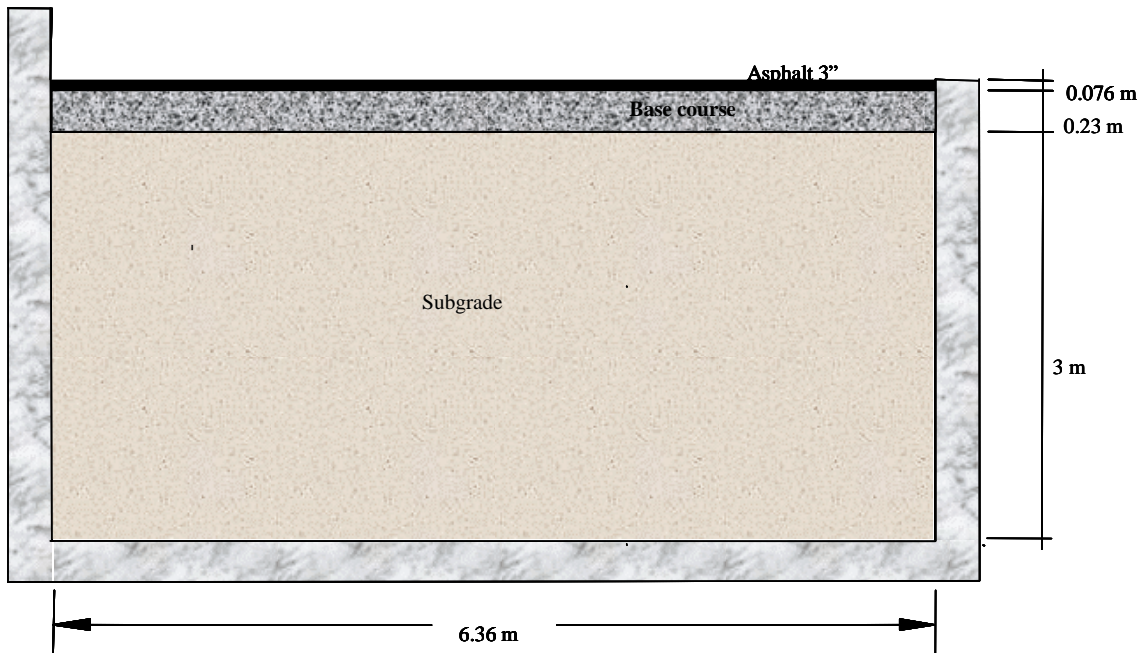
Figure 1 b. Transversal cross section.

MATERIAL PROPERTIES

Laboratory tests were conducted on representative samples of the subgrade soil and the base course soil. The battery of soil characterization tests included modified proctor, laboratory CBR, Atterberg limits, sieve analysis, hydrometer, and specific gravity tests.

Figure 1 shows grain size distributions for the subgrade soil and for the base course soil. The subgrade soil has approximately 88 percent passing the 0.074-mm (#200) sieve and 33 percent finer than 0.002 mm (clay content). The average liquid limit (LL) and plasticity index (PI) of the soil were 55 percent and 20 percent respectively. According to the American Association of Highway and Transportation Officials (AASHTO) soil classification system, this soil falls within the A-7-5 region, but near the boundary of the A-7-6 region. According to the Unified Soil Classification System, the subgrade soil was a MH soil (High liquid limit silt). The average specific gravity of the subgrade soil was 2.71.

The base course material was made of unbound crushed stone. It was classified as an AASHTO type A-1 soil. According to the Unified Soil Classification System, the base course soil was type GP-GM (mix of poorly graded gravel and silty gravel). About 11 percent by weight of the base course soil particles passed through the sieve 0.074-mm (#200) sieve. The fines were classified as non-plastic.


Figure 2. Grain size distribution for the subgrade soil and base course soils.
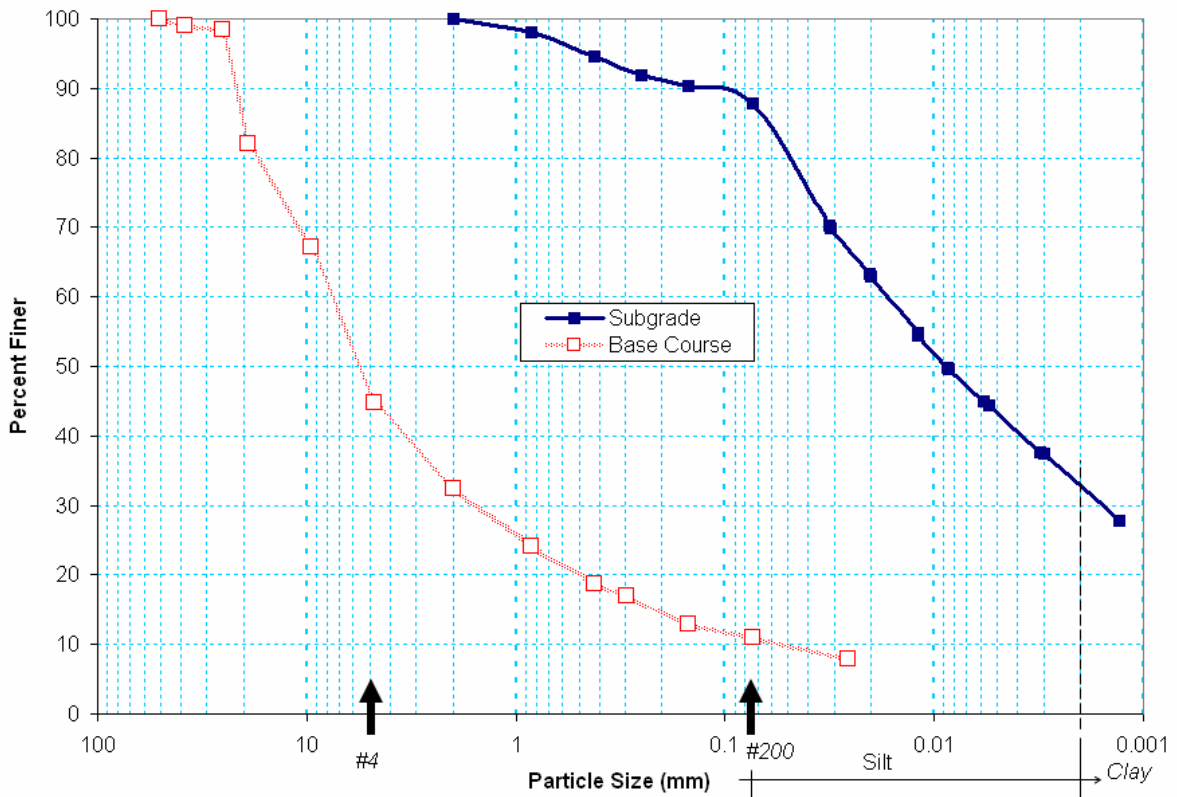
The maximum density and optimum gravimetric moisture content for the subgrade soil were 1700 kg/m^3 (106.1 pcf) and 20.5 percent respectively. The average as-built subgrade moisture content was 20 percent. The laboratory CBR for this moisture content was approximately 53 percent.
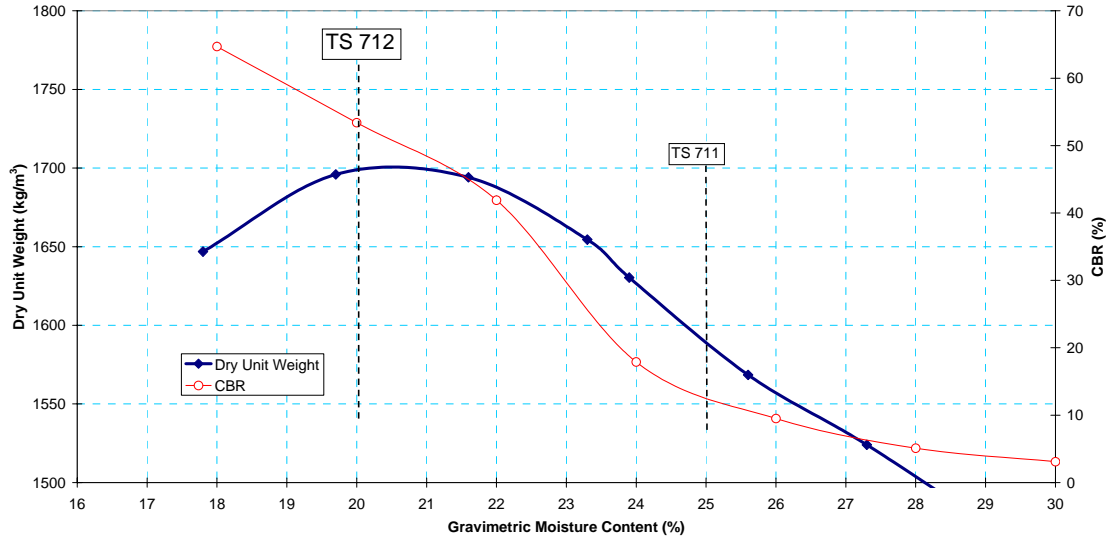

Figure 3. Subgrade modified Proctor and laboratory CBR test results.
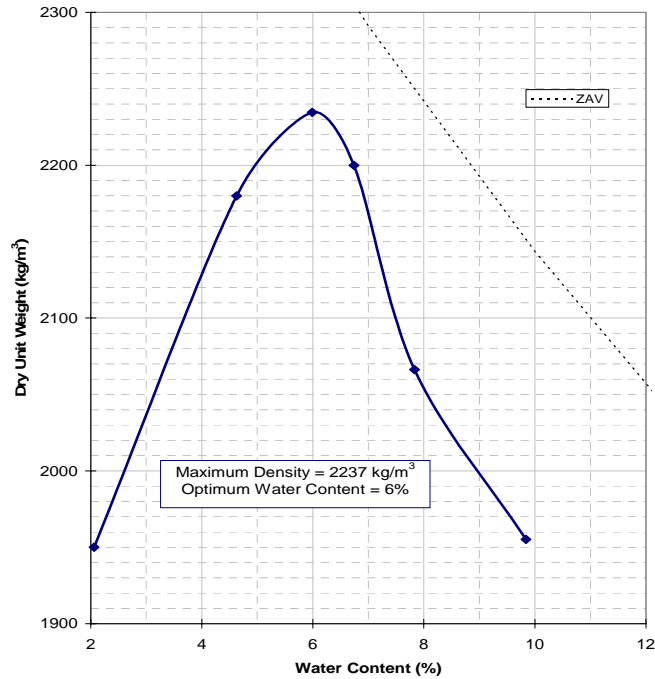

Figure 4. Base course modified Proctor test results.

The modified Proctor test results shown in Figure 4 indicate that the optimum gravimetric moisture content of the base course material was 6 percent and the maximum density was 2237 kg/m^3 (139.5 pcf). In practice, with high hydraulic conductivity

materials, it is difficult to obtain this optimum moisture content because some moisture drains down. The average moisture content of the base course material during construction was 4.7 percent. The moisture sensors embedded in the base course indicate that the moisture content did not significantly vary during the test period.

Table 2. Summary of properties of the subgrade soil used in Test Section 712.

AASHTO	A-7-5
USCS	MH
Spec. Gravity	2.71
LL (%)	55
PI	21
Optimum moisture content (%)	20.5
Maximum Density (kg/m^3)	1700
% passing #10	100
% passing #200	88
% finer than 0.002 mm	33

The asphalt concrete material of the binder course conformed to the Vermont Type II standard, with 19-mm maximum aggregate particle size and 4.5% of asphalt binder PG-58-34. The asphalt concrete material of the wearing course conformed to the Vermont Type III standard, with 13-mm maximum aggregate particle size and 5.3% of asphalt binder PG-58-34. The nominal thickness of the binder course was 51 mm. The nominal thickness of the wearing course was 25 mm.

CONSTRUCTION OF THE TEST SECTION

The subgrade was built in layers 150-mm (6-in.) thick. The soil was first placed at a moisture condition lower than the target moisture content. The soil was rototilled, and water was gradually added until the target soil moisture content was reached. Then, the soil was compacted with 8 passes of a 10-Ton (9,072-kg) steel roller in static mode, followed by 4 passes in vibratory mode. Moisture and density quality control measurements were taken using a nuclear gauge. Additional roller compacting was applied to any low density region until the density was at least 95 percent of the modified proctor density for the given moisture content.

The base course was placed in 2 layers 114.3-mm (4.5-in.) thick for a total of 228.6 mm (9 inches). Finally, the AC layer was placed in two lifts for a total of 76 mm (3 inches).

CONSTRUCTION QUALITY CONTROL

During the construction of the subgrade, a series of tests were conducted on each of the compacted layers. Measurements included layer thickness taken with a survey level, and moisture-density measurements taken with a nuclear gauge. Falling weight

deflectometer (FWD) tests were conducted on top of the asphalt concrete prior to traffic testing.

The mean moisture content of the subgrade was 20 percent. The average moisture content of the base course during construction was 5.9 percent.

The mean dry density of the subgrade was 1575 kg/m^3 (98.3 pcf). The mean dry density of the base course was 2350 kg/m ^{3} (146.7 pcf). The mean density of the AC was 2300 kg/m^3 (143.6 pcf).
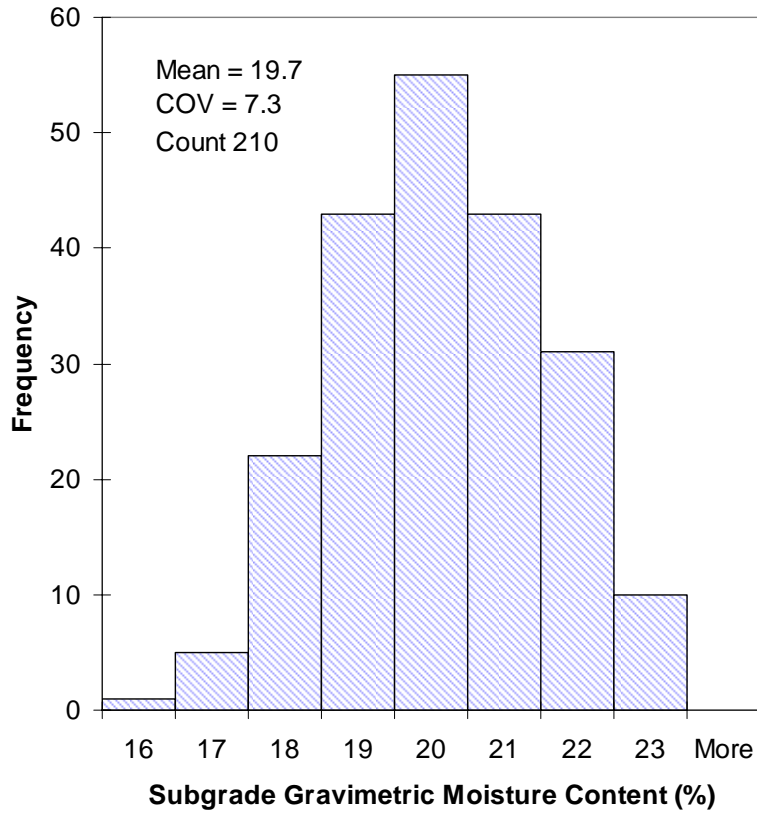

Figure 5. Subgrade moisture content.

Test Section 712 AASHTO A-7-5 subgrade soil at 20 percent (optimum) moisture content.
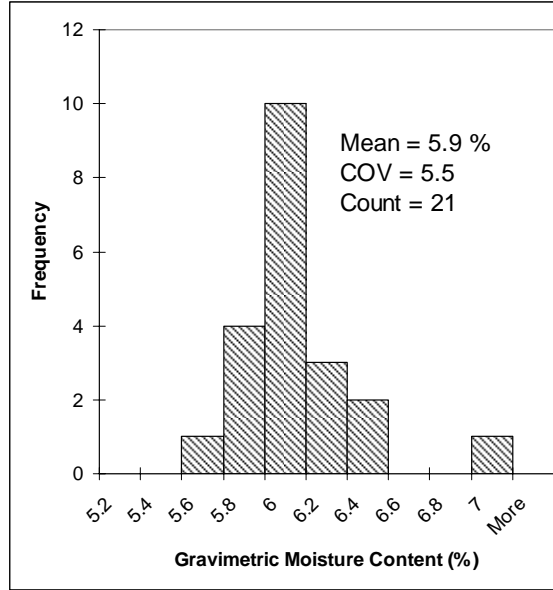

Figure 6. Base course gravimetric moisture content.
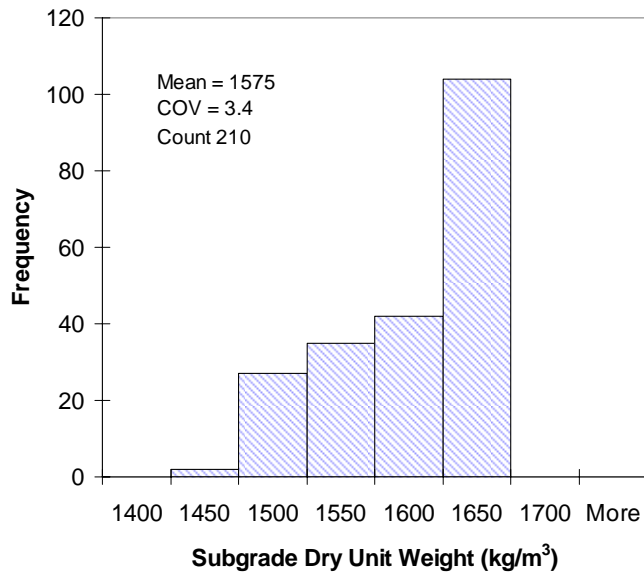

Figure 7. Subgrade dry unit weight.
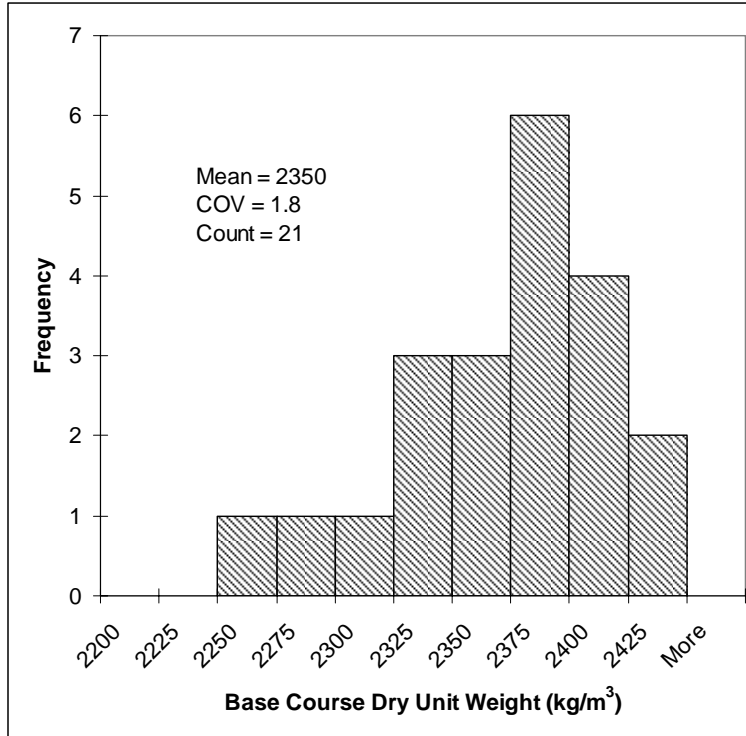
Figure 8. Base course dry unit weight.

INSTRUMENTATION

Instrumentation for measuring stress, strain, temperature, and moisture content were installed in the pavement structure during construction of the test section. More details about the instrumentation can be found in Janoo et al., 2002. The locations of the gages in the test section were similar to those in previous test sections.

Displacement measurements were made in the base and subgrade by means of εmu coils. Strain can be deducted from displacement measurements between coil pairs in either coaxial or co-planar arrangements. The sensors were placed 150 mm center to center. Displacements were measured in the longitudinal (x), transverse (y), and vertical (z) direction of loading. Displacements in the vertical direction were measured to a depth of 1.52 m.

Figure 9. Emu coils in a co-planar arrangement to measure longitudinal and transverse displacements. **A US 25-cent coin is included for scale reference.**

A triaxial Geokon® stress cell set was installed at a depth of 76 mm (3 in.) below the top of the subgrade in all test windows. In Test Window 2 an additional triaxial stress cell set was installed at a depth of 381 mm (15 in.) below the top of the subgrade. The diameter of these stress cells was 100 mm (4 in.).

Larger Geokon® stress cells were installed in the middle thickness of the base course in each of Test Windows 2 and 5 in triaxial sets. The diameter of these stress cells was 229 mm (9 in.).

In Test Window 6, Geokon stress cells were installed to measure stress only in the vertical direction at depths 51 mm (2 in.) below the bottom of the asphalt, at 25.4 mm (1 in.) above the base course-subgrade interface, and 127 mm (5 in.) below the top of the subgrade.


Figure 10. Small Geokon® stress cell used in the subgrade.
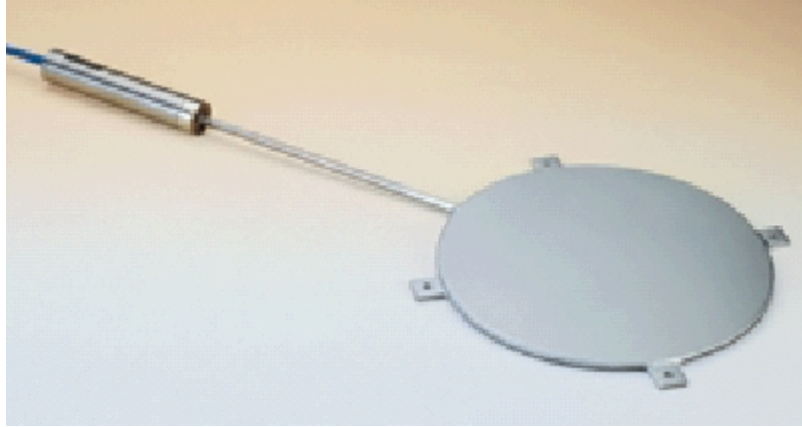
Figure 11. Large Geokon® stress cell used in the base course.

Campbell Scientific® reflectometer soil moisture probes model CS615 were used to measure the moisture content in the base and subgrade during the traffic tests. These sensors measure the oscillation frequency between two rods embedded in the moist soil. The oscillation frequency is related to the dielectric constant that changes with moisture content, and to a lesser degree with temperature. The sensor readings are also affected by salinity, mineralogy and presence of organic materials. Volumetric moisture content is converted to gravimetric moisture content through weight-volume relationships and soil specific gravity. These sensors alone are not accurate enough for the purpose of this study, but this deficiency was corrected by calibrating them with oven dry measurements taken during construction.

Moisture sensors were located at three depths at each of three horizontal locations. There were moisture sensors in the middle of the base course, and in the subgrade at 15 cm (6 in.) and 61 cm (2 ft.) below the top of the subgrade.
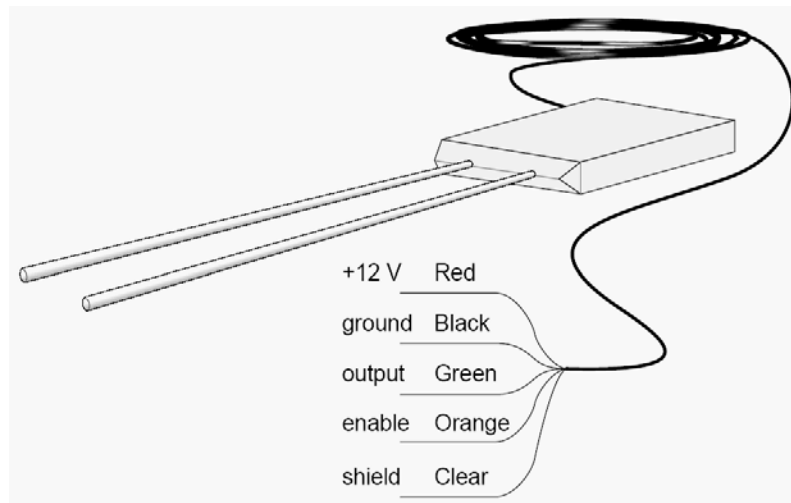

Figure 12. Campbell Scientific® reflectometer soil moisture probes model CS615.

Subsurface temperatures were taken using thermocouple sensors. The thermocouples have an accuracy of ± 0.5°C. The subsurface temperature sensors were installed at three horizontal locations within the test section in the asphalt concrete, base course and at two depths into the subgrade. Air temperatures were also measured.

TRAFFIC TESTING

The test windows were subjected to accelerated traffic loads using CRREL's Heavy Vehicle Simulator (HVS).

The following tests were conducted:

1. Prior to the accelerated load tests, FWD measurements were conducted on the surface of the AC layer at locations in a representative grid arrangement.
2. Initial transverse profiles of each test window were measured using a laser profilometer (Figure 13). The laser source and sensor were located 45 cm (1.5 ft.) above the pavement surface. Each cross section was composed of 512 measurements spaced at 5-mm (0.2-in.) intervals. Twenty profilometer transverse cross section measurements at 0.3-m (1-ft.) intervals were taken at each window (Figure 14). Surface profile measurements were made at each traffic stop to define the progression of surface rutting throughout the traffic tests. Rut depth was defined as the difference between the surface depth at a given number of passes and the corresponding depth measured at zero passes. A typical surface rut measurement and the definition of maximum rut depth are shown in Figure 15. Traffic testing was terminated when the average maximum surface rut depth of 12.5 mm was reached or exceeded.
3. In addition to the profilometer measurements, elevation measurements were conducted with a rod and level prior to the start and at the end of the traffic tests for each test window. Elevations were monitored at locations were the profilometer legs were placed during profilometer measurements to detect any potential change in elevation that would affect the profile measurements. In addition, the elevation of the projection of vertical εmu stack on the asphalt surface was also monitored with a rod and level system. The results from the level surveys indicated that the profilometer leg points were stationary throughout the test.

Test Section 712 AASHTO A-7-5 subgrade soil at 20 percent (optimum) moisture content.


Figure 13. Laser profilometer.
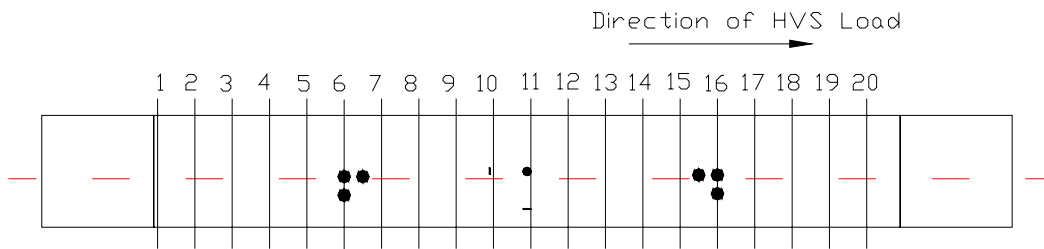
Figure 14. Locations for profile measurements in a test window.
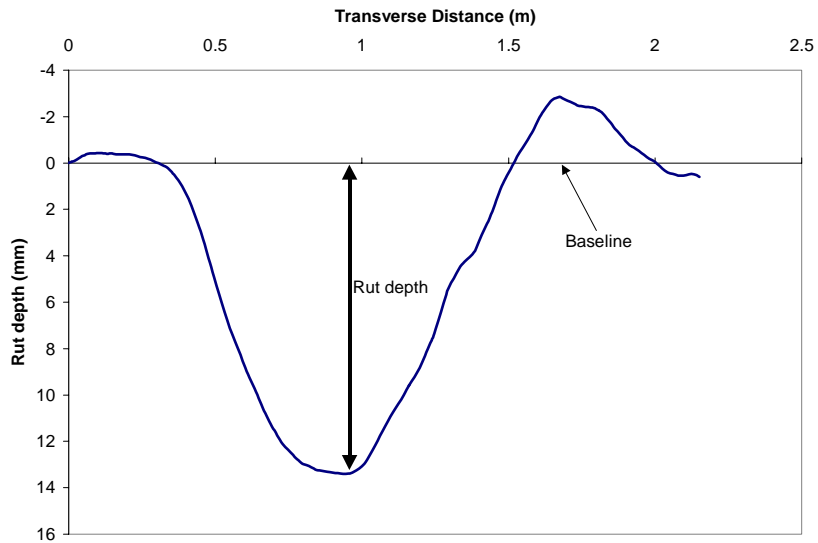
Figure 15. Definition of rut depth.

4. Subsurface stress and displacement measurements conducted in the vertical, longitudinal, and transverse directions relative to the direction of traffic. The measurements were conducted at various pass levels to define their progression throughout the traffic tests. The displacement measurements were conducted dynamically upon the passing of tire traffic, and also statically when no traffic was occurring. The dynamic displacements measured the resilient deformation during traffic load events. The static measurements were intended to measure permanent deformation.

5. In addition to the εmu coils embedded in the pavement, a mobile coil was placed on top of the asphalt over the vertical stack of embedded εmu coils as shown in Figure 16. This provided a means to measure the vertical permanent deformation in the asphalt layer.

Figure 16. Measuring vertical permanent deformation in the asphalt layer.

TRAFFIC LOADING

Traffic loading was applied by means of CRREL's Heavy Vehicle Simulator (HVS). The tire assembly was a dual-tire standard truck half axle. The traffic speed was 12 km/hr. The traffic was allowed to wander across a width of 0.91 m (3 ft.). The applied loads are summarized in Table 3. The tire pressure was set to 690-kPa (100 psi).

Table 3. Mean semi-axial loads on test windows

Test Window	Applied Loads	
	kips	kN
712C1	18	80
712C2	20	89
712C3	21	93.4
712C5	9	40

Table 4. Sequence of HVS tests on test windows

Test Section 712 AASHTO A-7-5 subgrade soil at 20 percent (optimum) moisture content.

Window	Start	End
712C1	08-Dec-2005	16-Feb-2006
712C2	28-Apr-2006	12-May-2006
712C3	21-Feb-2006	28-Feb-2006
712C5	01-Mar-2006	26-Apr-2006

TEMPERATURE AND MOISTURE

The test section was built inside a facility where temperature and moisture were controlled. The mean air temperature during the traffic test period was 20ºC (68ºF). Thermocouples embedded in the asphalt concrete, the base course and the top of the subgrade indicated that the mean temperatures in the various layers of the pavement structure were only slightly lower than the air temperature. The temperature differences between this test section and other test sections in this study were very small, and their effect on material properties is insignificant. Temperature and moisture measurements were taken at 4-hour intervals. The moisture sensors were Campbell Scientific model CS615. These sensors measure the oscillation frequency between two rods embedded in the moist soil. The oscillation frequency is related to the dielectric constant that changes with moisture content, and to a lesser degree with temperature. The sensor readings are also affected by salinity, mineralogy and presence of organic materials. The accuracy of the sensor calibration provided by the manufacturer was improved by field calibration based on oven-dry tests conducted during the construction of the test sections. Volumetric moisture content is converted to gravimetric moisture content through weight-volume relationships and soil specific gravity.

The moisture sensor data indicated that the moisture content remained practically constant throughout construction and testing. The test section was built above a concrete floor. It is surrounded by concrete walls, and it was finally covered by 76 mm (3 in.) of asphalt concrete. Neglecting water vapor diffusion through these very low permeability materials, one can consider the subgrade and base course system as a practically sealed system.

Figure 3 shows that, for this subgrade soil at 20 percent moisture content, the laboratory CBR value is approximately 53 percent. Figure 17 shows that this is equivalent to a resilient modulus (Mr) of 220.6 MPa (32 ksi).

Test Section 712 AASHTO A-7-5 subgrade soil at 20 percent (optimum) moisture content.
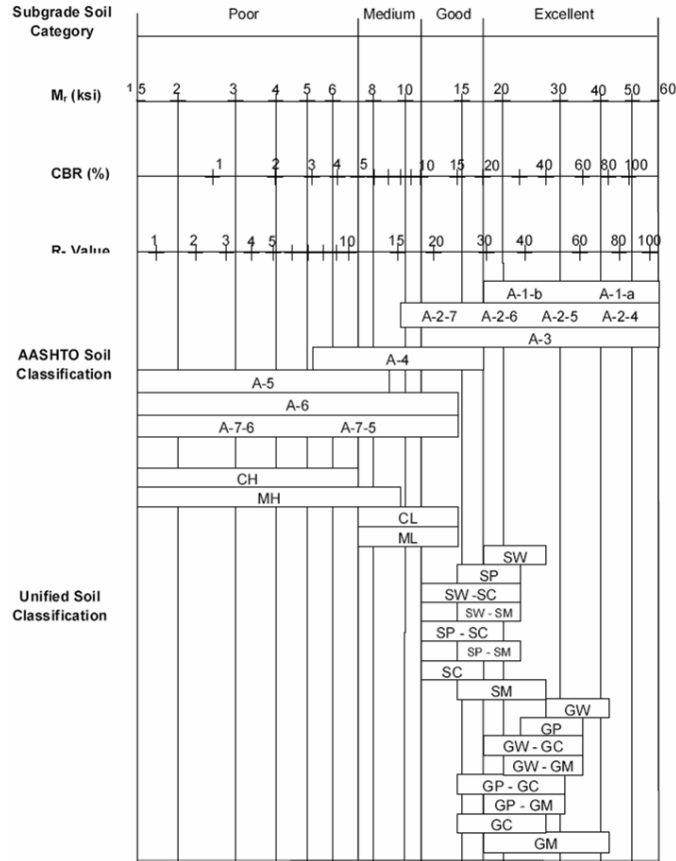
Figure 17. Relationships between CBR and resilient modulus for various soil types.
(Proposed AASHTO M-E Guide, 2004).

SURFACE RUTTING

Transverse surface profile measurements were taken before HVS testing, at several intermediate numbers of traffic passes, and at the end of testing. Rut depth was calculated as the difference between the profile measurements taken at the given pass level and the profile measurements taken prior to testing (pass level zero). Cross sectional profile measurements were taken at 305-mm (1-ft.) intervals along the effective test window for a total of 20 locations. A laser profilometer scanning at 5-mm intervals was used to make the measurements. For each test window, the maximum rut depth at each cross section was used to assemble a longitudinal profile. Using the average rut depth of the 20 cross sections for each test window, Figure 18 shows the progression of rut depths as a function of traffic repetitions for test windows subjected to various load intensities. Figure 18 also shows the axial load intensity applied to each test window. As expected, test windows tested with heavier loads deformed faster than those tested with lighter loads.
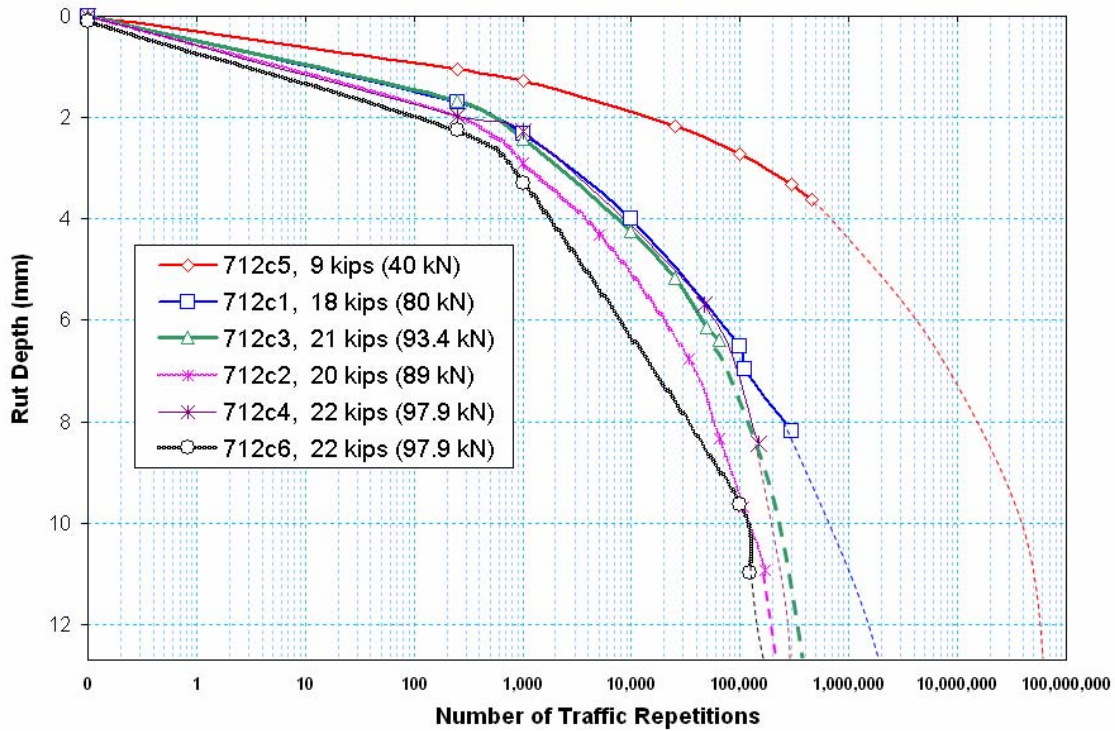
Figure 18. Average rut depth as function of traffic load repetitions and semi-axial load intensity.

The as-built gravimetric moisture content of the subgrade soil in Test Section 712 was 20 percent. The modified Proctor optimum moisture content was 20.5 percent. Laboratory test results presented in Figure 3 show that this subgrade soil at 20 percent moisture content has a CBR of 53 percent that indicates a relatively strong soil. Producing the target rut depth of 12.7 mm (0.5 inch) became time and cost prohibitive. For example, Test Window 712c5 was tested with the standard axial load of 80 kN (18 kips). After 500,000 traffic repetitions, the rut depth was only 3.6 mm. The axial load was increased for the remaining test windows, but even with the higher load intensities, for each test window, the number of traffic repetitions needed to produce 12.7 mm of rut depth had to be estimated by projecting the experimental rutting curve. For Test Window 712c5 with the standard axial load, failure was estimated to occur at approximately 60 million traffic repetitions.

Figures 26 to 31 present longitudinal rut depth profiles for each test window as a function of load repetitions. The semi-axial load applied to Test Window 711c5 was 40 kN (9 kips). This corresponds to the standard axial load of 80 kN (18 kips). Figure 18 shows that after 463,000 traffic repetitions this test window had developed a rut depth of only 3.6 mm. By projecting the experimental data curve it appears that this test section would require approximately 60 million traffic repetitions to produce a rut depth of 12.7 mm (0.5 in).

The axial load applied to Test Window 711c1 was 160 kN (36 kips). This is twice the load intensity of a standard axial load. Even with this overload, after 300,000 traffic

20

repetitions, the rut depth was 8.2 mm. By projecting the experimental data curve in Figure 18, the estimated number of traffic repetitions needed to produce a rut depth of 12.7 mm was 2 million.

No cracking was observed in any of the test windows of Test Section 712. This was probably due to the relatively strong subgrade. The subgrade gravimetric soil moisture content was 20.5 percent that approximately corresponds to its optimum moisture content. Test Section 711 was similar to Test Section 712 except that its subgrade soil moisture content was 25 percent. During the construction of that test section, a layer of soil was moistened more than intended, and the soil became very sticky and unworkable. Figure 19 shows a large rut caused by a rubber tire of our steel roller, and much muddy soil sticking to the tire. Moisture measurements on this layer of soil indicated values of gravimetric moisture content ranging from 27 to 35 percent. This subgrade soil tends to form lumps whereby the center of the lumps is dryer than the surrounding surface layer. This may explain why the workability and stability of this soil deteriorates rapidly past a threshold of strong and stable behavior. A similar soil behavior was observed in a test section from a previous study (Perkins and Cortez, 2005) that was built with this subgrade soil at 29 percent gravimetric moisture content. Also during the construction of the test section, the soil became unworkably sticky and unstable at some locations were minor increments of moisture content existed. Although this subgrade soil is relatively strong for a wide range of moisture contents, there appears to be a threshold beyond which even small increments of moisture content may render the soil unworkable. Figure 2 shows that the soil contains 33 percent of soil particles within the clay particle size range. The large clay content appears to govern the behavior of the soil mass.

Figure 19. Unstable soil behavior with gravimetric moisture contents between 27 and 35 percent..

Figure 20a. Test Window 712c1 before HVS traffic.

Figure 20b. Test Window 712c1 at the end of HVS traffic.

Figure 21a. Test Window 712c2 before HVS traffic.

Figure 21b. Test Window 712c2 at the end of HVS traffic.

Figure 22a. Test Window 712c3 before HVS traffic.

Figure 22b. Test Window 712c3 at the end of HVS traffic.

Figure 23a. Test Window 712c4 before HVS traffic.
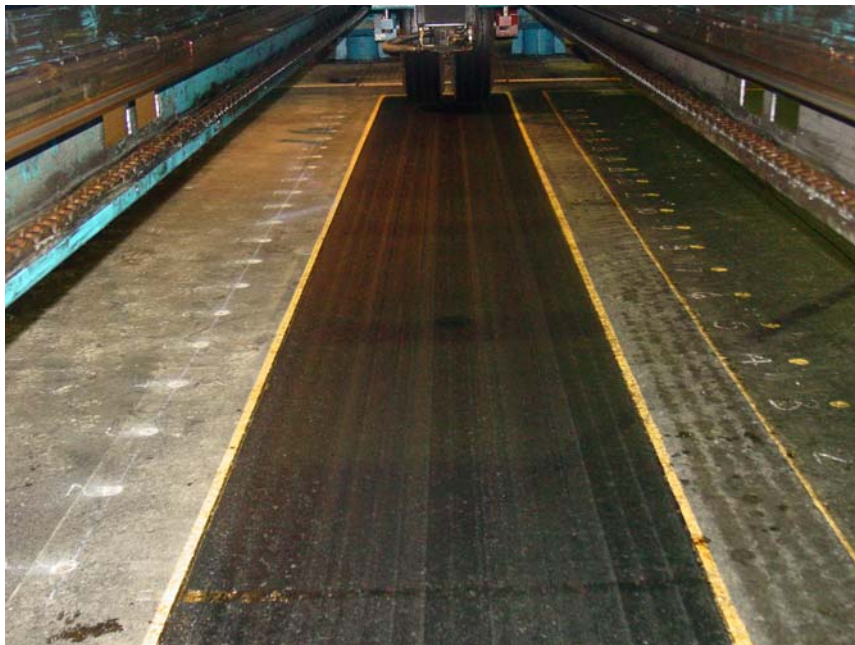
Figure 23. Test Window 712c4 at the end of HVS traffic.

Figure 24a. Test Window 712c5 before HVS traffic.

Figure 24b. Test Window 712c5 at the end of HVS traffic

Figure 25a. Test Window 712c6 before HVS traffic.

Figure 25b. Test Window 712c6 at the end of HVS traffic
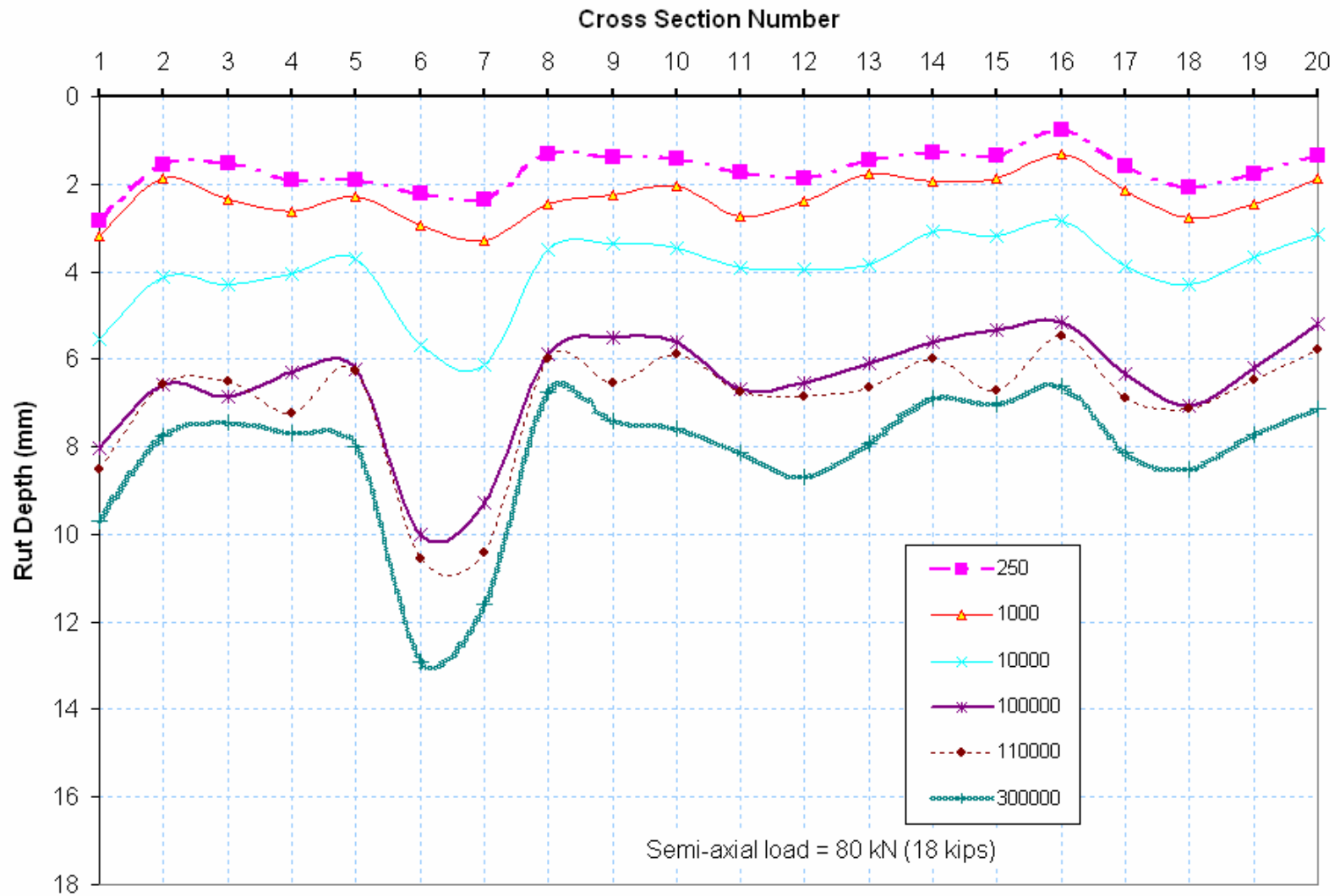
Figure 26. Progression of surface rutting along the center of the tire path in Test Window 712c1.

Test Section 712 AASHTO A-7-5 subgrade soil at 20 percent (optimum) moisture content.
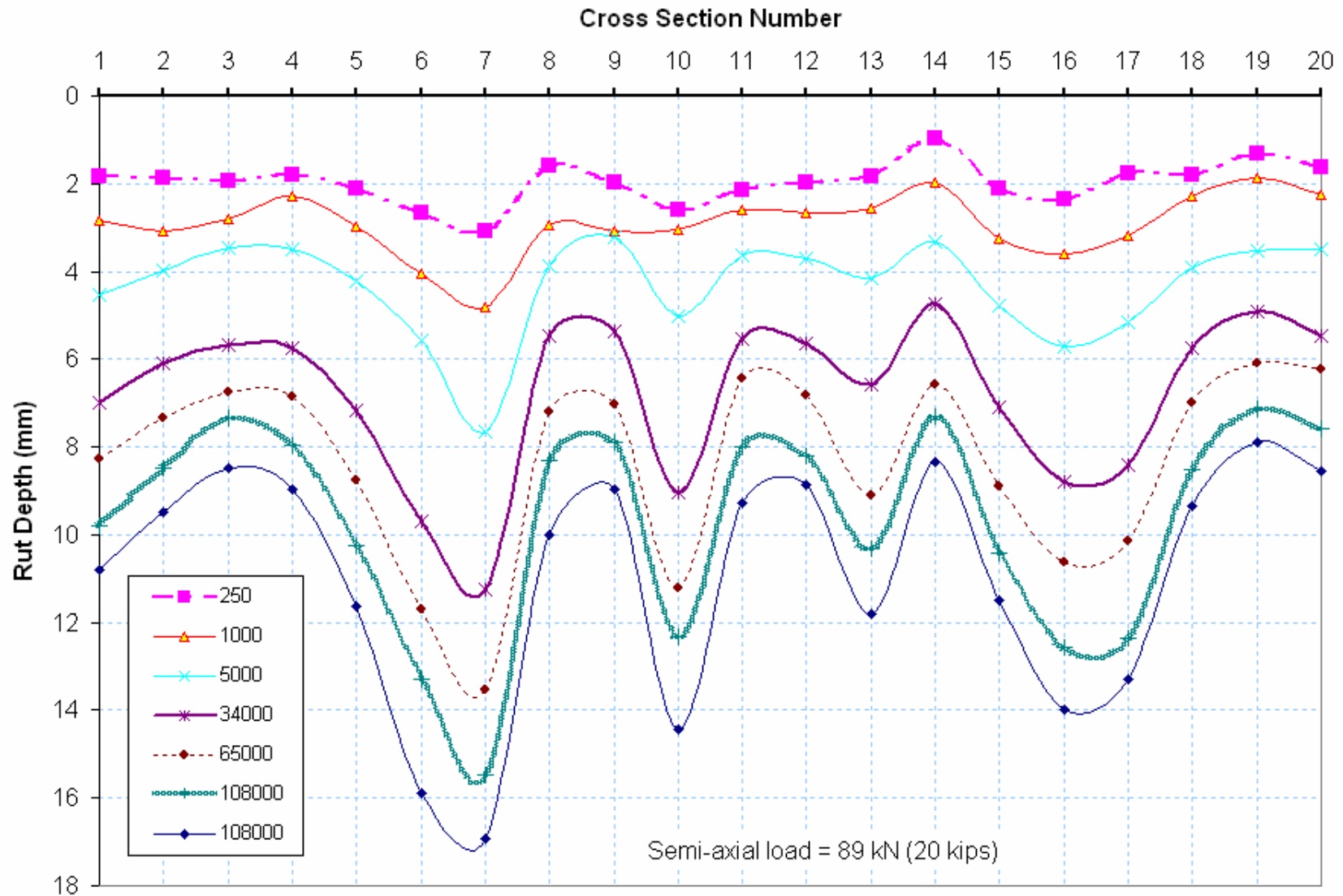
Figure 27. Progression of surface rutting along the center of the tire path in Test Window 712c2.

Test Section 712 AASHTO A-7-5 subgrade soil at 20 percent (optimum) moisture content.
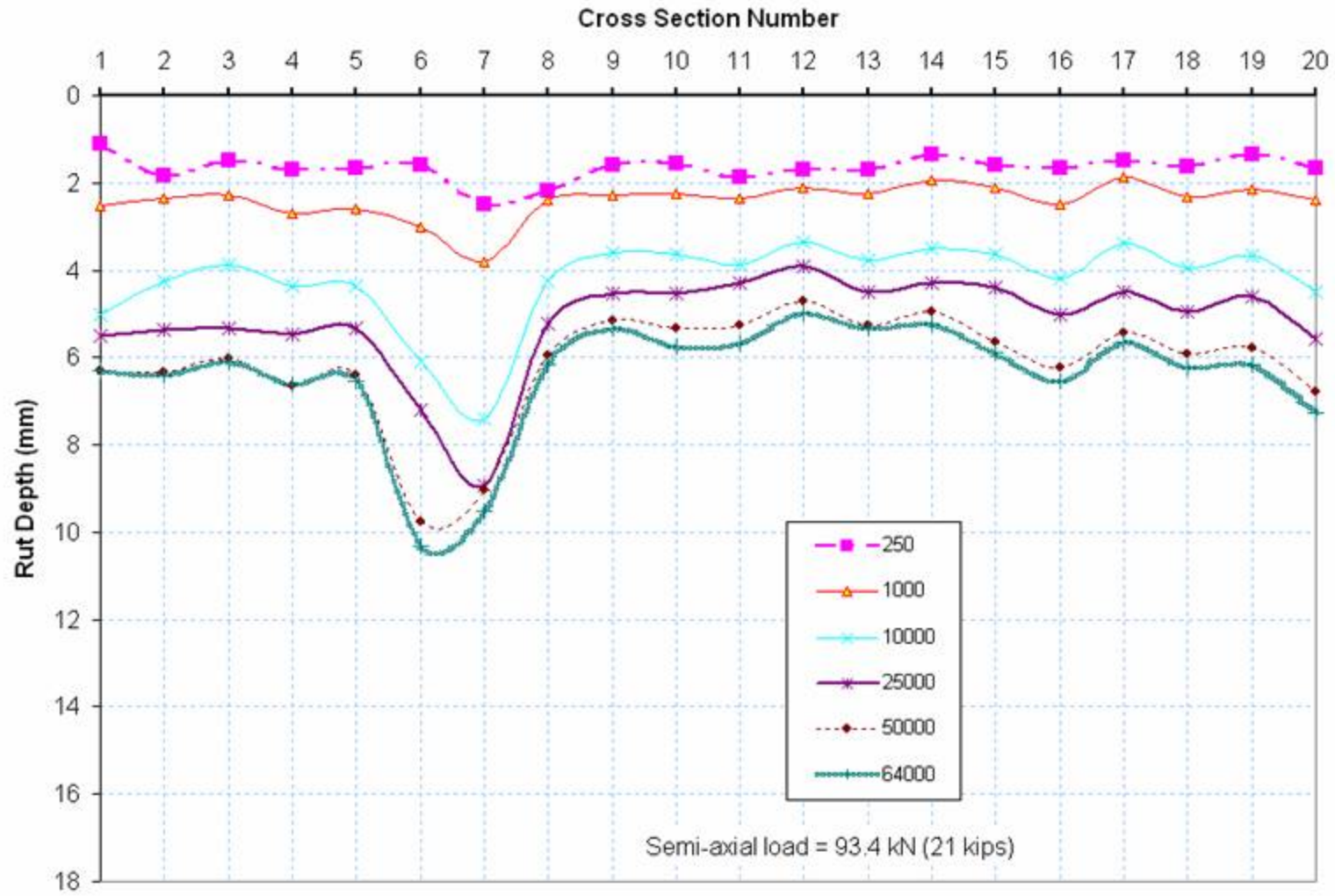
Figure 28. Progression of surface rutting along the center of the tire path in Test Window 712c3.

Test Section 712 AASHTO A-7-5 subgrade soil at 20 percent (optimum) moisture content.
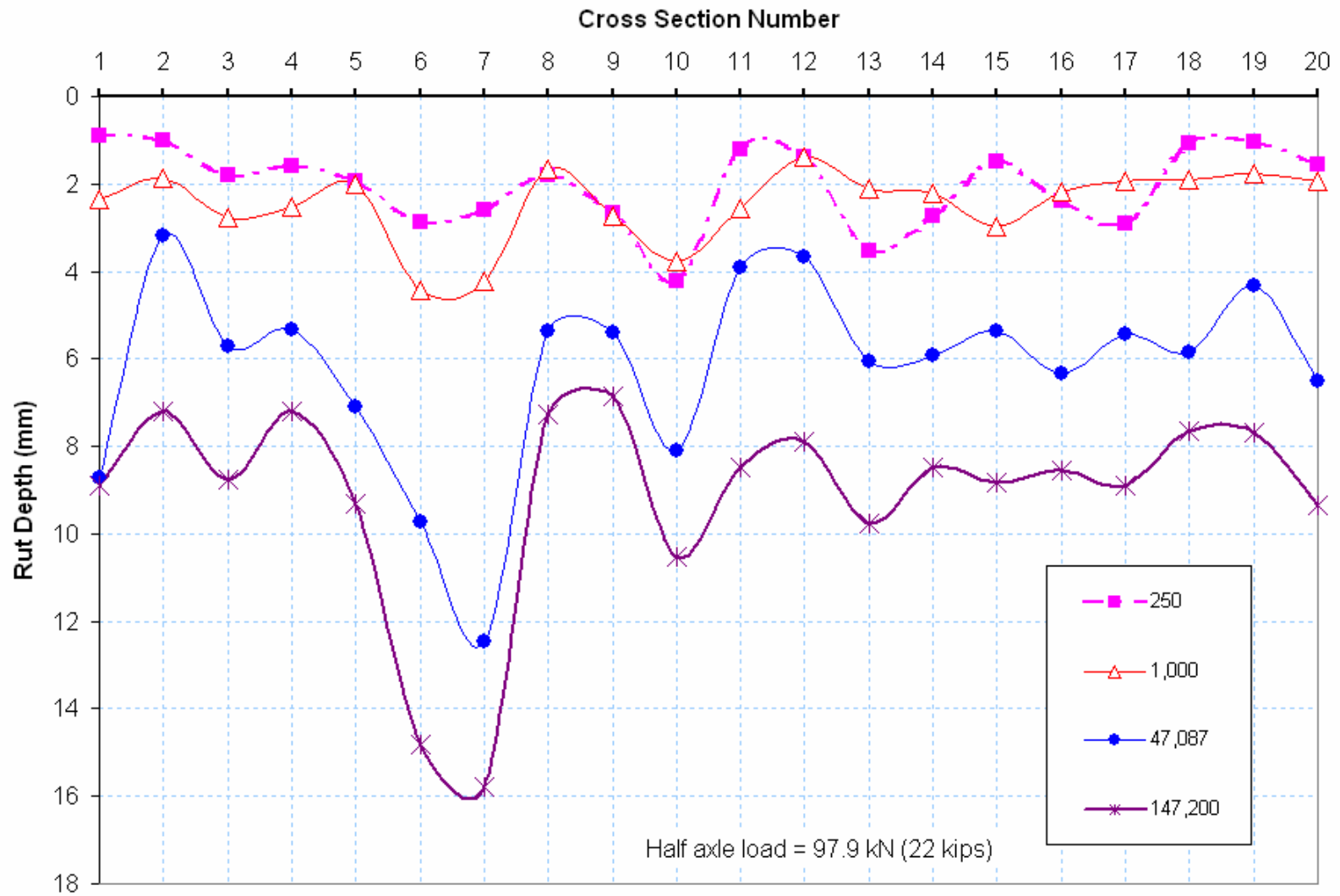
Figure 29. Progression of surface rutting along the center of the tire path in Test Window 712c4.

Test Section 712 AASHTO A-7-5 subgrade soil at 20 percent (optimum) moisture content.
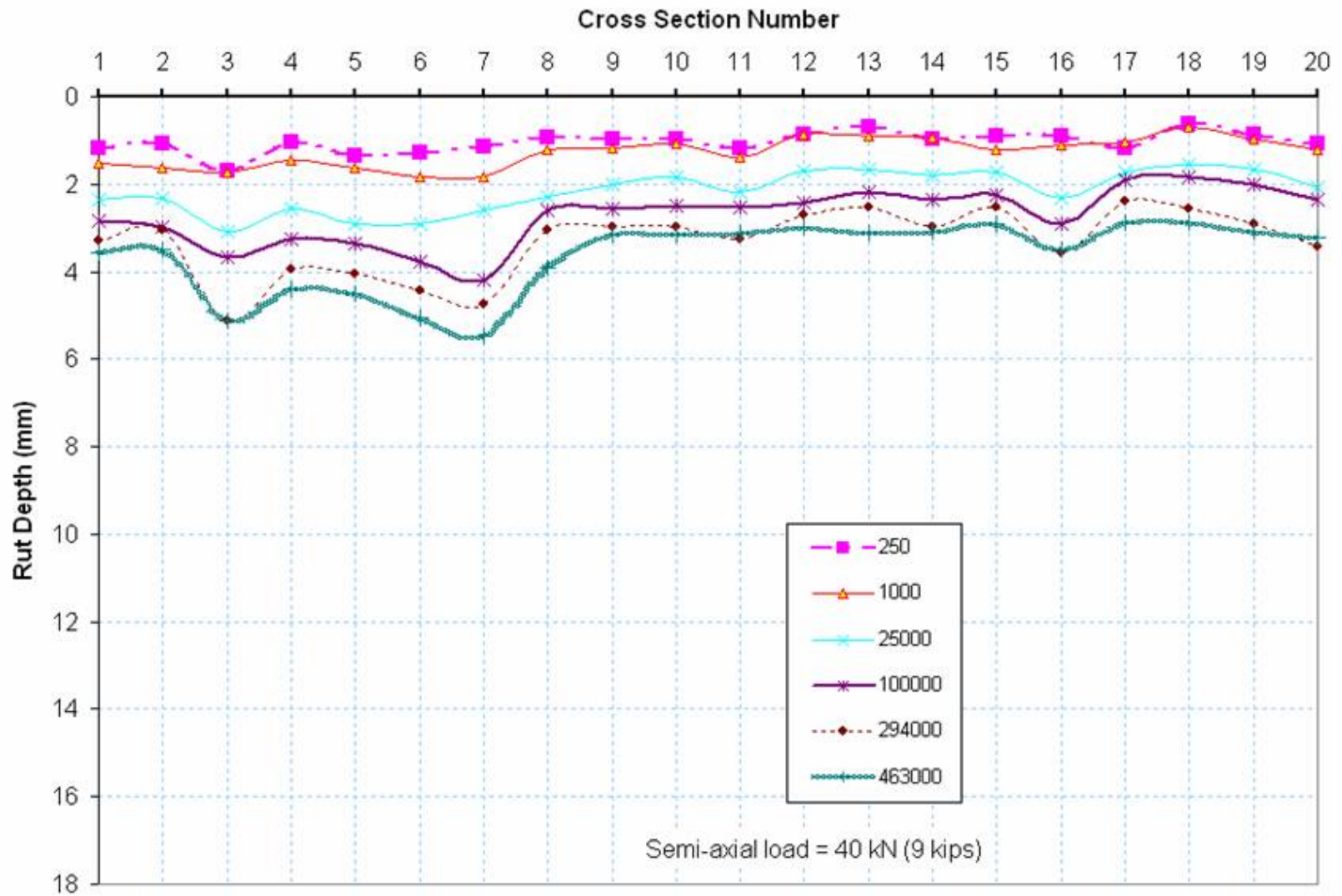
Figure 30. Progression of surface rutting along the center of the tire path in Test Window C5
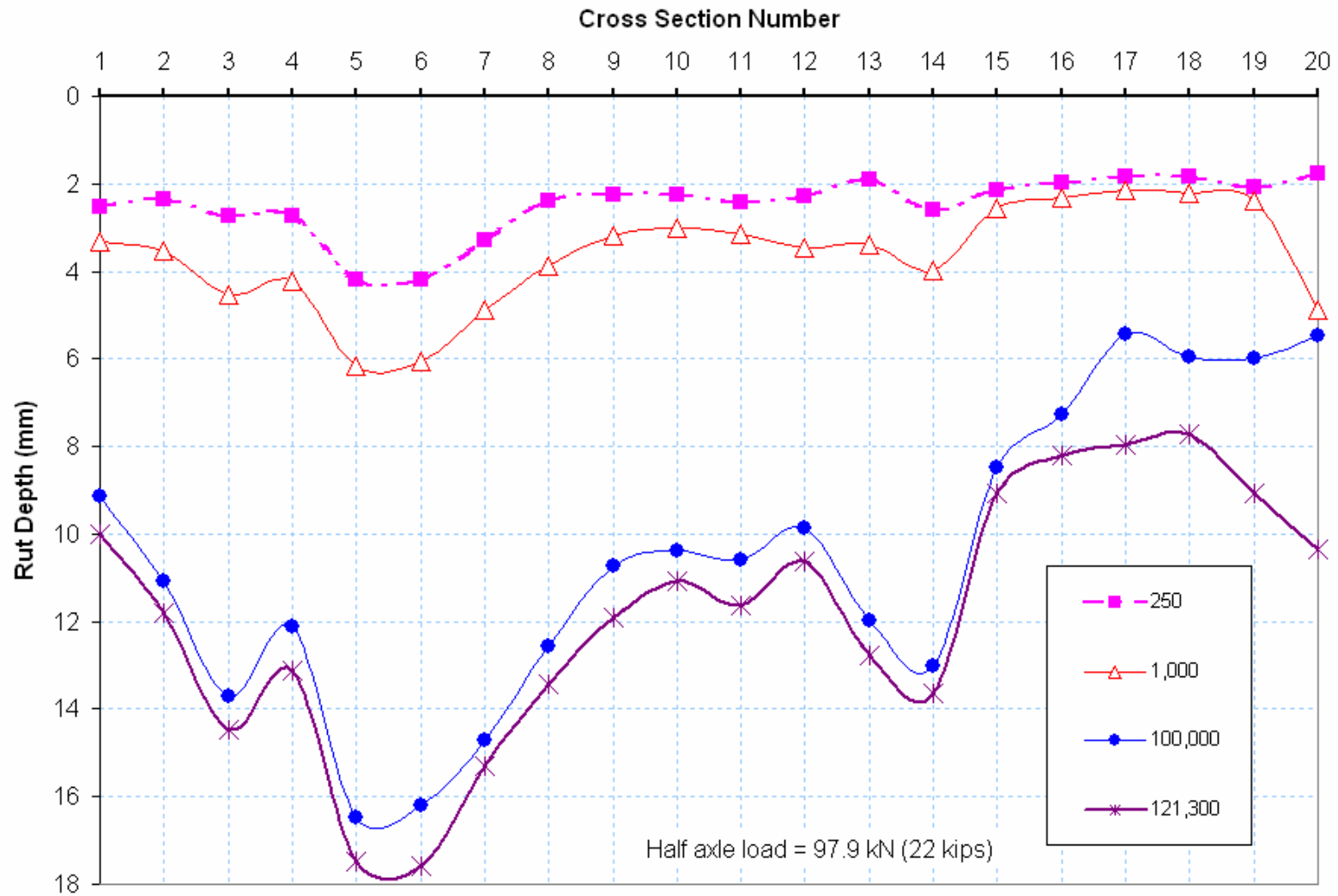
Figure 31. Progression of surface rutting along the center of the tire path in Test Window 712c6.
.

Table 8 shows the number of traffic passes required to cause a rut depth of 12.7 mm (0.5 in) estimated from the projections of the experimental data. Figure 32 graphically shows the relationship between load intensity and number of traffic passes to failure, and also a power function that fits the experimental data with an R^2 value of 0.996.

Table 8. Load Repetitions to reach failure of 12.7 mm

Test Window	Load (kN)	$N_{failure}$
c5	40	60,000,000
c1	80	2,000,000
c2	89	380,000
c3	93.4	210,000
c4, c6	97.9	180,000
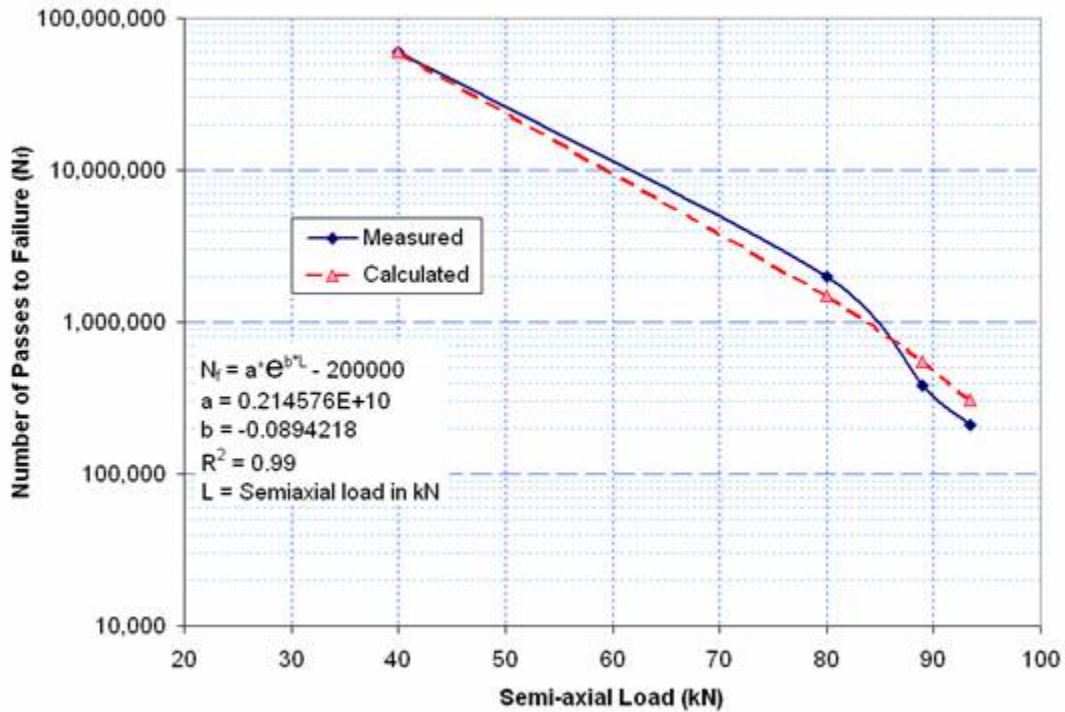
Figure 32 Load repetitions to failure as a function of load intensity.

DEFORMATION AND STRAIN

Emu inductance coil sensors were used to measure the distance between pairs of coils at various stages throughout the traffic testing. Comparing the distance between a

35

pair of coils to the initial distance, the deformation of the soil between the coils can be established. An average strain value can then be calculated by dividing this deformation by the initial coil distance. By convention, we assign this strain value to a point located in the middle between a coil pair. Coil distance measurements were conducted at stages with the HVS stopped to obtain permanent deformation, and also dynamically during traffic applications to obtain resilient deformations.

a) Permanent Deformations

Permanent deformation measurements were collected from εmu coils embedded in the base and the subgrade. Measurements were conducted before traffic began and at various stages throughout the traffic tests. An additional mobile εmu coil was placed at the asphalt surface and paired with a coil embedded just below the bottom of the asphalt concrete (AC) to measure the vertical deformation that occurred in the asphalt layer. Three stacks of εmu coils were embedded to form triaxial arrangements in the base and subgrade. Vertical pairs of εmu coils were embedded down to a depth of 1.52 m (5 ft) from the asphalt surface. Previous experiments have shown that, at this depth, the strains are normally small compared to electronic noise.
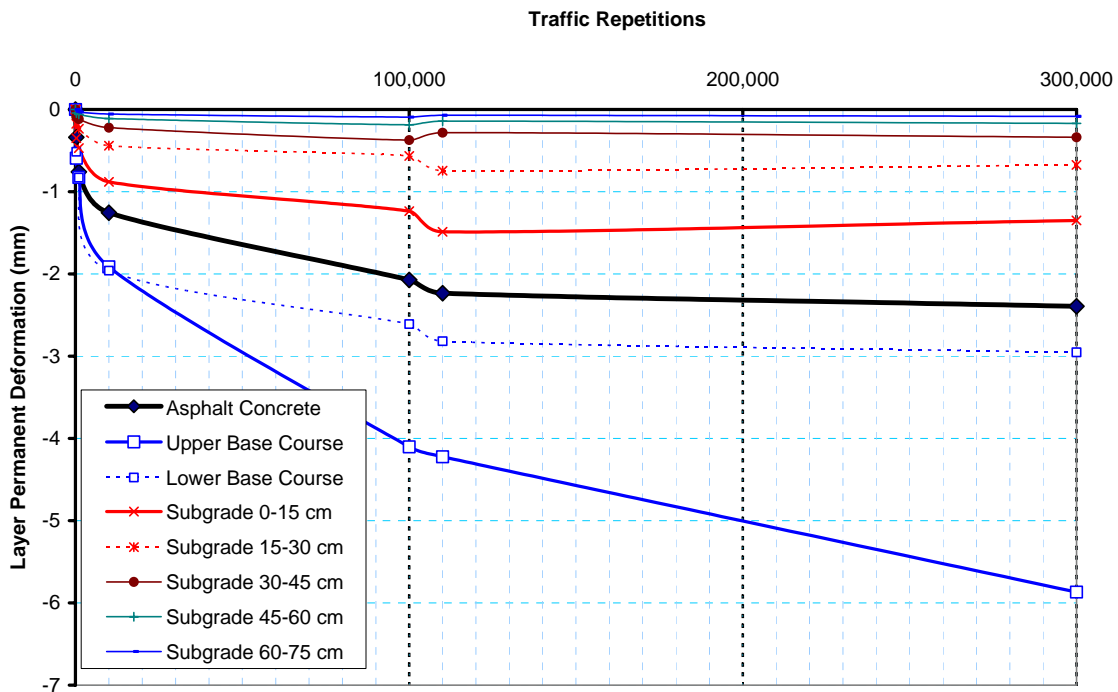
Figure 33a. Layer by layer vertical permanent deformation in Test Window 712c1 with 80 kN semi-axial load.
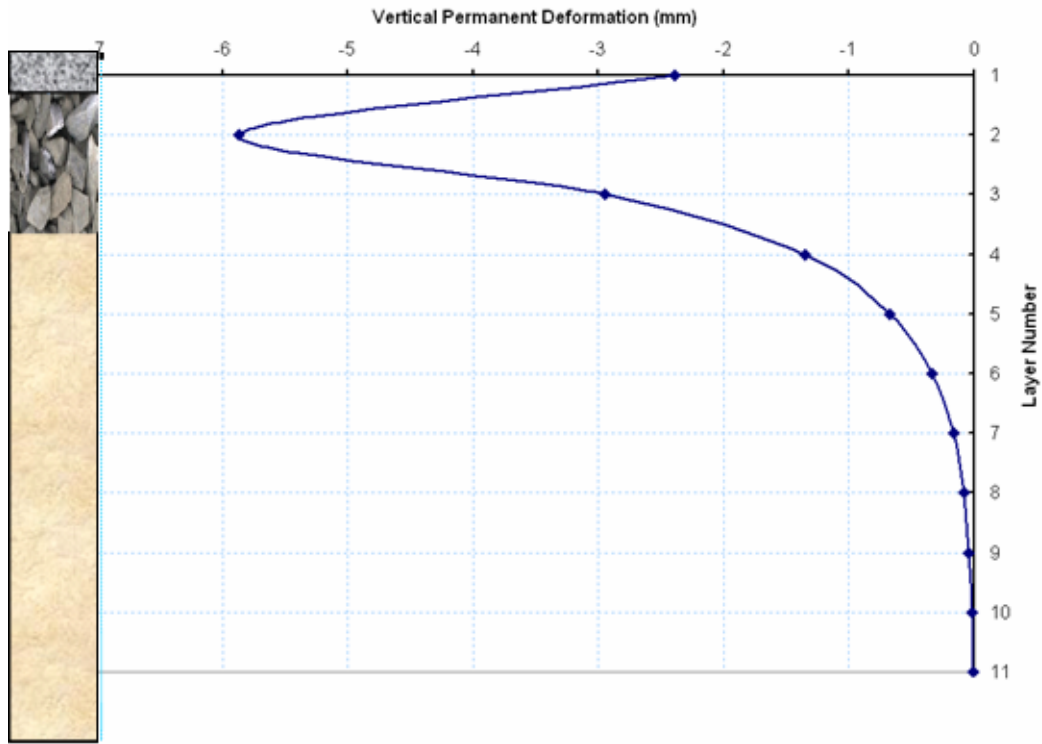
Figure 33b. Layer by layer vertical permanent deformation at failure in Test Window 712c1 with 80-kN semi-axial load.
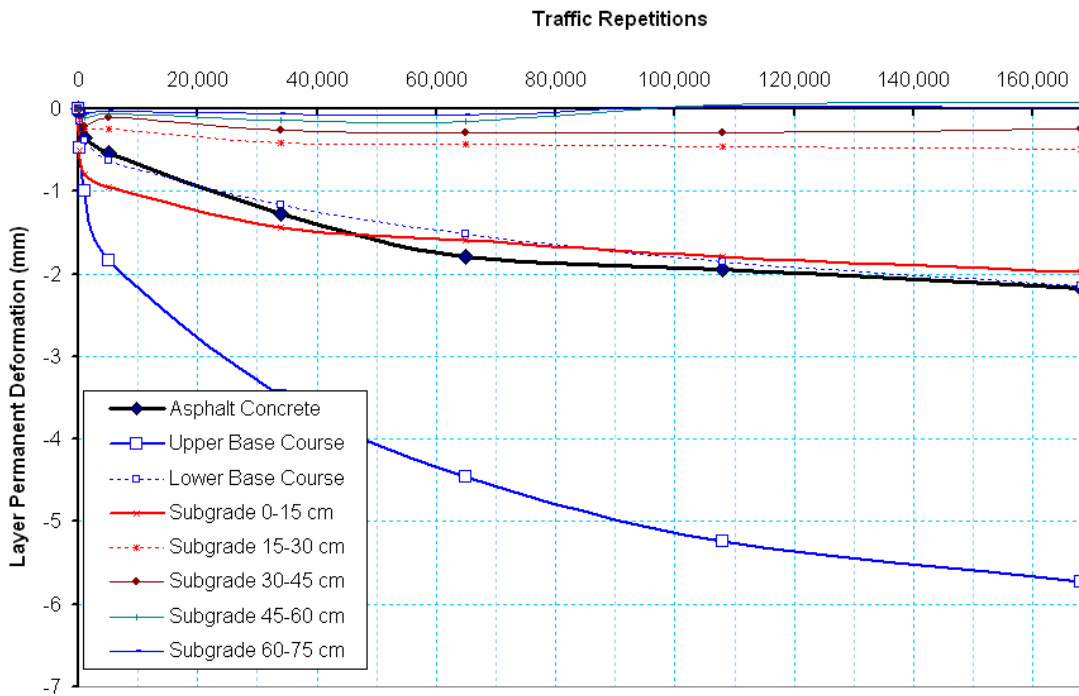
Figure 34a. Layer by layer vertical permanent deformation in Test Window 712c2 with 89-kN semi-axial load.
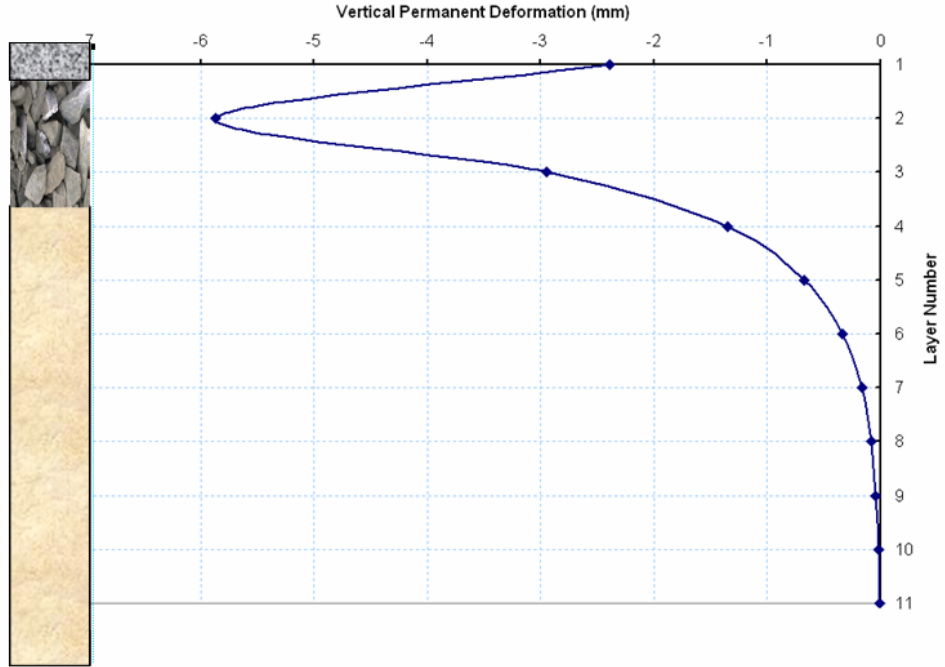
Figure 34b. Layer by layer vertical permanent deformation at failure in Test Window 712c2 with 89-kN semi-axial load.
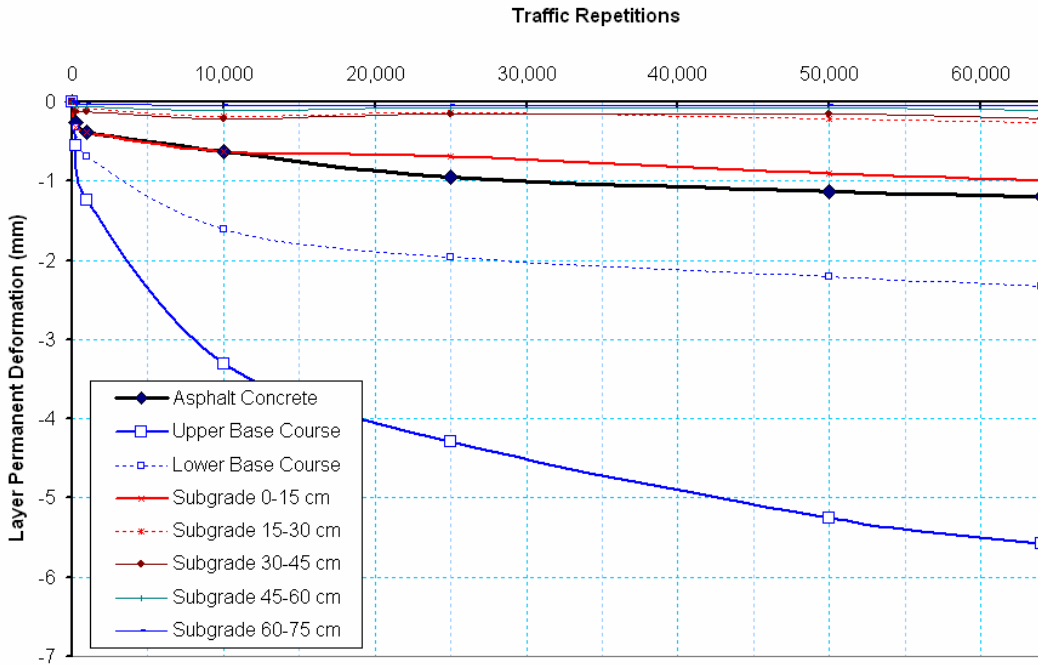
Figure 35a. Layer by layer vertical permanent deformation in Test Window 712c3 with 93.4-kN semi-axial load.
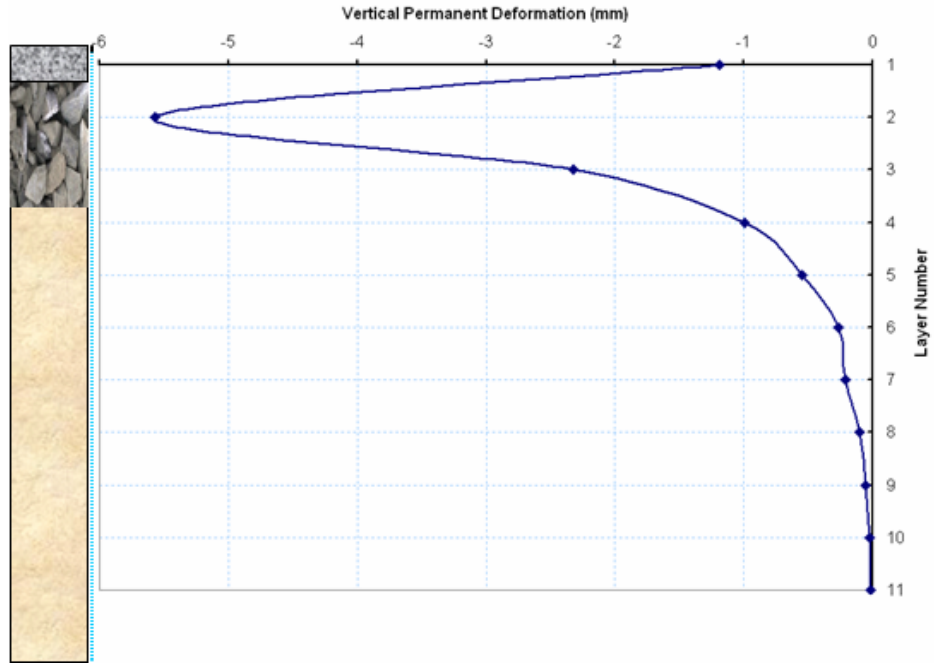
Figure 35b. Layer by layer vertical permanent deformation at failure in Test Window 713c3 with 93.4-kN semi-axial load.
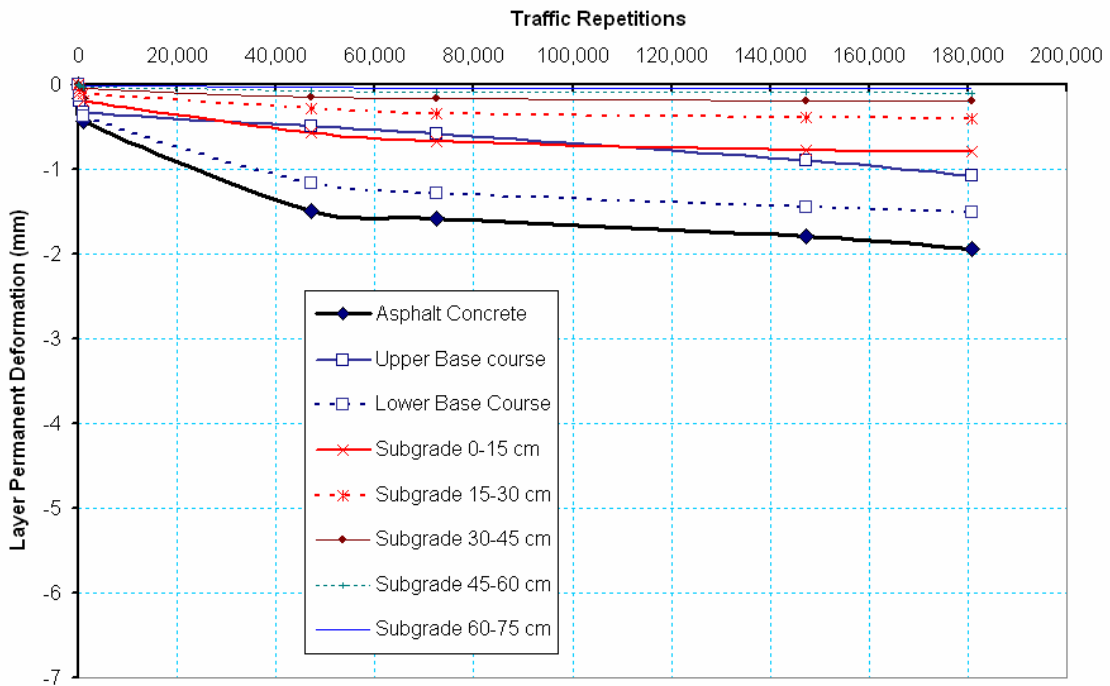
Figure 36a. Layer by layer vertical permanent deformation in Test Window 712c4 with 97.9-kN semi-axial load.
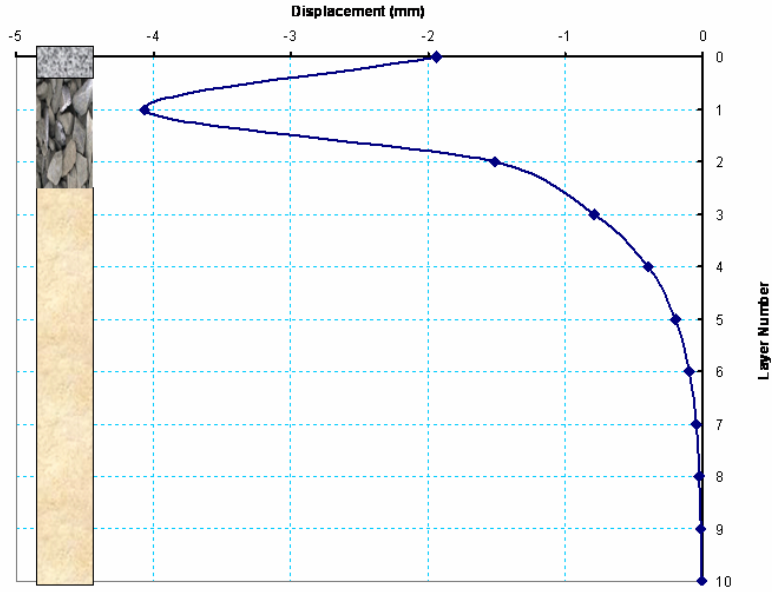
Figure 36b. Layer by layer vertical permanent deformation at failure in Test Window 713c4 with 97.9-kN semi-axial load.
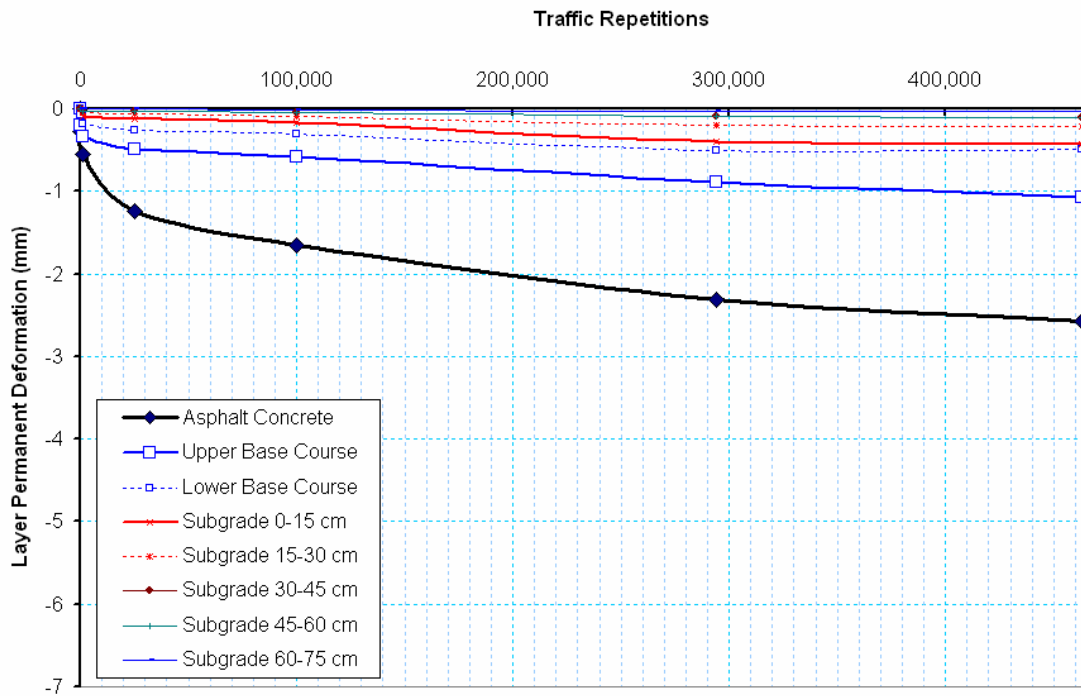
Figure 37a. Layer by layer vertical permanent deformation in Test Window 712c5 with 40 kN semi-axial load.

40
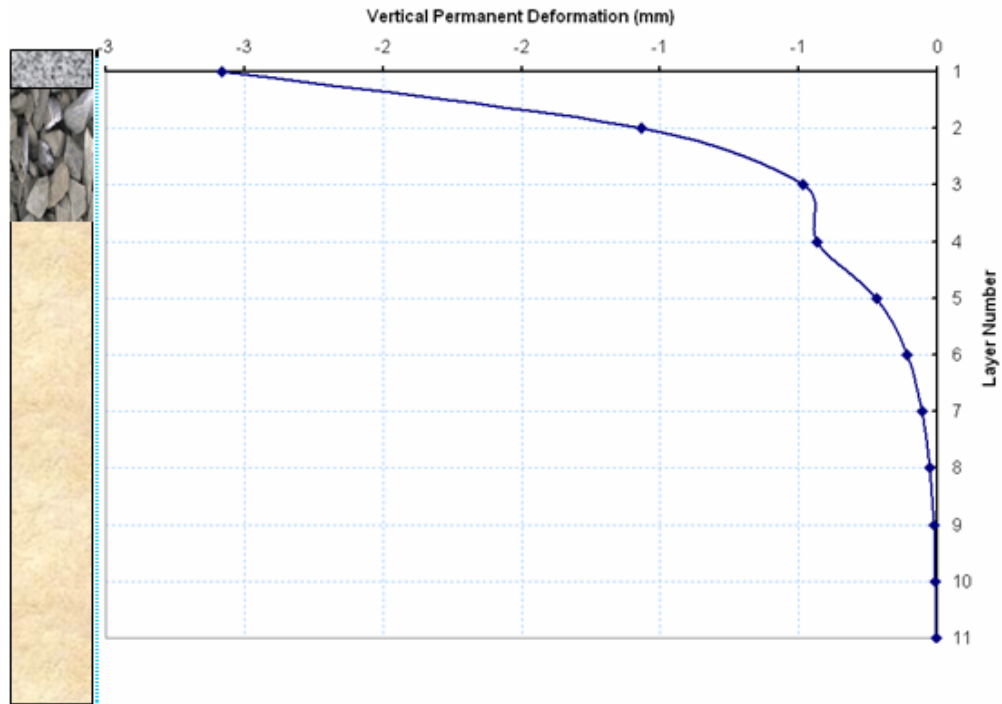
Figure 37b. Layer by layer vertical permanent deformation at end of traffic in Test Window 712c5 with 40-kN half axle load.
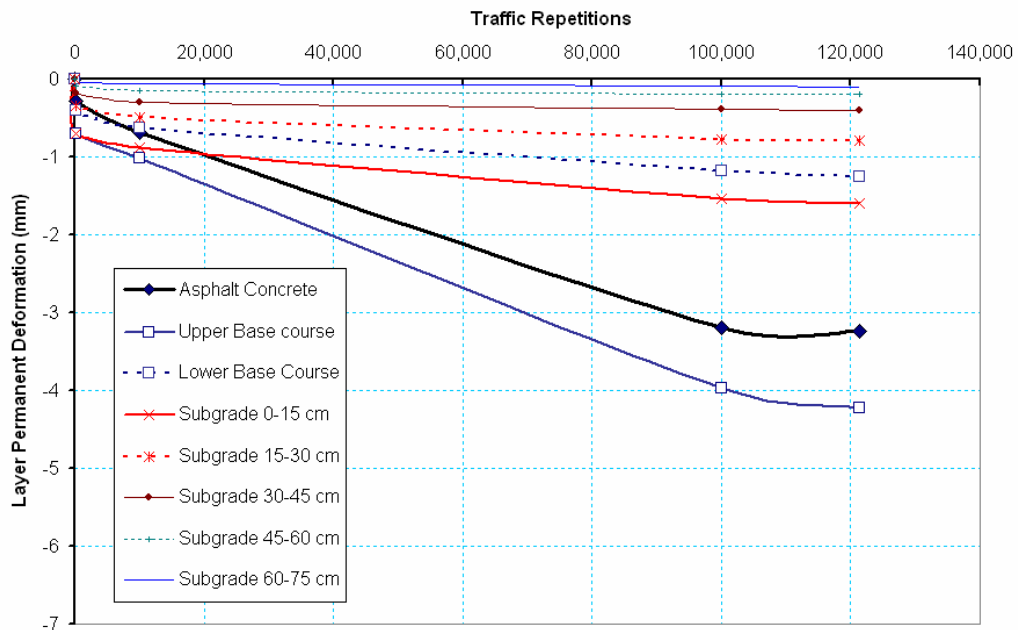
Figure 38a. Layer by layer vertical permanent deformation in Test Window 712c6 with 97.9-kN half axle load.
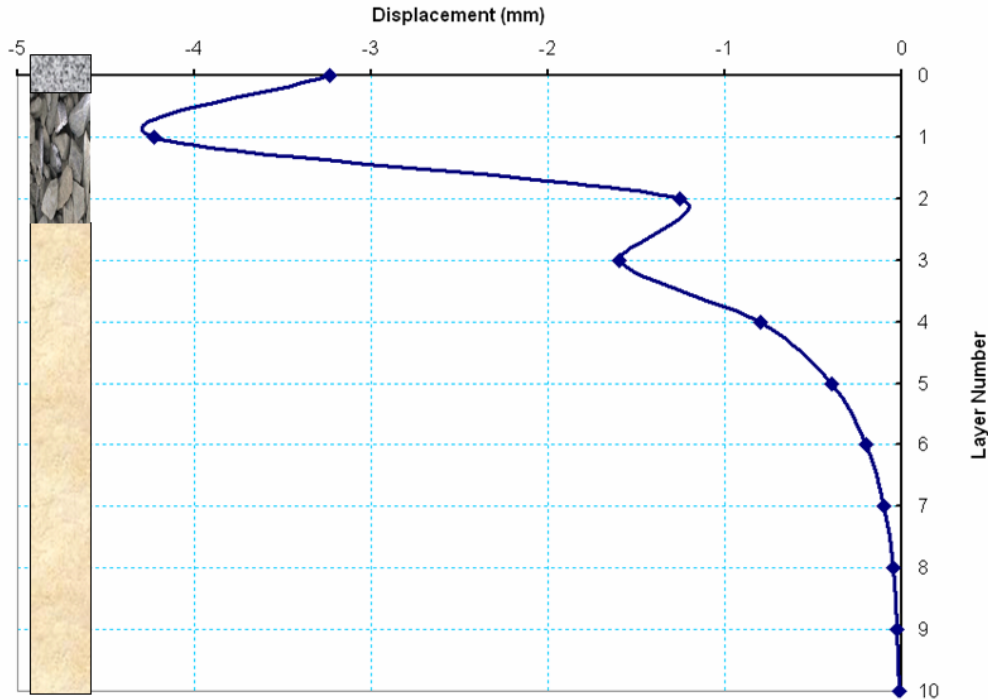
Figure 38b. Layer by layer vertical permanent deformation at end of traffic in Test Window 712c6 with 97.9-kN half axle load.

b) Resilient Deformations and Strains

As with previous test sections, resilient deformations were measured with the εmu coil gages in two layers in the base course and eight layers in the subgrade. The vertical resilient deformations and strains were compressive. The transverse resilient deformations and strains were extensive. The longitudinal resilient deformations and strains were initially compressive until the tire assembly was located directly above the sensors, and thereafter suddenly reversed into extensive deformations and strains. Resilient deformations are induced by the dynamic rolling of the truck tires over the pavement test section and over the sensors. Observing the static permanent deformation and the dynamic measurements, one can conclude that for each traffic load event, most deformation is recoverable (resilient), but a small component of (permanent) deformation remains and cumulates with traffic repetitions. However, the ratio of permanent to resilient deformations decreases when the number of traffic repetitions increases. This report we will focus on vertical stress and strains. A later report will examine relationships between vertical and horizontal components of stress and strain in order to model soil behavior, and define the mechanical behavior of the pavement structure as affected by multiple parameters.

42

In general, resilient deformation and strain increased in proportion to the traffic load intensity. Resilient strains as a function of load repetitions are presented in Figure 45 for a location 76 mm (3 in.) below the top of the subgrade. It can be seen that, in this test section, the resilient strains remained nearly constant throughout the traffic tests.
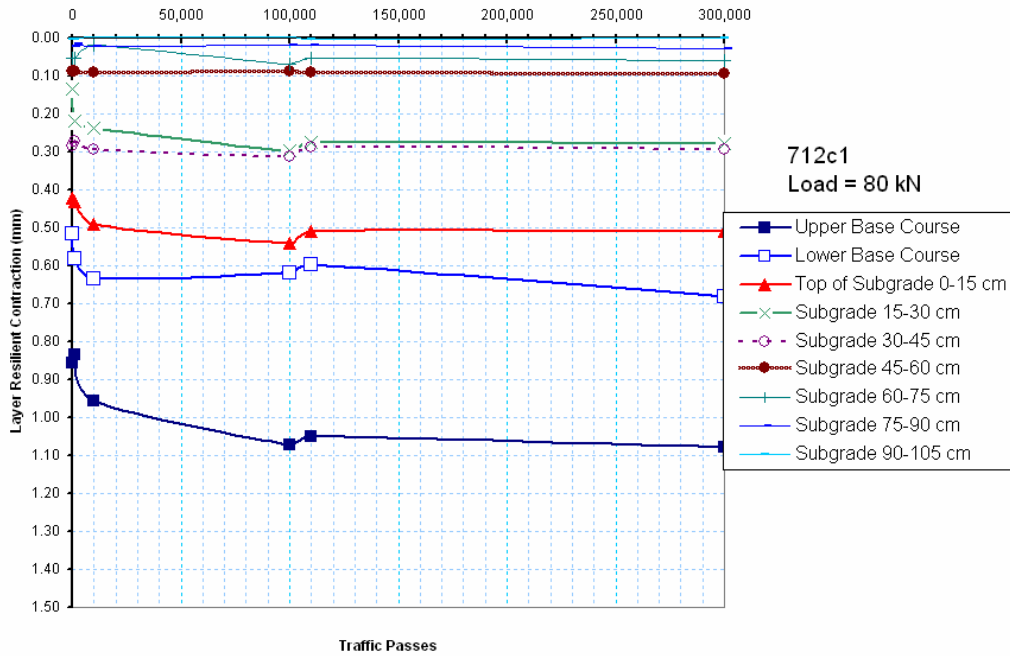
Figure 39. Resilient vertical deformations at various layers in Test Window 712c1.

Test Section 712 AASHTO A-7-5 subgrade soil at 20 percent (optimum) moisture content.
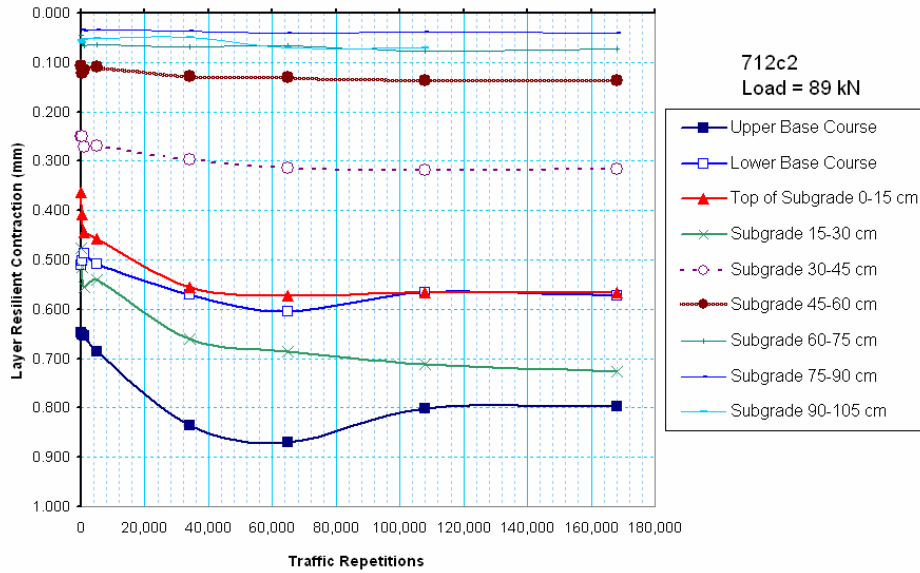
Figure 40. Resilient vertical deformations at various layers in Test Window 712c2.
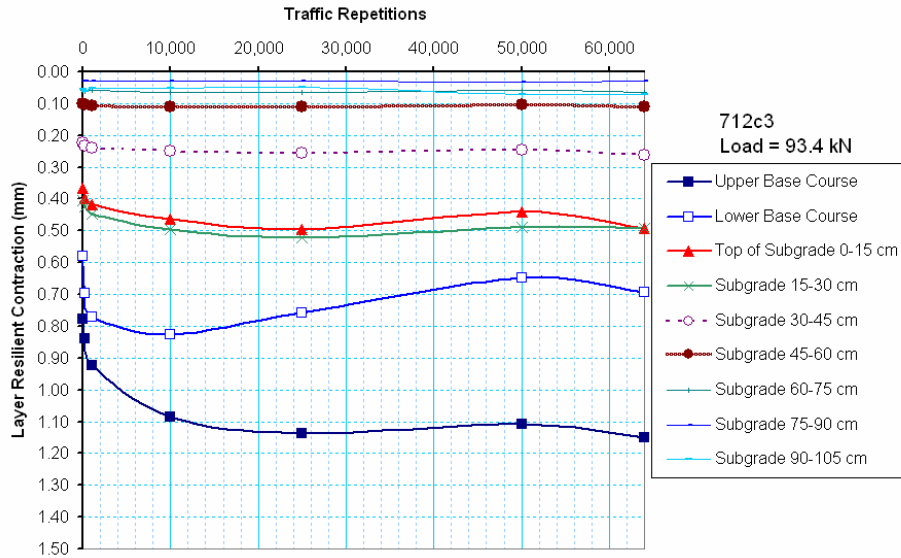
Figure 41. Resilient vertical deformations at various layers in Test Window 712c3.

Test Section 712 AASHTO A-7-5 subgrade soil at 20 percent (optimum) moisture content.
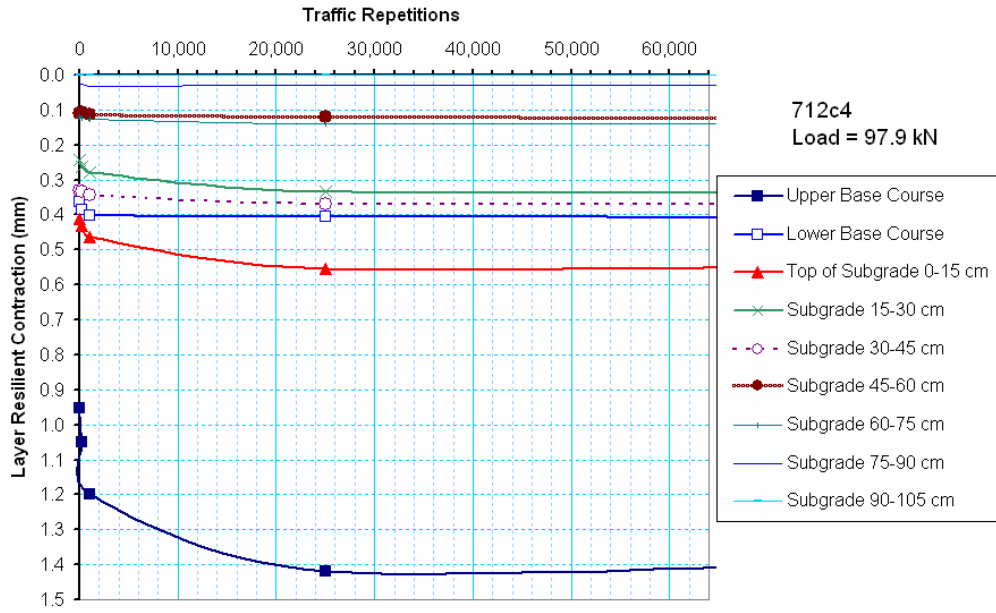
Figure 42. Resilient vertical deformations at various layers in Test Window 712c4.
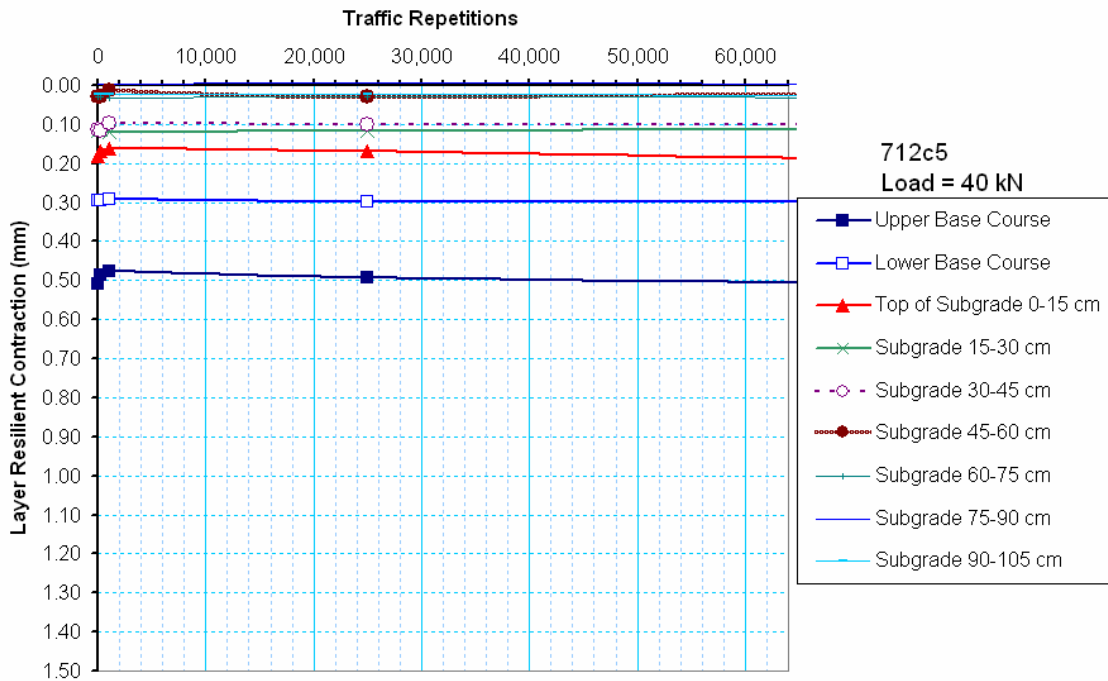
Figure 43. Resilient vertical deformations at various layers in Test Window 712c5.

Test Section 712 AASHTO A-7-5 subgrade soil at 20 percent (optimum) moisture content.
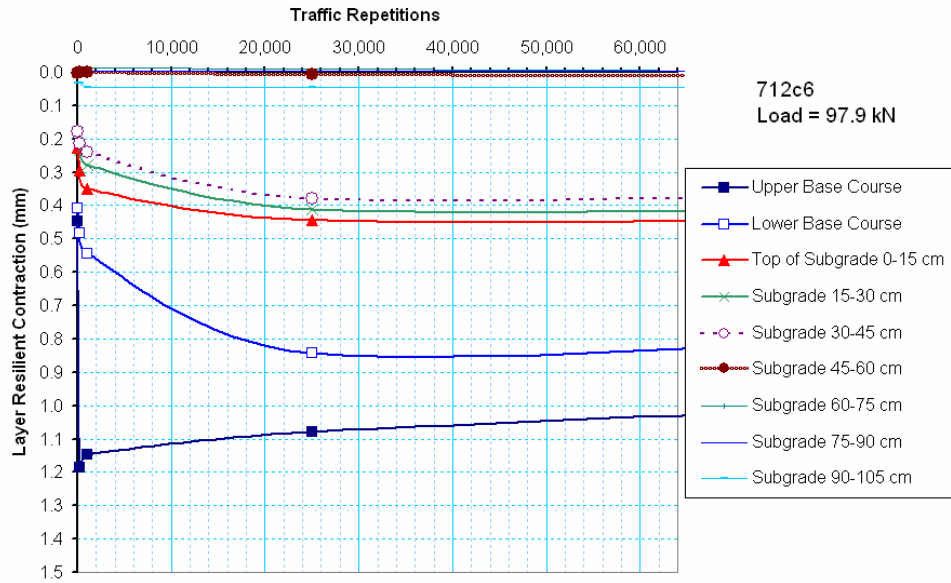
Figure 44. Resilient vertical deformations at various layers in Test Window 712c6.
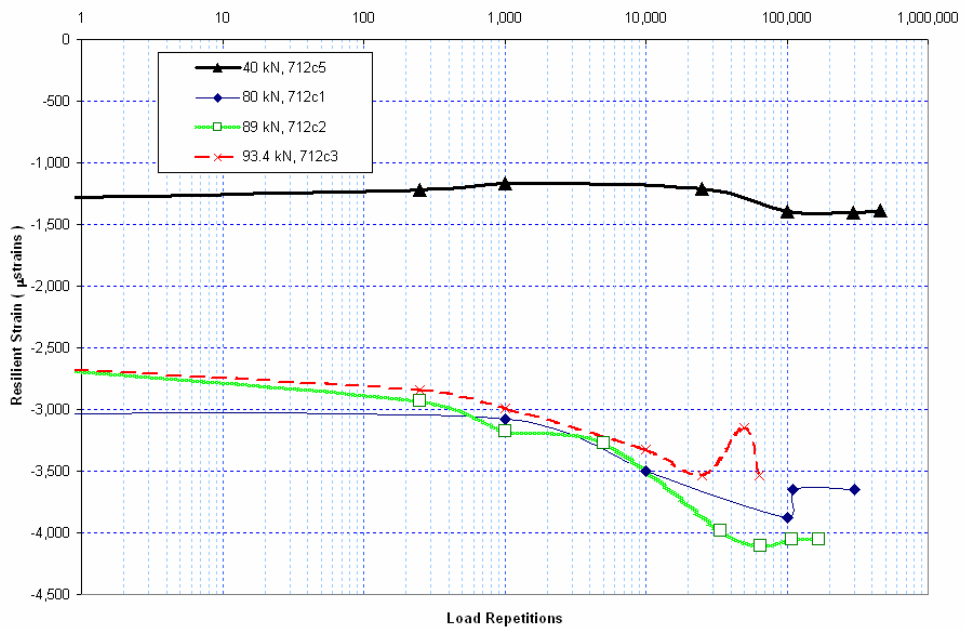
Figure 45. Resilient vertical strain at the top of the subgrade for various loads.

46
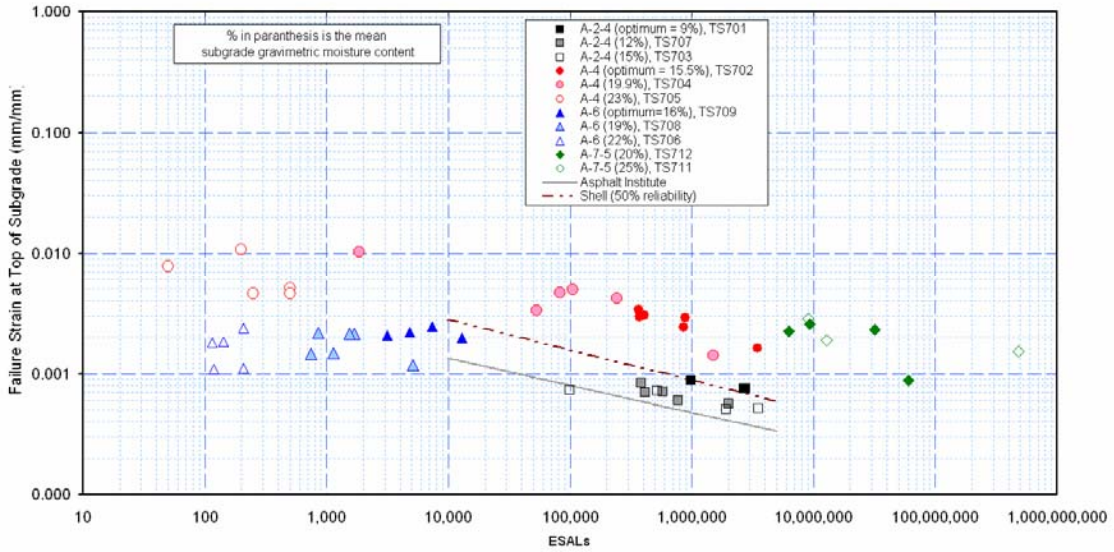
Figure 46. Effect of soil type and moisture content on subgrade failure criteria.

Figure 46 shows the resilient strain at the top of the subgrade at failure for all the subgrade soils included in this study. The existing subgrade failure criteria established by the Asphalt Institute and the Shell corporation are also graphed for comparison. It can be seen that the resilient behavior of the subgrade soil A-2-4 is consistent with the two established criteria, but significant differences occur for other soils. The data suggests that subgrade resilient strain criteria must be tailored to soil type.

STRESS

Stress measurements were conducted by means of Geokon® gauges. Figure 47 shows the stress measurements in the middle of the base course in Test Windows 712c2 and 712c5. The semi-axial load were 89 kN (20 kips) and 40 kN (9 kips) respectively.
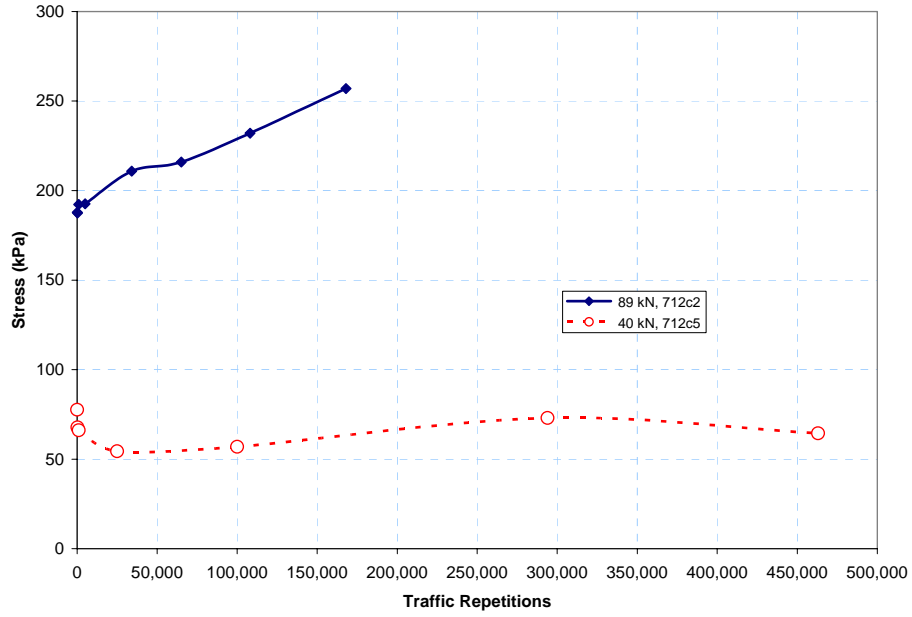
Figure 47. Stress measurements in the middle of the base course in Test Windows 712c2 and 712c5.
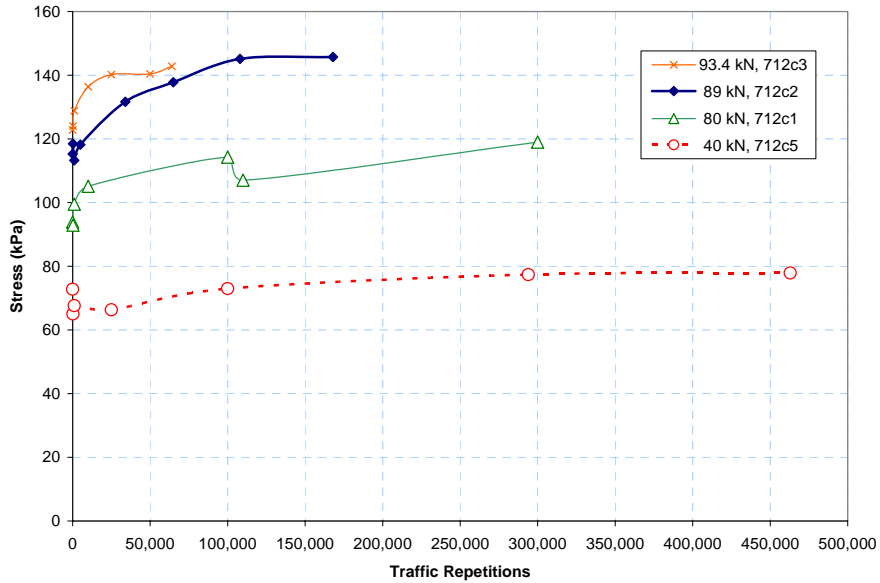
Figure 48. Vertical stress measurements at a depth of 76 mm below the top of the subgrade for several semi-axial load intensities.
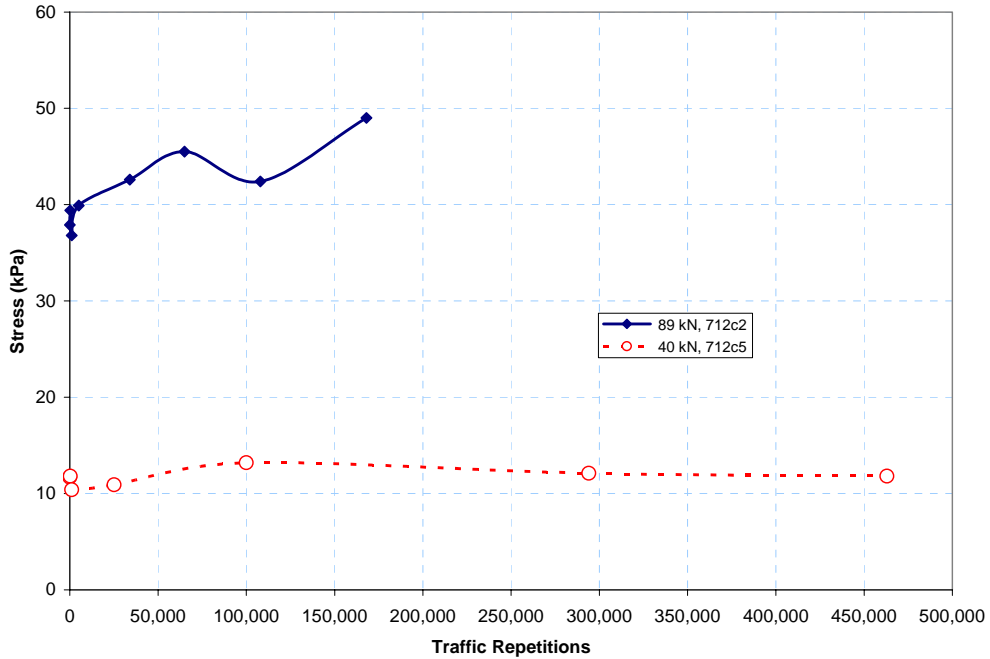
Figure 49. Stress measurements at a depth of 686 mm (27 in.) below the top of the asphalt concrete for semi-axial loads of 40 kN (9 kips) 89 kN (20 kips).
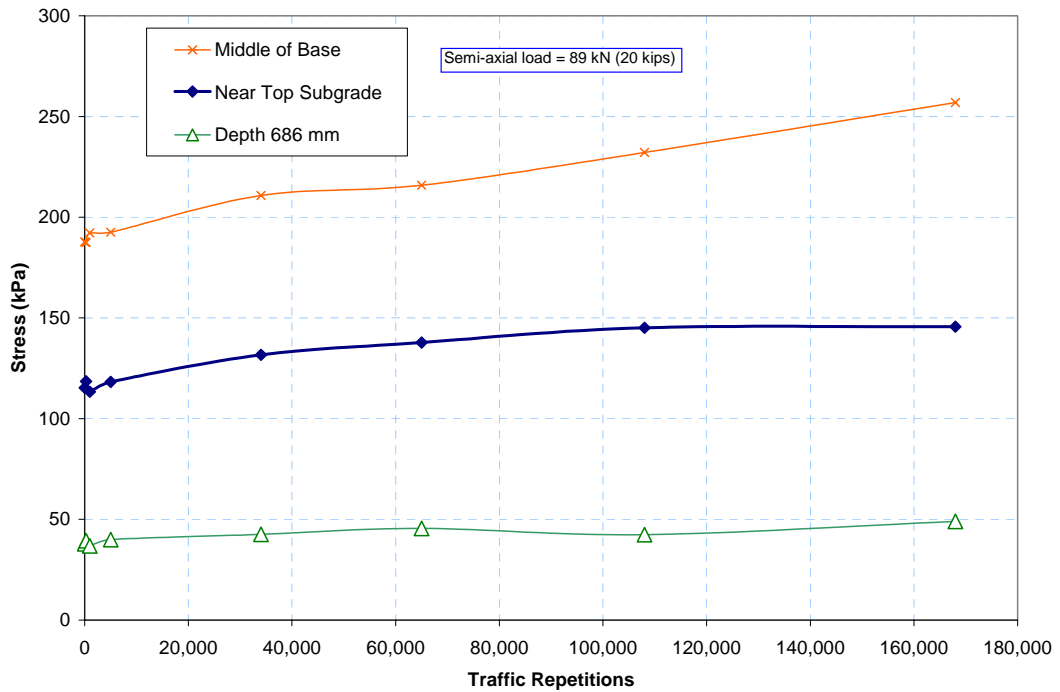
Figure 50. Stress measurements at various depths in Test Window 712c2 with a semi-axial load of 89 kN (20 kips).

In most cases, stress increased slightly with traffic repetitions (stress hardening). This is probably due to packing of soil particles under the action of traffic.

49

FORENSIC EVALUATION

A forensic evaluation was conducted to establish the condition of the pavement structure at the end of the traffic tests. Two trenches were cut across the test windows. One trench was excavated across test windows 1, 2, and 3 on the south region of the test section. This trench will be referred to as the "South Trench". Another trench was excavated in the north region of the test section. This trench cut across test windows 4, 5, and 6. The boundaries of the trenches were carefully located and marked to avoid damaging the embedded sensors and wires. Dry saw cutting was used to avoid disturbing the base and subgrade moisture contents. Base course and subgrade soil samples were taken immediately after exposure to determine their moisture contents by the oven-dry method. The side surfaces were carefully scrapped and dusted off to be able to measure asphalt and base layer thickness.
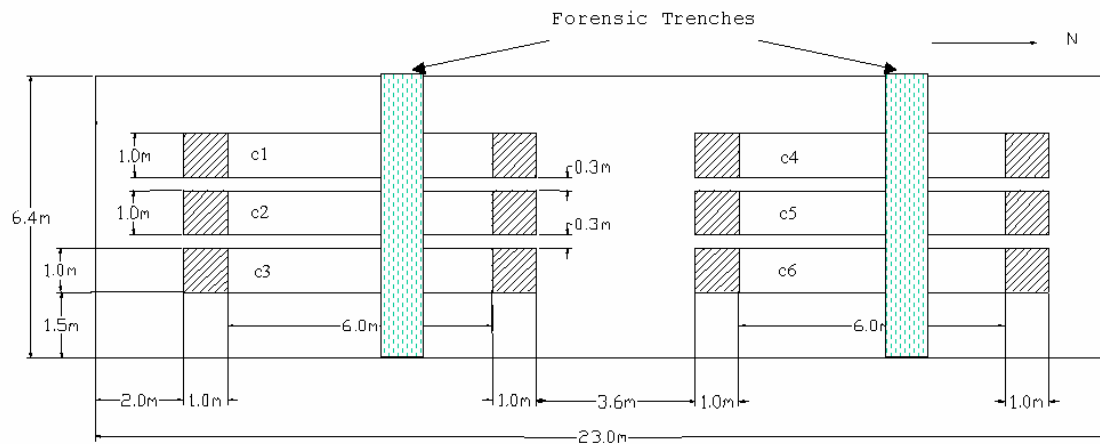
Figure 51. Location of the forensic trenches in Test Section 712

Figure 52 shows a view of the test section at the end of traffic. The distress mode in all the test windows in this test section were limited to smooth rutting. No other form of distress (cracking, delamination, shoving, etc.) was observed. Test window 712c4 was traffic tested first.

50

Figure 52. View of test section at the end of traffic tests.

       Moisture and density measurements were conducted inside the trenches in the base course and in the upper subgrade down to a depth of 0.91 m (3 ft.) below the top of the asphalt concrete. Figure 53 and 56 show the gravimetric moisture contents in the south and north trenches respectively. The measured values are consistent with those obtained during the construction. Figures 57 and 60 show density measurements for the south and north trenches at each test window and also at locations outside the traffic areas at the east and west sides of the test windows. Most measured values are above 90 percent of modified Proctor density.
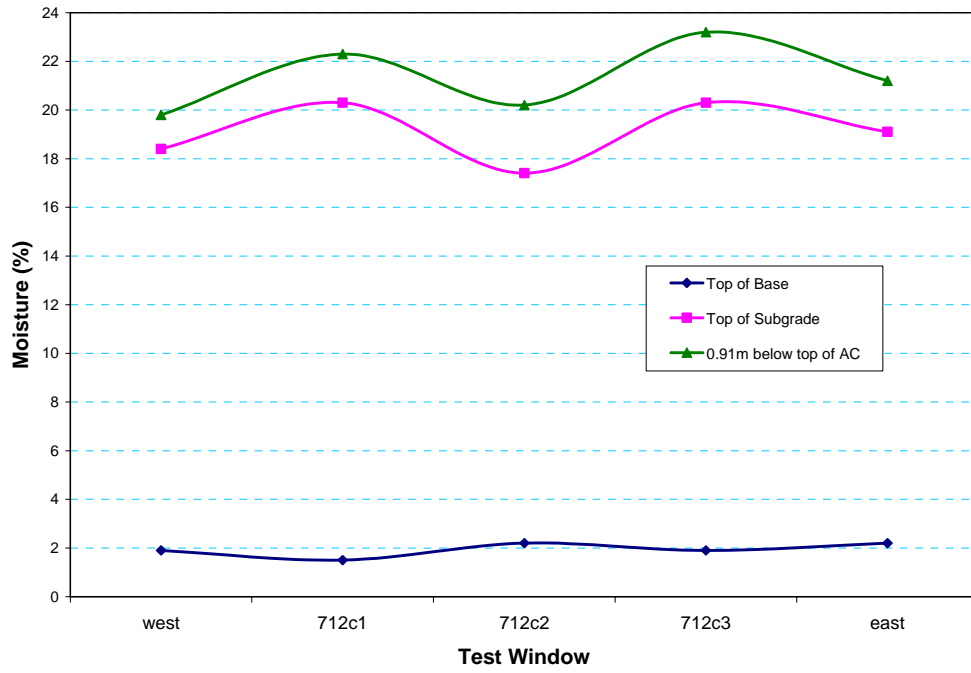
Figure 53. Moisture content in the base and upper subgrade in the south trench.
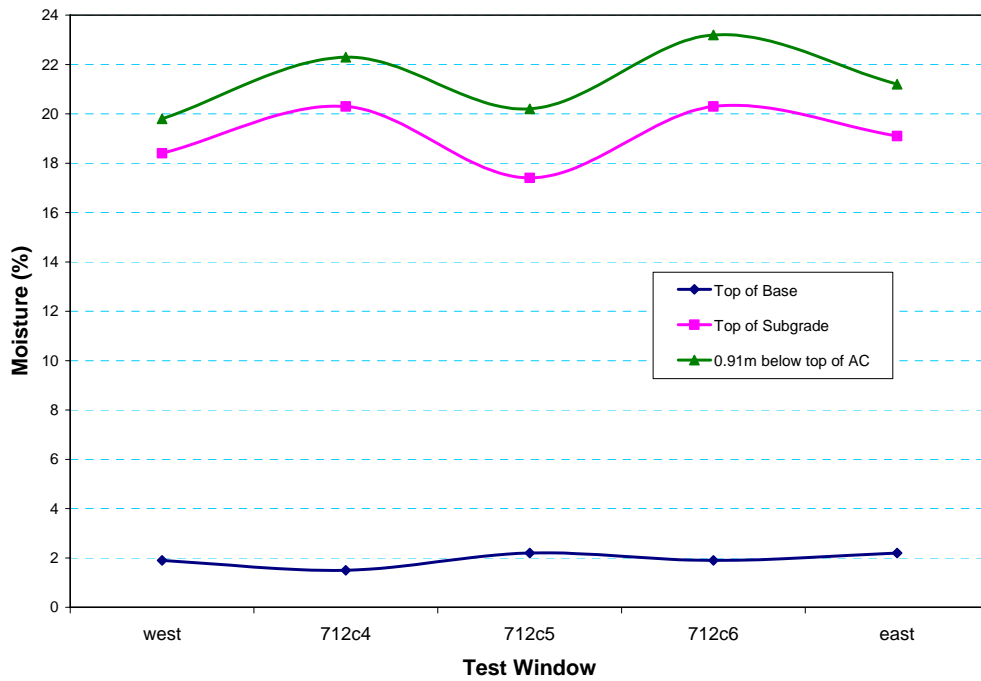
Figure 54. Moisture content in the base and upper subgrade in the north trench.
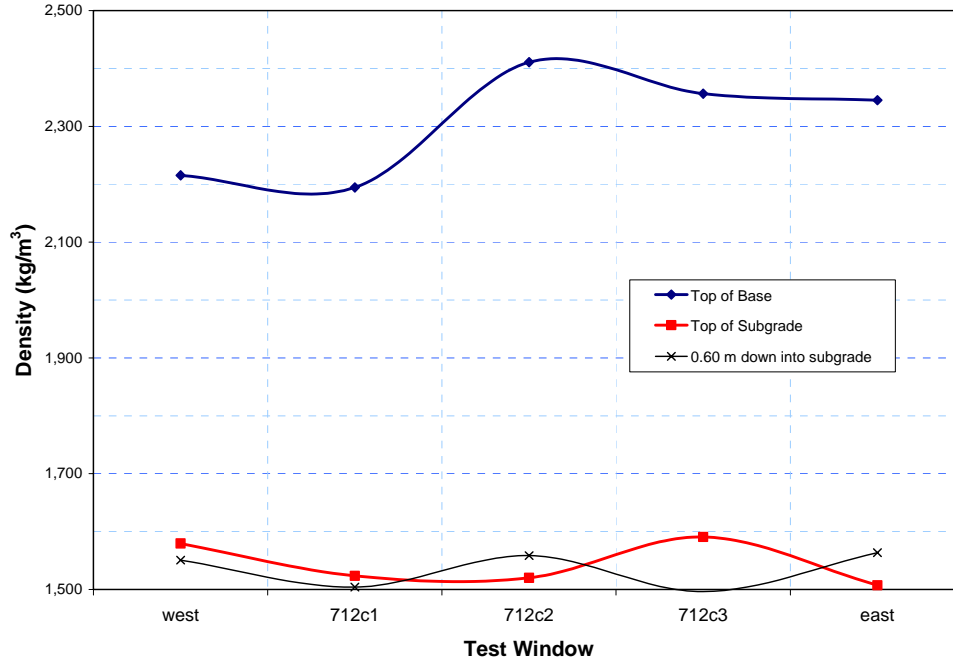
Figure 55. Density measurements in the base and upper subgrade in the south trench.
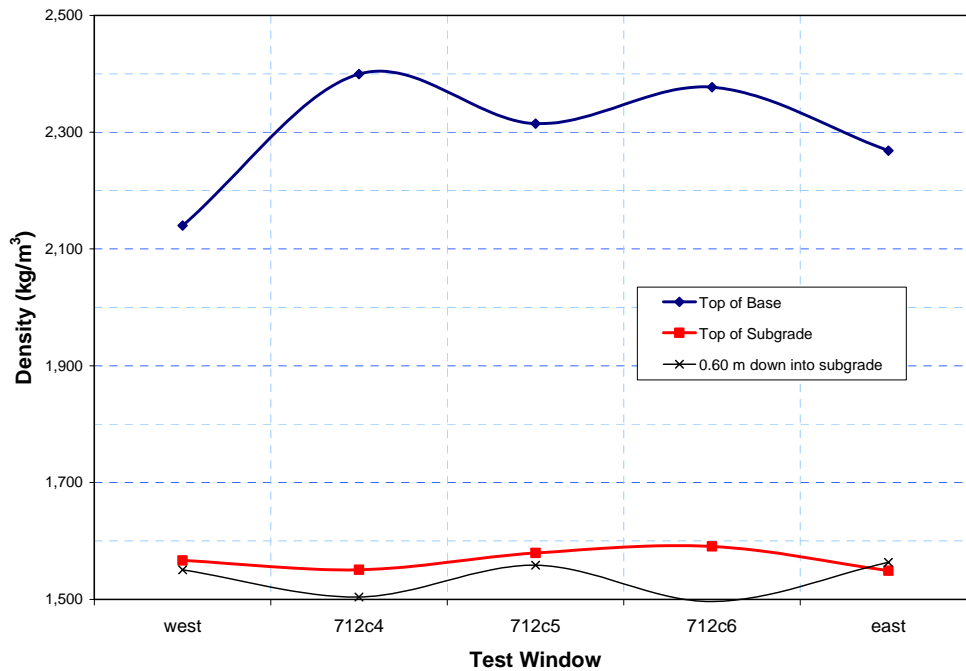
Figure 56. Density measurements in the base and upper subgrade in the north trench.

Asphalt and base course layer thickness measurements for each test window are presented in Figures 57 through 62. In Test Window 712c1 the asphalt thickness was approximately as thick as intended. The average base course was also very close to its design value of 229 mm (9 in.).

The average asphalt thickness and the base thickness in Test Window 712c2 were also very close to the target values.

In Test Window 712c3, the asphalt thickness was at the target value, but the base course was slightly thinner than intended.

In Test Window 712c4 the asphalt and base thicknesses were thicker than intended on opposite sides relative to the center line. These differences must be considered in the data analysis.

In Test Window 712c5 the average asphalt and base course thicknesses were slightly thicker than intended.

In Test Window 712c6 the average asphalt thickness was thicker than intended, but the base course was 25 mm (1 in.) thinner than intended at the center of the test window.
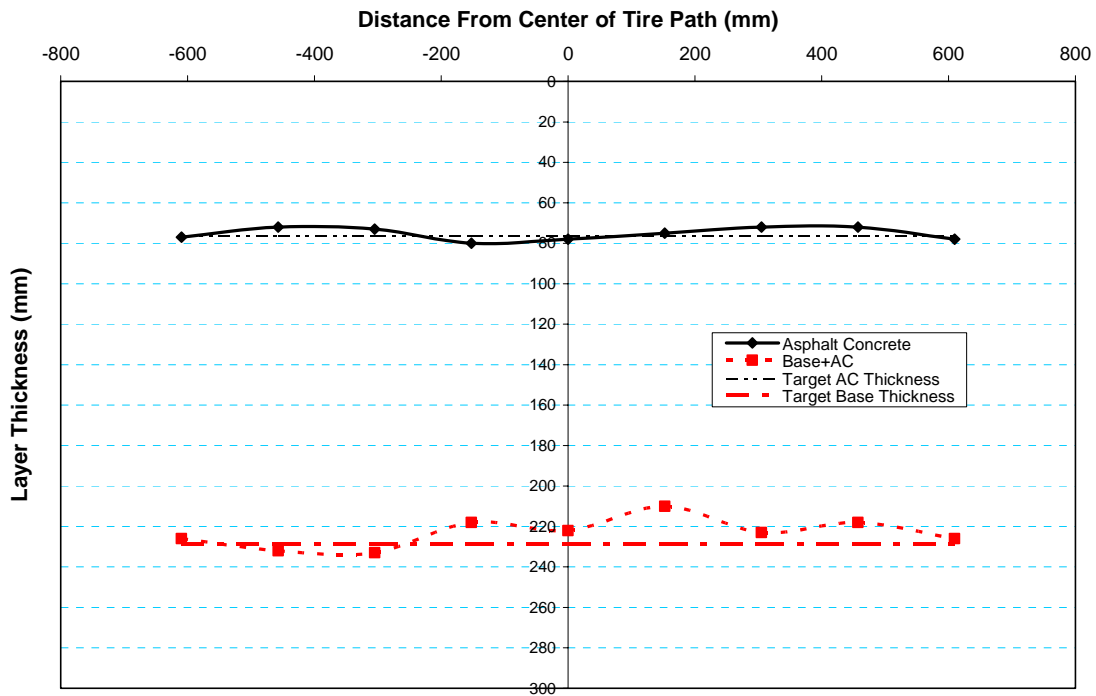
Figure 57. Layer thickness measurements across Test Window C1.

54

Test Section 712 AASHTO A-7-5 subgrade soil at 20 percent (optimum) moisture content.
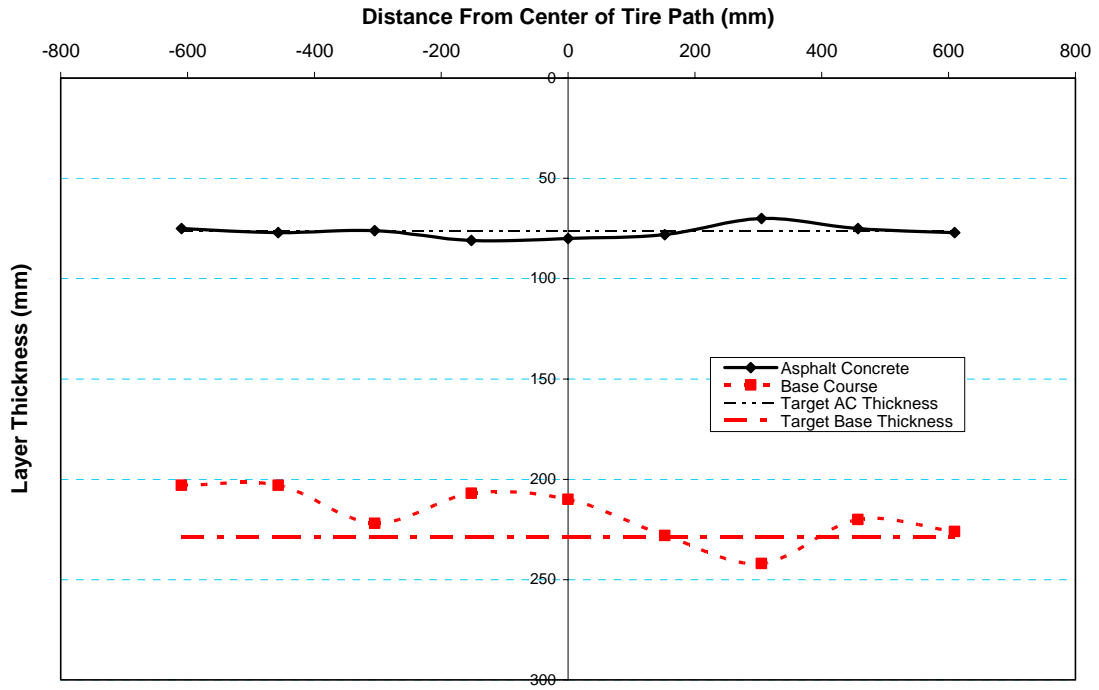
Figure 58. Layer thickness measurements across Test Window C2.
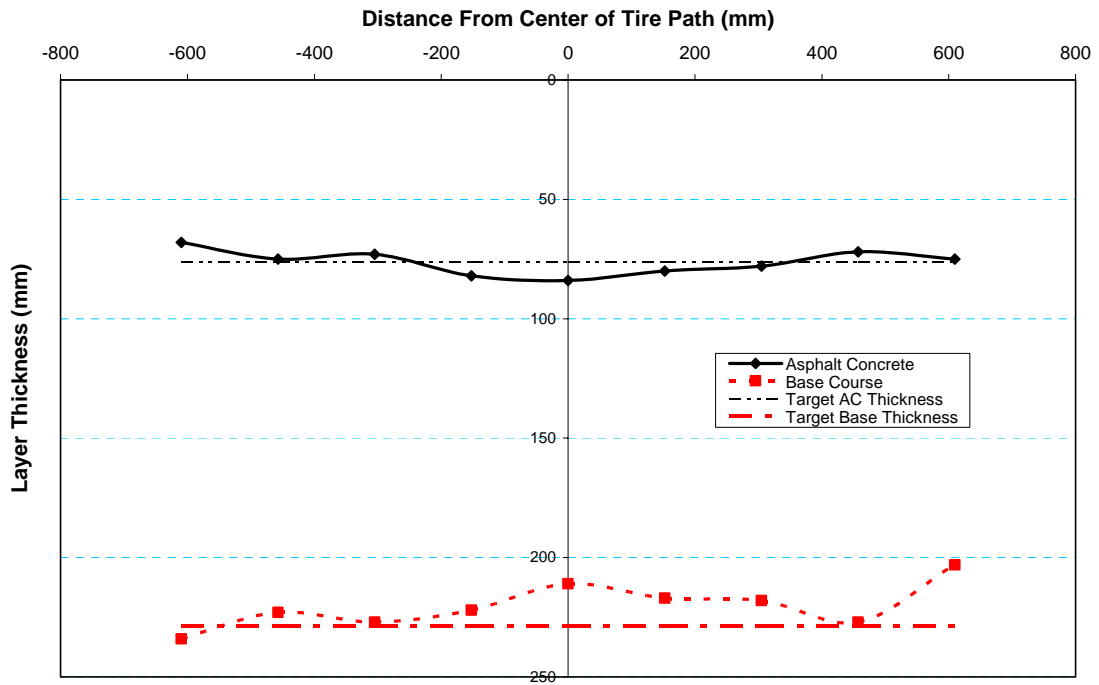
Figure 59. Layer thickness measurements across Test Window C3.

Test Section 712 AASHTO A-7-5 subgrade soil at 20 percent (optimum) moisture content.
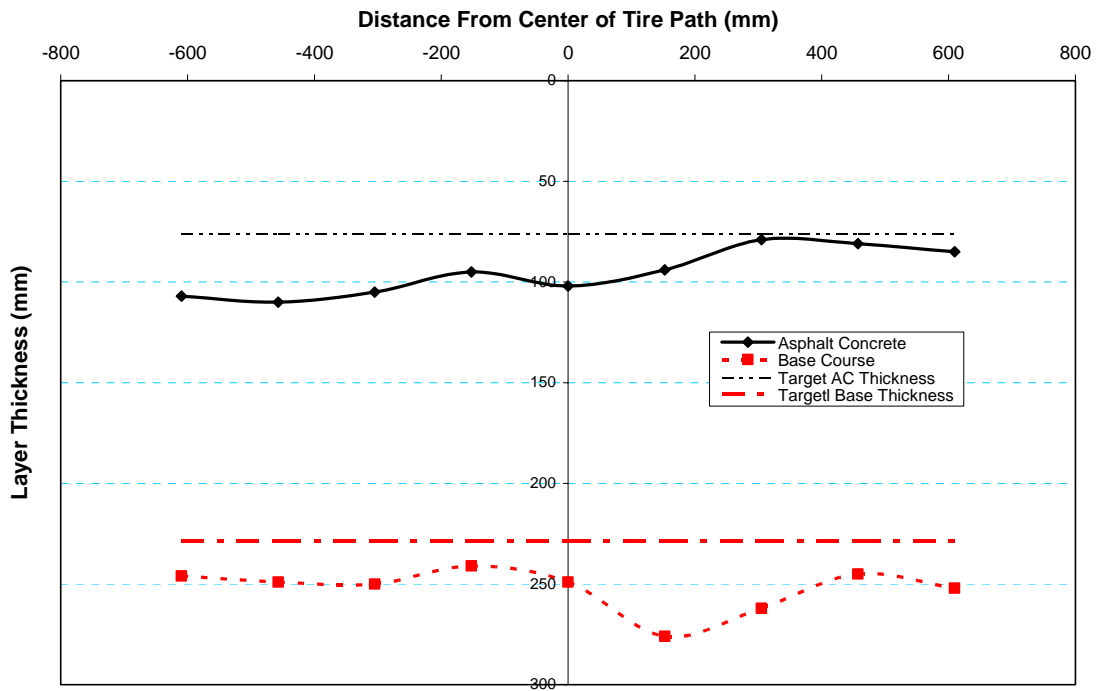
Figure 60. Layer thickness measurements across Test Window C4.
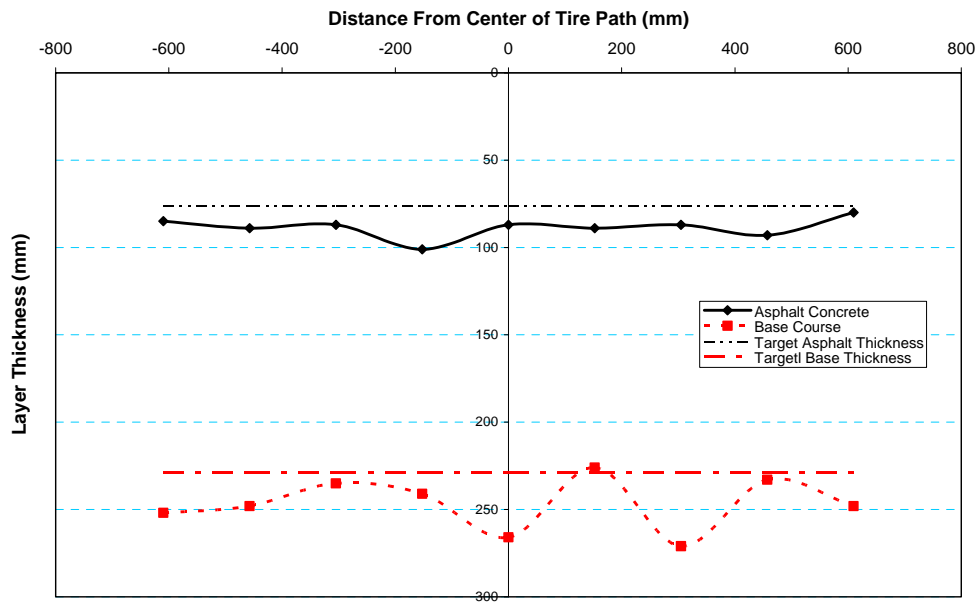
Figure 61. Layer thickness measurements across Test Window C5.
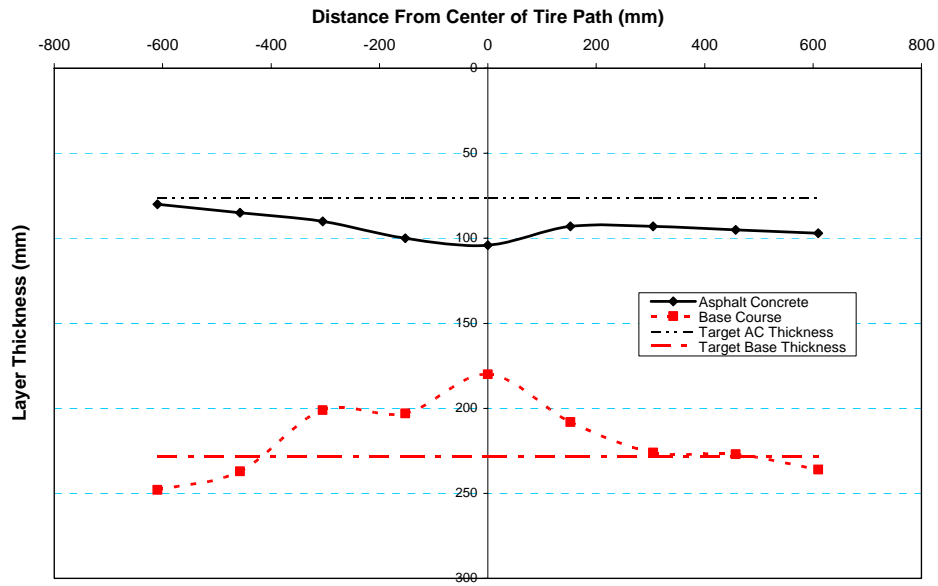
Figure 62. Layer thickness measurements across Test Window C6.

Dynamic cone penetrometer (DCP) measurements were conducted from the top of the subgrade down to a depth of at least 0.61 m (2 ft.). Figures 63 through 68 show profiles of CBR values obtained through DCP-CBR correlations. The average subgrade CBR value was 16 percent. According to Figure 19, this corresponds to a resilient modulus of 103 MPa (14,939 psi).
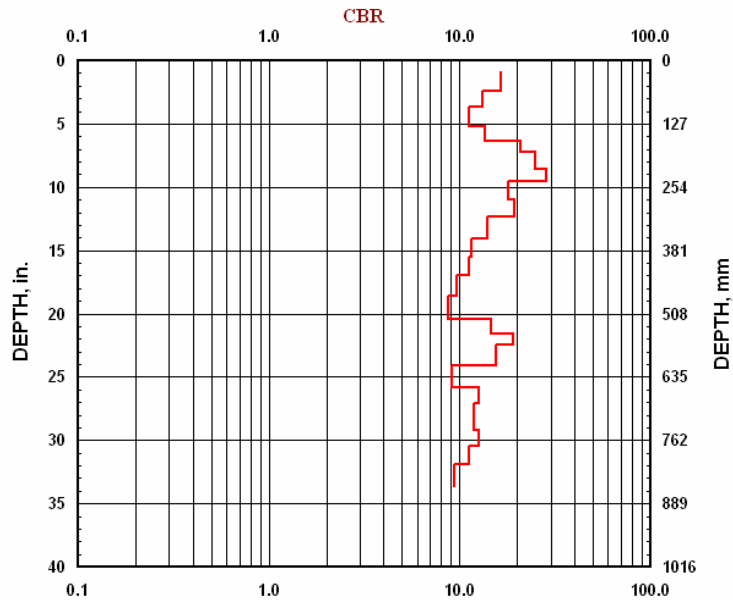
Figure 63. Subgrade CBR in Test Window C1.

57

Test Section 712 AASHTO A-7-5 subgrade soil at 20 percent (optimum) moisture content.
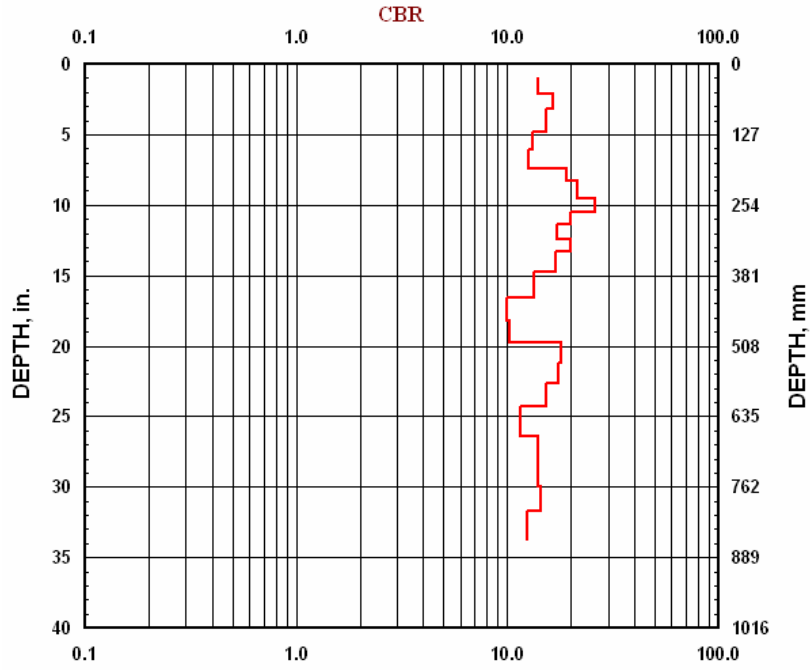
Figure 64. Subgrade CBR in Test Window C2.
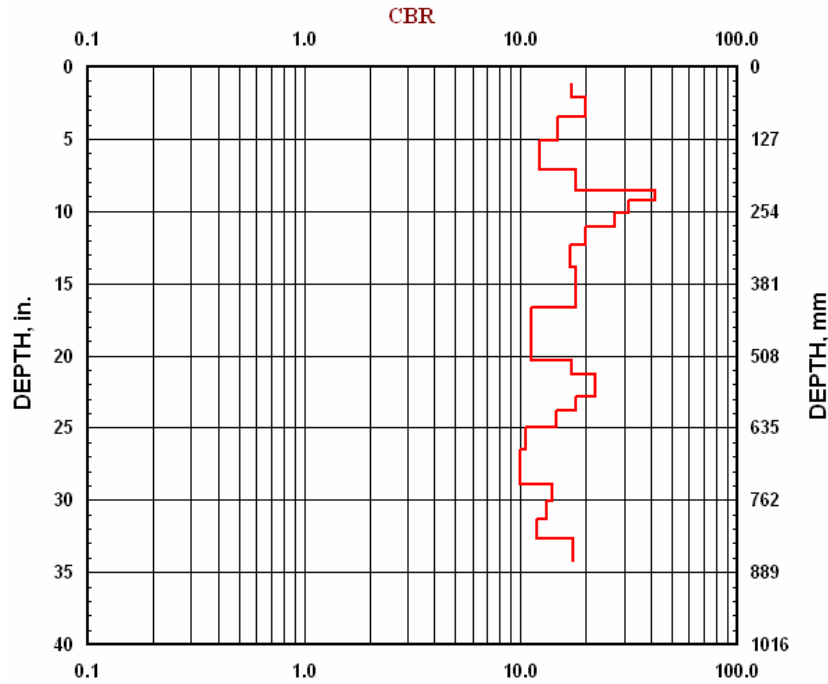
Figure 65. Subgrade CBR in Test Window C3.

Test Section 712 AASHTO A-7-5 subgrade soil at 20 percent (optimum) moisture content.
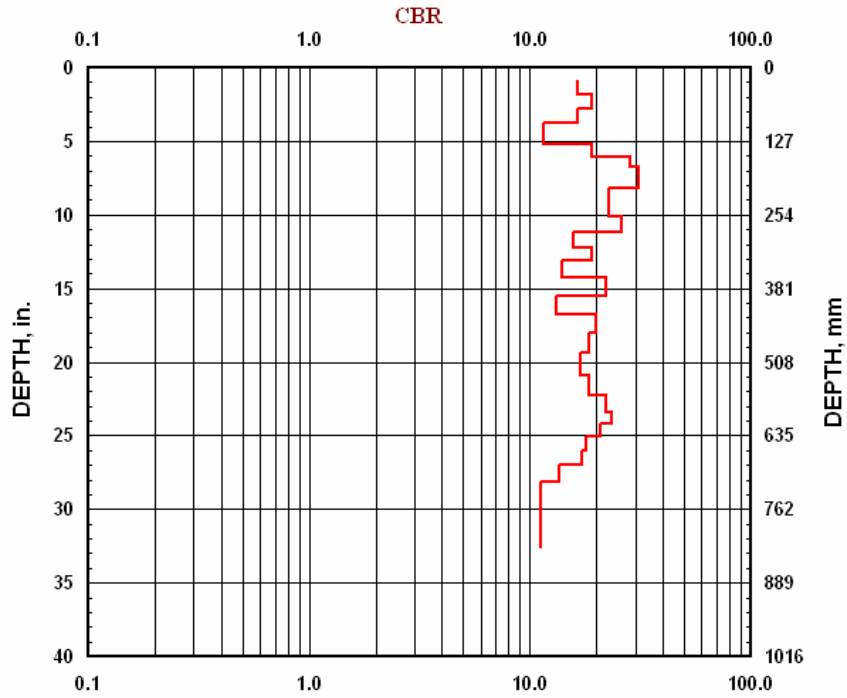
Figure 66. Subgrade CBR in Test Window C4.
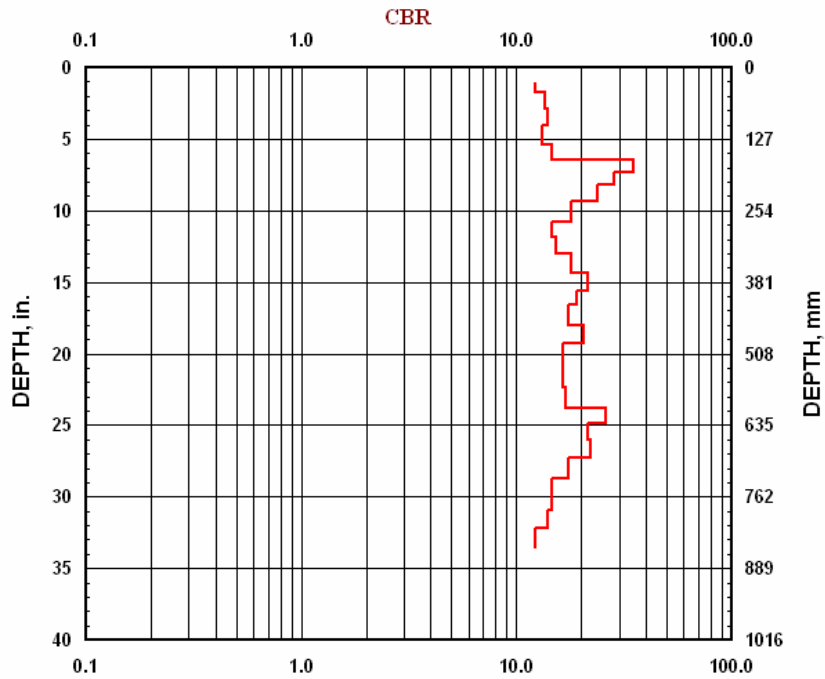
Figure 67. Subgrade CBR in Test Window C5.

59

Test Section 712 AASHTO A-7-5 subgrade soil at 20 percent (optimum) moisture content.
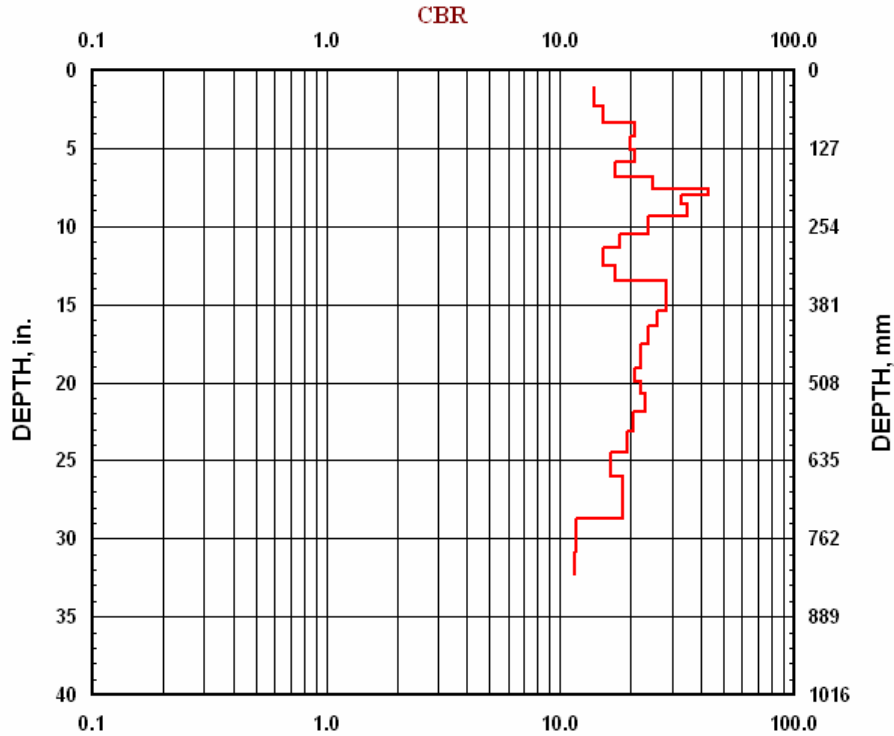
Figure 68. Subgrade CBR in Test Window C6.

SUMMARY AND CONCLUSIONS

Accelerated pavement testing (APT) was conducted on a test section with a subgrade soil that was classified as AASHTO type A-7-5 (USCS type MH). The as-built gravimetric moisture content of the subgrade soil in Test Section 712 was 20 percent. The modified Proctor optimum moisture content was 20.5 percent. Laboratory test results presented in Figure 3 show that this subgrade soil at 20 percent moisture content has a CBR of 53 percent. Figure 17 shows that resilient modulus (M_r) for a CBR value of 53 percent is 220.6 MPa (32 ksi). This value is consistent with the DCP measurements conducted in the subgrade during the forensic evaluation. Therefore, at this moisture condition, this is a relatively strong subgrade soil. However, during the construction of the test section, it was observed that, for this soil, past a threshold, even small increases of moisture can render the soil weak, unstable and unworkable as shown in Figure 19.

The test section was instrumented with stress, strain, temperature and moisture sensors. Traffic was applied by means of CRREL's Heavy Vehicle Simulator (HVS). All test windows were built equally in terms of materials and geometry, but the traffic load intensity was varied from test window to test window. However, the traffic load was kept constant throughout the traffic test for a particular test window. The test loads varied between 40 to 93.4-kN (9 to 21 kips). The load was applied by means of a standard dual truck tire assembly that constitutes half of a truck axle. Therefore, for example, 40 kN (9

60

kips) is equivalent to a full axial load of 80 kN (18 kips). The tire pressure was kept constant at 690-kPa (100 psi). Traffic speed was also kept constant at 12 km/hour (7.46 miles/hour) for all test windows. Traffic was evenly wandered within a strip 0.91 m (3 ft) wide. Because the experiments were conducted indoors, the ambient and pavement temperatures were practically constant throughout the test period. The average ambient temperature was 20 ºC (68ºF). Soil moisture was also kept practically constant because the base and subgrade soils were enclosed in a space limited by very low permeability materials. The bottom and sides of the test section were made of portland cement concrete, and the top surface was made of asphalt concrete. Aside for vapor diffusion, the pavement was practically a sealed system for soil moisture. At various stages during the accelerated pavement testing (APT), dynamic stresses, resilient strain, permanent strains, and surface rut depth measurements were collected for each test window. Arrays of sensors were embedded in each test window to measure vertical, longitudinal and transverse components of stress and strain at critical locations. Transverse profiles on top of the asphalt concrete were taken by means of a laser profilometer. Surface deformation profiles were produced by subtracting corresponding profiles at various pass levels to a baseline profile taken before traffic began. Surface rut progressions with traffic repetitions are presented in Figures 26 through 31. Subsurface deformation and stress data from sensors embedded in the pavement are presented in Figures 33 through 50.

The asphalt concrete surface displayed surface rutting, but no crack or other mode of deterioration was identified in any of the test windows. The relatively strong subgrade soil may have contributed to the good asphalt performance. Delamination and cracking were observed in similar test sections built with softer subgrade soils.

Figure 46 shows the resilient strain at the top of the subgrade at failure for all the subgrade soils included in this study. The existing subgrade failure criteria established by the Asphalt Institute and the Shell corporation are also graphed for comparison. It can be seen that the resilient behavior of the subgrade soil A-2-4 is consistent with the two established criteria, but significant differences occur for other soils. The data suggests that subgrade resilient strain criteria must be tailored to soil type. Figure 46 also shows that the AASHTO type A-2-4 soil is significantly less susceptive to moisture content than the other soil types. Subgrade soil AASHTO type A-4 is most susceptible to moisture variations. This is a silty soil, and therefore, it is also most susceptible to frost heaving and spring thaw weakening. Unfortunately, this is also the most abundant subgrade soil type found in the United States and in the world (Rollings, R., 2004).

As explained above, our experiments were conducted at constant speed of 12 km/hour (7.46 miles/hour). In order to compare with these results to those from the AASHO Road tests, where the test speed was 48 km/hr, a reduction factor of 0.63 was applied to the strain data. This correction factor was based on results from experiments at the MnRoad experimental facility (Dai and Van Deusen, 1998). In order to compare to our data to that of a reference highway speed of 88 km/hour (55 miles/hour), a reduction factor of 0.48 would be needed.

Test Section 712 is the last of a set of 12 test sections included in this study. A database containing a summary of the experimental data is available. Analyses of the experimental data and of subgrade performance models are presented in a project Final Report. This effort is in support to the new AASHTO Mechanistic-Empirical Pavement Design Guide.

REFERENCE

Dai, S.T., D.Van Deusen, D.Rettner and G.Cochran. "Investigation of Flexible Pavement Response to Truck Speed and FWD Load Through Instrumented Pavements", Proceedings of the 8th International Conference on Flexible Pavements. Seattle, Washington, pp.141-160. 1997.

Hilderbrand, G. and L. Irwin, "Theoretical Analysis of Pavement Test Sections in the FERF", Internal Report, 1994.

Janoo, V., L. Irwin, R. Eaton, and R. Haehnel, "Pavement Subgrade Performance Study: Project Overview, ERDC Report TR15, 2002.

APPENDIX A

SURFACE PROFILE TEST RESULTS

Test Section 712 AASHTO A-7-5 subgrade soil at 20 percent (optimum) moisture content.

Table A1. Surface rut measurements in 712C1

Cross Section	Rut Depth (mm)						
	Pass Number						
	0	250	1,000	10,000	100,000	110,000	300,000
1	0.0	-2.8	-3.2	-5.5	-8.0	-8.5	-9.7
2	0.0	-1.6	-1.9	-4.1	-6.6	-6.6	-7.8
3	0.0	-1.5	-2.4	-4.3	-6.9	-6.5	-7.5
4	0.0	-1.9	-2.6	-4.1	-6.3	-7.2	-7.7
5	0.0	-1.9	-2.3	-3.7	-6.2	-6.3	-8.0
6	0.0	-2.7	-3.9	-6.7	-11.0	-11.6	-13.9
7	0.0	-2.3	-3.3	-6.1	-9.3	-10.4	-11.6
8	0.0	-1.3	-2.5	-3.5	-5.9	-6.0	-6.7
9	0.0	-1.4	-2.3	-3.4	-5.5	-6.5	-7.4
10	0.0	-1.4	-2.1	-3.5	-5.6	-5.9	-7.6
11	0.0	-1.7	-2.7	-3.9	-6.7	-6.7	-8.1
12	0.0	-1.9	-2.4	-3.9	-6.5	-6.9	-8.7
13	0.0	-1.4	-1.8	-3.9	-6.1	-6.7	-7.9
14	0.0	-1.3	-1.9	-3.1	-5.6	-6.0	-6.9
15	0.0	-1.4	-1.9	-3.2	-5.3	-6.7	-7.0
16	0.0	-0.8	-1.3	-2.9	-5.1	-5.5	-6.6
17	0.0	-1.6	-2.1	-3.9	-6.3	-6.9	-8.1
18	0.0	-2.1	-2.8	-4.3	-7.0	-7.1	-8.5
19	0.0	-1.7	-2.4	-3.7	-6.2	-6.5	-7.7
20	0.0	-1.3	-1.9	-3.2	-5.2	-5.8	-7.1

Test Section 712 AASHTO A-7-5 subgrade soil at 20 percent (optimum) moisture content.

Table A 2. Surface rut measurements in 710C2

Cross Section	Rut Depth (mm)							
	Pass Number							
	0	250	1000	5000	34000	65000	108000	168000
1	0.0	-1.8	-2.8	-4.5	-7.0	-8.3	-9.8	-10.8
2	0.0	-1.9	-3.1	-4.0	-6.1	-7.4	-8.5	-9.5
3	0.0	-1.9	-2.8	-3.5	-5.7	-6.7	-7.3	-8.5
4	0.0	-1.8	-2.3	-3.5	-5.7	-6.8	-8.0	-9.0
5	0.0	-2.1	-3.0	-4.2	-7.2	-8.7	-10.3	-11.6
6	0.0	-2.7	-4.1	-5.6	-9.7	-11.7	-13.3	-15.9
7	0.0	-3.1	-4.8	-7.7	-11.3	-13.5	-15.5	-16.9
8	0.0	-1.6	-2.9	-3.9	-5.5	-7.2	-8.3	-10.0
9	0.0	-2.0	-3.1	-3.2	-5.4	-7.0	-7.9	-9.0
10	0.0	-2.6	-3.1	-5.0	-9.0	-11.2	-12.3	-14.4
11	0.0	-2.1	-2.6	-3.6	-5.5	-6.4	-8.0	-9.3
12	0.0	-2.0	-2.7	-3.7	-5.7	-6.8	-8.2	-8.8
13	0.0	-1.8	-2.6	-4.2	-6.6	-9.1	-10.3	-11.8
14	0.0	-1.0	-2.0	-3.3	-4.7	-6.6	-7.3	-8.3
15	0.0	-2.1	-3.2	-4.8	-7.1	-8.9	-10.4	-11.5
16	0.0	-2.4	-3.6	-5.7	-8.8	-10.6	-12.6	-14.0
17	0.0	-1.8	-3.2	-5.2	-8.4	-10.1	-12.3	-13.3
18	0.0	-1.8	-2.3	-3.9	-5.7	-7.0	-8.5	-9.3
19	0.0	-1.3	-1.9	-3.5	-4.9	-6.1	-7.1	-7.9
20	0.0	-1.6	-2.2	-3.5	-5.5	-6.2	-7.6	-8.5

Test Section 712 AASHTO A-7-5 subgrade soil at 20 percent (optimum) moisture content.

Table A 3. Surface rut measurements in 712C3

Cross Section	Rut Depth (mm)						
	Pass Number						
	0	250	1000	10000	25000	50000	64000
1	0.0	-1.1	-2.5	-5.0	-5.5	-6.3	-6.3
2	0.0	-1.8	-2.4	-4.3	-5.4	-6.3	-6.4
3	0.0	-1.5	-2.3	-3.9	-5.3	-6.0	-6.1
4	0.0	-1.7	-2.7	-4.4	-5.5	-6.7	-6.6
5	0.0	-1.7	-2.6	-4.4	-5.3	-6.4	-6.5
6	0.0	-2.6	-4.0	-7.6	-9.2	-10.8	-11.3
7	0.0	-2.5	-3.8	-7.4	-8.9	-10.0	-10.5
8	0.0	-2.2	-2.4	-4.3	-5.2	-5.9	-6.2
9	0.0	-1.6	-2.3	-3.6	-4.5	-5.1	-5.3
10	0.0	-1.6	-2.2	-3.6	-4.5	-5.3	-5.7
11	0.0	-1.9	-2.3	-3.9	-4.3	-5.3	-5.7
12	0.0	-1.7	-2.1	-3.4	-3.9	-4.7	-5.0
13	0.0	-1.7	-2.2	-3.8	-4.5	-5.3	-5.3
14	0.0	-1.4	-2.0	-3.5	-4.3	-4.9	-5.2
15	0.0	-1.6	-2.1	-3.6	-4.4	-5.6	-5.9
16	0.0	-1.6	-2.5	-4.2	-5.0	-6.2	-6.6
17	0.0	-1.5	-1.9	-3.4	-4.5	-5.5	-5.7
18	0.0	-1.6	-2.3	-3.9	-5.0	-5.9	-6.2
19	0.0	-1.3	-2.2	-3.7	-4.6	-5.8	-6.2
20	0.0	-1.7	-2.4	-4.5	-5.6	-6.8	-7.3

Test Section 712 AASHTO A-7-5 subgrade soil at 20 percent (optimum) moisture content.

Table A 4. Surface rut measurements in 712C4

Test Window	kips	kN			
712C4	22.0	97.9			
			Pass Number		
Cross Section	0.1	250	1,000	47,087	147,200
1	0	0.9	2.3	8.7	8.9
2	0	1.0	1.9	3.2	7.2
3	0	1.8	2.8	5.7	8.8
4	0	1.6	2.5	5.3	7.2
5	0	2.0	2.0	7.1	9.3
6	0	2.9	4.4	9.7	14.8
7	0	2.6	4.2	12.5	15.8
8	0	1.8	1.7	5.4	7.3
9	0	2.7	2.7	5.4	6.8
10	0	4.2	3.8	8.1	10.5
11	0	1.2	2.6	3.9	8.5
12	0	1.4	1.4	3.7	7.9
13	0	3.5	2.1	6.1	9.8
14	0	2.8	2.2	5.9	8.5
15	0	1.5	3.0	5.4	8.8
16	0	2.4	2.2	6.3	8.6
17	0	2.9	1.9	5.4	8.9
18	0	1.1	1.9	5.9	7.6
19	0	1.0	1.8	4.3	7.7
20	0	1.5	1.9	6.5	9.3
Average	0	2.0	2.3	5.7	8.4

Test Section 712 AASHTO A-7-5 subgrade soil at 20 percent (optimum) moisture content.

Table A 5. Surface rut measurements in 712C5

Cross Section	Rut Depth (mm)						
	Pass Number						
	0	250	1000	25000	100000	294000	463000
1	0.0	-1.2	-1.5	-2.4	-2.9	-3.3	-3.6
2	0.0	-1.1	-1.6	-2.3	-3.0	-3.1	-3.5
3	0.0	-1.7	-1.7	-3.1	-3.7	-5.1	-5.1
4	0.0	-1.0	-1.5	-2.6	-3.2	-3.9	-4.4
5	0.0	-1.4	-1.6	-2.9	-3.4	-4.1	-4.5
6	0.0	-1.3	-1.8	-2.9	-3.8	-4.4	-5.0
7	0.0	-1.1	-1.8	-2.6	-4.2	-4.8	-5.5
8	0.0	-0.9	-1.2	-2.3	-2.6	-3.0	-3.9
9	0.0	-1.0	-1.2	-2.0	-2.5	-3.0	-3.2
10	0.0	-1.0	-1.1	-1.8	-2.5	-3.0	-3.2
11	0.0	-1.2	-1.4	-2.2	-2.5	-3.2	-3.1
12	0.0	-0.9	-0.9	-1.7	-2.4	-2.7	-3.0
13	0.0	-0.7	-0.9	-1.7	-2.2	-2.5	-3.1
14	0.0	-1.0	-1.0	-1.8	-2.4	-3.0	-3.1
15	0.0	-0.9	-1.2	-1.7	-2.3	-2.5	-2.9
16	0.0	-0.9	-1.1	-2.3	-2.9	-3.6	-3.5
17	0.0	-1.2	-1.0	-1.7	-1.9	-2.4	-2.9
18	0.0	-0.6	-0.7	-1.6	-1.8	-2.5	-2.9
19	0.0	-0.9	-1.0	-1.7	-2.0	-2.9	-3.1
20	0.0	-1.1	-1.2	-2.1	-2.3	-3.4	-3.2

Test Section 712 AASHTO A-7-5 subgrade soil at 20 percent (optimum) moisture content.

Table A 5. Surface rut measurements in 712C5

Test Window	kips	kN			
712C6	22.0	97.9			
			Pass Number		
Cross Section	0.1	250	1,000	100,000	121,300
1	0	2.5	3.3	9.1	10.0
2	0	2.3	3.5	11.1	11.8
3	0	2.7	4.5	13.7	14.5
4	0	2.8	4.2	12.1	13.1
5	0	4.2	6.2	16.5	17.5
6	0	4.2	6.1	16.2	17.6
7	0	3.3	4.9	14.7	15.3
8	0	2.4	3.9	12.6	13.4
9	0	2.3	3.2	10.7	11.9
10	0	2.2	3.0	10.4	11.1
11	0	2.4	3.1	10.6	11.6
12	0	2.3	3.5	9.9	10.6
13	0	1.9	3.4	12.0	12.8
14	0	2.6	4.0	13.0	13.6
15	0	2.1	2.6	8.5	9.1
16	0	2.0	2.3	7.3	8.2
17	0	1.8	2.1	5.4	8.0
18	0	1.8	2.2	6.0	7.7
19	0	2.1	2.4	6.0	9.1
20	0	1.8	4.9	5.5	10.3
Average	0.1	2.2	3.3	9.6	11.0

APPENDIX B

PERMANENT DEFORMATION

AND

PERMANENT STRAIN

TEST RESULTS

Test Section 712 AASHTO A-7-5 subgrade soil at 20 percent (optimum) moisture content.

Table B 1. Vertical permanent deformation (mm) in 712C1

Test Window	kips	kN						
712C1	18	80						

Layer	Depth	Traffic Passes						
	(mm)	0	250	1,000	10,000	100,000	110,000	300,000
AC	0-75	0	-0.34	-0.76	-1.25	-2.07	-2.23	-2.39
Base-Top	75-195	0	-0.59	-0.83	-1.91	-4.10	-4.22	-5.87
Base-Bottom	195-305	0	-0.51	-0.83	-1.96	-2.61	-2.82	-2.95
Subgrade-Top	305-455	0	-0.35	-0.47	-0.88	-1.24	-1.49	-1.35
Subgrade	455-615	0	-0.17	-0.23	-0.44	-0.56	-0.74	-0.67
Subgrade	615-755	0	-0.09	-0.12	-0.22	-0.37	-0.28	-0.34
Subgrade	755-925	0	-0.04	-0.06	-0.11	-0.19	-0.14	-0.17
Subgrade	925-1055	0	-0.02	-0.03	-0.05	-0.09	-0.07	-0.08
Subgrade	1055-1235	0	-0.01	-0.01	-0.03	-0.05	-0.04	-0.04
Subgrade	1235-1355	0	-0.01	-0.01	-0.01	-0.02	-0.02	-0.02
Subgrade	1355-1545	0	0.00	0.00	-0.01	-0.01	-0.01	-0.01
	Sum	0	-2.14	-3.34	-6.88	-11.32	-12.06	-13.90

Table B 2. Vertical permanent deformation (mm) in 712C2

Test Window	kips	kN						
712C2	20.0	89.0						

Layer	Depth	Traffic Passes						
	(mm)	0	250	1,000	5,000	34,000	65,000	108,000	168,000
AC	0-75	0	-0.06	-0.35	-0.53	-1.28	-1.79	-1.95	-2.17
Base-Top	75-195	0	-0.48	-0.99	-1.84	-3.48	-4.45	-5.23	-5.72
Base-Bottom	195-305	0	-0.16	-0.38	-0.64	-1.16	-1.51	-1.85	-2.15
Subgrade-Top	305-455	0	-0.50	-0.79	-0.95	-1.43	-1.59	-1.79	-1.98
Subgrade	455-615	0	-0.23	-0.39	-0.37	-0.60	-0.66	-0.72	-0.77
Subgrade	615-755	0	-0.14	-0.24	-0.24	-0.41	-0.43	-0.45	-0.49
Subgrade	755-925	0	-0.01	-0.22	-0.11	-0.26	-0.29	-0.30	-0.24
Subgrade	925-1055	0	-0.01	-0.11	-0.06	-0.13	-0.15	0.04	0.07
Subgrade	1055-1235	0	0.00	-0.05	-0.03	-0.07	-0.07	0.03	0.02
Subgrade	1235-1355	0	0.00	-0.03	-0.01	-0.03	-0.04	0.04	0.02
Subgrade	1355-1545	0	0.00	-0.01	-0.01	-0.02	-0.02	0.07	0.10
	Sum	0	-1.58	-3.57	-4.78	-8.86	-10.99	-12.11	-13.30

Test Section 712 AASHTO A-7-5 subgrade soil at 20 percent (optimum) moisture content.

Table B3. Vertical permanent deformation (mm) in 712C3

Test Window	kips	kN					
712C3	21.0	93.4					

Layer	Depth	Traffic Passes						
	(mm)	0	250	1,000	10,000	25,000	50,000	64,000
AC	0-75	0	-0.254	-0.381	-0.632	-0.943	-1.129	-1.190
Base-Top	75-195	0	-0.554	-1.240	-3.315	-4.284	-5.253	-5.569
Base-Bottom	195-305	0	-0.325	-0.688	-1.603	-1.965	-2.206	-2.326
Subgrade-Top	305-455	0	-0.315	-0.383	-0.628	-0.682	-0.901	-0.995
Subgrade	455-615	0	-0.190	-0.223	-0.372	-0.355	-0.479	-0.551
Subgrade	615-755	0	-0.102	-0.096	-0.184	-0.135	-0.210	-0.263
Subgrade	755-925	0	-0.124	-0.118	-0.211	-0.157	-0.156	-0.209
Subgrade	925-1055	0	-0.062	-0.059	-0.106	-0.079	-0.078	-0.105
Subgrade	1055-1235	0	-0.031	-0.029	-0.053	-0.039	-0.039	-0.052
Subgrade	1235-1355	0	-0.015	-0.015	-0.026	-0.020	-0.019	-0.026
Subgrade	1355-1545	0	-0.008	-0.007	-0.013	-0.010	-0.010	-0.013
Sum		0	-1.98	-3.24	-7.14	-8.67	-10.479	-11.30

Table B4. Vertical permanent deformation (mm) in 712C4

Test Window	kips	kN					
712C4	22.0	97.9					

Layer	Depth	Traffic Passes						
	(mm)	0	250	1,000	47,087	72,500	147,200	180,800
AC	0-75	0	-0.16	-0.44	-1.49	-1.59	-1.79	-1.94
Base-Top	75-195	0	-0.24	-0.74	-3.25	-3.53	-3.95	-4.07
Base-Bottom	195-305	0	-0.13	-0.37	-1.17	-1.29	-1.45	-1.51
Subgrade-Top	305-455	0	-0.08	-0.20	-0.57	-0.68	-0.77	-0.79
Subgrade	455-615	0	-0.04	-0.10	-0.29	-0.34	-0.38	-0.40
Subgrade	615-755	0	-0.02	-0.05	-0.14	-0.17	-0.19	-0.20
Subgrade	755-925	0	-0.01	-0.02	-0.07	-0.08	-0.10	-0.10
Subgrade	925-1055	0	-0.01	-0.01	-0.04	-0.04	-0.05	-0.05
Subgrade	1055-1235	0	0.00	-0.01	-0.02	-0.02	-0.02	-0.02
Subgrade	1235-1355	0	0.00	0.00	-0.01	-0.01	-0.01	-0.01
Subgrade	1355-1545	0	0.00	0.00	0.00	-0.01	-0.01	-0.01
Sum		0	-0.70	-1.93	-7.05	-7.75	-8.72	-9.10

Test Section 712 AASHTO A-7-5 subgrade soil at 20 percent (optimum) moisture content.

Table B5. Vertical permanent deformation (mm) in 712C5

Test Window	kips	kN
712C5	9.0	40.0

Layer	Depth	Traffic Passes						
	(mm)	0	250	1,000	25,000	100,000	294,000	463,000
AC	0-75	0	-0.28	-0.56	-1.24	-1.65	-2.32	-2.58
Base-Top	75-195	0	-0.20	-0.33	-0.49	-0.59	-0.89	-1.07
Base-Bottom	195-305	0	-0.08	-0.19	-0.26	-0.31	-0.50	-0.49
Subgrade-Top	305-455	0	0.01	-0.10	-0.12	-0.17	-0.40	-0.43
Subgrade	455-615	0	0.00	-0.05	-0.06	-0.09	-0.20	-0.22
Subgrade	615-755	0	0.00	-0.02	-0.03	-0.04	-0.10	-0.11
Subgrade	755-925	0	0.00	-0.01	-0.01	-0.02	-0.05	-0.05
Subgrade	925-1055	0	0.00	-0.01	-0.01	-0.01	-0.02	-0.03
Subgrade	1055-1235	0	0.00	0.00	0.00	-0.01	-0.01	-0.01
Subgrade	1235-1355	0	0.00	0.00	0.00	0.00	-0.01	-0.01
Subgrade	1355-1545	0	0.00	0.00	0.00	0.00	0.00	0.00
Sum		0	-0.54	-1.28	-2.23	-2.88	-4.50	-5.00

Table B6. Vertical permanent deformation (mm) in 712C6

Test Window	kips	kN
712C6	22.0	97.9

Layer	Depth	Traffic Passes				
	(mm)	0	250	10,000	100,000	121,300
AC	0-75	0	-0.28	-0.68	-3.19	-3.24
Base-Top	75-195	0	-0.70	-1.02	-3.97	-4.23
Base-Bottom	195-305	0	-0.40	-0.63	-1.18	-1.26
Subgrade-Top	305-455	0	-0.70	-0.88	-1.54	-1.59
Subgrade	455-615	0	-0.35	-0.49	-0.77	-0.80
Subgrade	615-755	0	-0.17	-0.29	-0.39	-0.40
Subgrade	755-925	0	-0.09	-0.15	-0.19	-0.20
Subgrade	925-1055	0	-0.04	-0.06	-0.10	-0.10
Subgrade	1055-1235	0	-0.02	-0.04	-0.05	-0.05
Subgrade	1235-1355	0	-0.01	-0.01	-0.02	-0.02
Subgrade	1355-1545	0	-0.01	-0.01	-0.01	-0.01
Sum		0	-2.77	-4.26	-11.41	-11.90

Test Section 712 AASHTO A-7-5 subgrade soil at 20 percent (optimum) moisture content.

Table B7. Vertical permanent strain (microstrains) in 712C1

Test Window	kips	kN					
712C1	18	80					

Layer	Depth	Traffic Passes						
	(mm)	0	250	1,000	10,000	100,000	110,000	300,000
AC	Surface	0	-3,451	-7,727	-12,804	-21,136	-22,784	-24,425
Base-Top	135	0	-5,185	-7,219	-16,749	-36,922	-35,852	-51,336
Base-Bottom	250	0	-4,498	-7,244	-17,143	-24,573	-22,901	-25,827
Subgrade-Top	380	0	-2,492	-3,358	-6,298	-10,644	-8,085	-9,653
Subgrade	535	0	-1,142	-1,539	-2,886	-4,878	-3,706	-4,424
Subgrade	685	0	-571	-770	-1,443	-2,439	-1,853	-2,212
Subgrade	840	0	-286	-385	-722	-1,220	-926	-1,106
Subgrade	990	0	-143	-192	-361	-610	-463	-553
Subgrade	1145	0	-71	-96	-180	-305	-232	-277
Subgrade	1295	0	-36	-48	-90	-152	-116	-138
Subgrade	1450	0	-18	-24	-45	-76	-58	-69

Table B8. Vertical permanent strain (microstrains) in 712C2

Test Window	kips	kN					
712C2	20	89					

Layer	Depth	Traffic Passes						
	(mm)	0	250	1,000	5,000	34,000	65,000	108,000	168,000
AC	Surface	0	-605	-3,614	-5,404	-13,043	-18,219	-19,925	-22,184
Base-Top	134	0	-4,172	-8,693	-16,088	-30,419	-38,936	-45,798	-50,082
Base-Bottom	248	0	-1,377	-3,367	-5,558	-10,122	-13,209	-16,162	-18,782
Subgrade-Top	381	0	-3,569	-5,663	-6,770	-10,271	-11,380	-12,831	-14,160
Subgrade	534	0	-1,519	-2,546	-2,413	-3,909	-4,301	-4,701	-5,048
Subgrade	686	0	-886	-1,591	-1,588	-2,688	-2,848	-2,981	-3,193
Subgrade	838	0	-67	-1,413	-742	-1,722	-1,927	-1,949	-1,566
Subgrade	991	0	-33	-707	-371	-861	-964	291	491
Subgrade	1143	0	-17	-353	-186	-430	-482	199	146
Subgrade	1296	0	-8	-177	-93	-215	-241	267	138
Subgrade	1448	0	-4	-88	-46	-108	-120	431	654

Test Section 712 AASHTO A-7-5 subgrade soil at 20 percent (optimum) moisture content.

Table B9. Vertical permanent strais (microstrains) in 712C3

Test Window	kips	kN						
712C3	21.0	93.4						
Layer	Depth	Traffic Passes						
	(mm)	0	250	1,000	10,000	25,000	50,000	64,000
AC	Surface	0	-2,594	-3,884	-6,448	-9,626	-11,519	-12,147
Base-Top	133	0	-4,847	-10,849	-29,006	-37,483	-45,955	-48,724
Base-Bottom	248	0	-2,841	-6,023	-14,025	-17,190	-19,296	-20,348
Subgrade-Top	381	0	-2,256	-2,740	-4,498	-4,880	-6,447	-7,124
Subgrade	533	0	-1,250	-1,462	-2,439	-2,326	-3,145	-3,616
Subgrade	686	0	-667	-631	-1,210	-887	-1,379	-1,727
Subgrade	838	0	-811	-774	-1,387	-1,032	-1,022	-1,372
Subgrade	991	0	-405	-387	-693	-516	-511	-686
Subgrade	1143	0	-203	-193	-347	-258	-256	-343
Subgrade	1295	0	-101	-97	-173	-129	-128	-172
Subgrade	1448	0	-51	-48	-87	-65	-64	-86

Table B10. Vertical permanent strain (microstrains) in 712C4

Test Window	kips	kN						
712C4	22.0	97.9						
Layer	Depth	Traffic Passes						
	(mm)	0	250	1,000	47,087	72,500	147,200	180,800
AC	Surface	0	-2,155	-5,710	-19,494	-20,836	-23,499	-25,481
Base-Top	133	0	-2,111	-6,403	-28,237	-30,719	-34,305	-35,357
Base-Bottom	248	0	-1,118	-3,187	-10,166	-11,189	-12,640	-13,149
Subgrade-Top	381	0	-726	-1,729	-4,992	-5,881	-6,692	-6,897
Subgrade	533	0	-363	-865	-2,496	-2,940	-3,346	-3,449
Subgrade	686	0	-182	-432	-1,248	-1,470	-1,673	-1,724
Subgrade	838	0	-91	-216	-624	-735	-837	-862
Subgrade	991	0	-45	-108	-312	-368	-418	-431
Subgrade	1143	0	-23	-54	-156	-184	-209	-216
Subgrade	1295	0	-11	-27	-78	-92	-105	-108
Subgrade	1448	0	-6	-14	-39	-46	-52	-54

Table B11. Vertical permanent strain (microstrains) in 712C5

Test Window	kips	kN
712C5	9	40

Layer	Depth	Traffic Passes						
	(mm)	0	250	1,000	25,000	100,000	294,000	463,000
AC	Surface	0	-3,662	-7,300	-16,294	-21,622	-30,390	-33,860
Base-Top	134	0	-1,697	-2,899	-4,240	-5,098	-7,775	-9,295
Base-Bottom	248	0	-700	-1,647	-2,301	-2,669	-4,340	-4,224
Subgrade-Top	381	0	52	-860	-1,038	-1,486	-3,437	-3,777
Subgrade	534	0	26	-430	-519	-743	-1,718	-1,888
Subgrade	686	0	13	-215	-259	-372	-859	-944
Subgrade	838	0	6	-108	-130	-186	-430	-472
Subgrade	991	0	3	-54	-65	-93	-215	-236
Subgrade	1143	0	2	-27	-32	-46	-107	-118
Subgrade	1296	0	1	-13	-16	-23	-54	-59
Subgrade	1448	0	0	-7	-8	-12	-27	-30

Table B12. Vertical permanent strain (microstrains) in 712C6

Test Window	kips	kN
712C6	22.0	97.9

Layer	Depth	Traffic Passes				
	(mm)	0	250	10,000	100,000	121,300
AC	Surface	0	-3,700	-3,700	-41,840	-42,494
Base-Top	133	0	-6,108	-7,089	-34,550	-36,772
Base-Bottom	248	0	-3,455	-2,897	-10,264	-10,922
Subgrade-Top	381	0	-6,054	-3,263	-13,413	-13,868
Subgrade	533	0	-3,027	-1,631	-6,707	-6,934
Subgrade	686	0	-1,513	-816	-3,353	-3,467
Subgrade	838	0	-757	-408	-1,677	-1,734
Subgrade	991	0	-378	-204	-838	-867
Subgrade	1143	0	-189	-102	-419	-433
Subgrade	1295	0	-95	-51	-210	-217
Subgrade	1448	0	-47	-25	-105	-108

APPENDIX C

RESILIENT STRAIN

TEST RESULTS

Test Section 712 AASHTO A-7-5 subgrade soil at 20 percent (optimum) moisture content.

Table C 1. Resilient vertical strain (microstrains) in 712c1

Test Window	kips	kN					
712C1	18	80					

Layer	Depth	Traffic Passes					
	(mm)	0.1	1,000	10,000	100,000	110,000	300000
Base-Top	135	-7,489	-7,287	-8,378	-9,380	-9,190	-9,432
Base-Bottom	250	-4,524	-5,084	-5,544	-5,416	-5,230	-5,949
Subgrade-Top	380	-3,029	-3,077	-3,501	-3,874	-3,648	-3,645
Subgrade	535	-874	-1,440	-1,554	-1,958	-1,799	-1,816
Subgrade	685	-1,862	-1,794	-1,936	-2,049	-1,880	-1,931
Subgrade	840	-571	-565	-599	-574	-591	-607
Subgrade	990	-355	-356	-131	-458	-356	-395
Subgrade	1145	-139	-111	-146	-126	-126	-175
Subgrade	1295	-17	-22	11	13	-11	-1
Subgrade	1450	-239	-204	-221	-247	-232	-271

Table C 2. Resilient vertical strain (microstrains) in 712c2

Test Window	kips	kN						
712C2	20	89						

Layer	Depth	Traffic Passes						
	(mm)	0.1	250	1,000	5,000	34,000	65,000	108,000	168,000
Base-Top	135	-5,661	-5,708	-5,720	-5,992	-7,313	-7,617	-7,002	-6,969
Base-Bottom	250	-4,465	-4,387	-4,268	-4,447	-4,994	-5,289	-4,956	-5,011
Subgrade-Top	380	-2,602	-2,926	-3,175	-3,276	-3,982	-4,106	-4,050	-4,051
Subgrade	535	-3,128	-3,382	-3,641	-3,550	-4,327	-4,497	-4,666	-4,767
Subgrade	685	-1,645	-1,646	-1,777	-1,771	-1,949	-2,056	-2,090	-2,072
Subgrade	840	-707	-796	-761	-709	-842	-859	-894	-895
Subgrade	990	-301	-406	-439	-425	-443	-432	-503	-470
Subgrade	1145	-226	-219	-243	-222	-241	-273	-255	-262
Subgrade	1295	-151	-206	-213	-251	-202	-216	-154	-234
Subgrade	1450	-88	14	-135	-84	-138	-187	-55	-161

Test Section 712 AASHTO A-7-5 subgrade soil at 20 percent (optimum) moisture content.

Table C 3. Resilient vertical strain (microstrains) in 712c3

Test Window	kips	kN					
712C3	21.0	93.4					
Layer	Depth	Traffic Passes					
	(mm)	0.1	250	1,000	10,000	25,000	50,000	64,000
Base-Top	135	-6,794	-7,339	-8,089	-9,500	-9,952	-9,689	-10,058
Base-Bottom	250	-5,061	-6,088	-6,737	-7,232	-6,643	-5,667	-6,078
Subgrade-Top	380	-2,613	-2,842	-2,989	-3,324	-3,538	-3,153	-3,534
Subgrade	535	-2,656	-2,787	-2,936	-3,260	-3,427	-3,218	-3,227
Subgrade	685	-1,468	-1,533	-1,567	-1,638	-1,685	-1,626	-1,716
Subgrade	840	-656	-689	-692	-722	-716	-680	-728
Subgrade	990	-379	-397	-388	-431	-421	-386	-434
Subgrade	1145	-193	-192	-191	-201	-190	-212	-202
Subgrade	1295	-358	-396	-344	-337	-323	-466	-468
Subgrade	1450	0	-33	-72	56	37	-52	70

Table C 4. Resilient vertical strain (microstrains) in 712c4

Test Window	kips	kN					
712C4	22.0	97.9					
Layer	Depth	Traffic Passes					
	(mm)	0	250	1,000	47,087	72,500	147,200	180,800
Base-Top	135	8342	9,178	10,493	12,426	12,301	13,407	12,662
Base-Bottom	250	3178	3,380	3,519	3,544	3,561	3,606	3,576
Subgrade-Top	380	2942	3,091	3,314	3,964	3,891	3,863	3,692
Subgrade	535	1597	1,714	1,833	2,180	2,212	2,251	2,200
Subgrade	685	2162	2,194	2,251	2,422	2,428	2,443	2,397
Subgrade	840	718	701	740	795	803	793	839
Subgrade	990	777	798	832	915	917	901	889
Subgrade	1145	198	180	206	201	192	207	266
Subgrade	1295	-5	-11	-6	-1	-9	-13	-7

Test Section 712 AASHTO A-7-5 subgrade soil at 20 percent (optimum) moisture content.

Table C 5. Resilient vertical strain (microstrains) in 712c5

Test Window	kips	kN						
712C5	9	40						
Layer	Depth	Traffic Passes						
	(mm)	0.1	250	1,000	25,000	100,000	294,000	463,000
Base-Top	135	-4,452	-4,251	-4,162	-4,311	-4,495	-4,893	-5,292
Base-Bottom	250	-2,577	-2,579	-2,546	-2,615	-2,622	-2,812	-2,841
Subgrade-Top	380	-1,303	-1,216	-1,162	-1,208	-1,398	-1,406	-1,390
Subgrade	535	-761	-746	-778	-759	-737	-871	-885
Subgrade	685	-752	-761	-630	-665	-672	-836	-811
Subgrade	840	-187	-197	-90	-185	-100	-49	-181
Subgrade	990	-195	-196	-213	-201	-204	-227	-210
Subgrade	1145	28	26	29	35	29	35	34
Subgrade	1295	-153	-153	-156	-156	-179	-147	-152
Subgrade	1450	-68	-44	-65	-42	-50	28	-36

Table C 6. Resilient vertical strais (microstrains) in 712c6

Test Window	kips	kN				
712C6	22.0	97.9				
Layer	Depth	Traffic Passes				
	(mm)	0	250	10,000	100,000	121,300
Base-Top	135	3,917	10,377	10,034	9,437	8,649
Base-Bottom	250	3,563	4,230	4,769	7,366	6,901
Subgrade-Top	380	1,623	2,101	2,513	3,169	3,160
Subgrade	535	1,182	1,541	1,838	2,703	2,678
Subgrade	685	1,167	1,402	1,582	2,486	2,383
Subgrade	840	11	9	8	45	86
Subgrade	990	-82	-81	-79	-57	1
Subgrade	1145	-11	-40	-24	-23	-36
Subgrade	1295	214	211	292	305	326
Subgrade	1450	-66	1	-3	32	45

APPENDIX E

STRESS MEASUREMENTS

Test Section 712 AASHTO A-7-5 subgrade soil at 20 percent (optimum) moisture content.

Table E 1. Vertical stress (kPa) in 712C1.

Test Window	kips	kN						
712C1	18.0	80.0						
Depth		Traffic Passes						
Layer	(mm)	0	250	1,000	10,000	100,000	110,000	300,000
Top of subgrade	381	93.9	92.9	99.5	105.1	114.3	107	119

Table E 2. Vertical stress (kPa) in 712C2.

Test Window	kips	kN						
712C2	20	89						
Depth		Traffic Passes						
Layer	(mm)	0	250	1,000	5,000	34,000	65,000	108,000	168,000
Middle of base	191	187.8	187.4	192.2	192.6	210.8	215.9	232.1	257.0
Top of subgrade	381	115.3	118.5	113.3	118.2	131.7	137.8	145.1	145.7
Depth = 0.69 m	686	37.9	39.4	36.8	39.9	42.6	45.5	42.4	49.0

Table E 3. Vertical stress (kPa) in 712C3.

Test Window	kips	kN					
712C3	21.0	93.4					
Depth		Traffic Passes					
Layer	(mm)	0	250	1,000	10,000	25,000	50,000	64,000
Top of subgrade	381	122.8	124	128.8	136.4	140.2	140.4	142.8

Table E 4. Vertical stress (kPa) in 712C4.

Test Window	kips	kN					
712C4	22.0	97.9					
Depth		Traffic Passes					
(mm)	0	250	1,000	47,087	72,500	147,200	180,800
381	152	152.6	154.2	156.1	156.8	157	157.2

Test Section 712 AASHTO A-7-5 subgrade soil at 20 percent (optimum) moisture content.

Table E 5. Vertical stress (kPa) in 712C5.

Test Window	kips	kN						
712C5	9.0	40.0						
Depth		Traffic Passes						
Layer	(mm)	0	250	1,000	25,000	100,000	294,000	463,000
Middle of base	191	77.6	67.7	66.1	54.4	56.9	73.0	64.5
Top of subgrade	381	72.8	65.0	67.6	66.3	73.0	77.4	77.9
Depth = 0.69 m	686	11.7	11.8	10.4	10.9	13.2	12.1	11.8

Table E 6. Vertical stress (kPa) in 712C6.

Test Window	kips	kN			
712C6	22.0	97.9			
Depth		Traffic Passes			
(mm)	0	250	10,000	100,000	121,300
381	174.1	179.2	169.5	193.2	189.0

Test Section 712 AASHTO A-7-5 subgrade soil at 20 percent (optimum) moisture content.

APPENDIX F

## FALLING WEIGHT DEFLECTOMETER MEASUREMENTS

Test Section 712 AASHTO A-7-5 subgrade soil at 20 percent (optimum) moisture content.
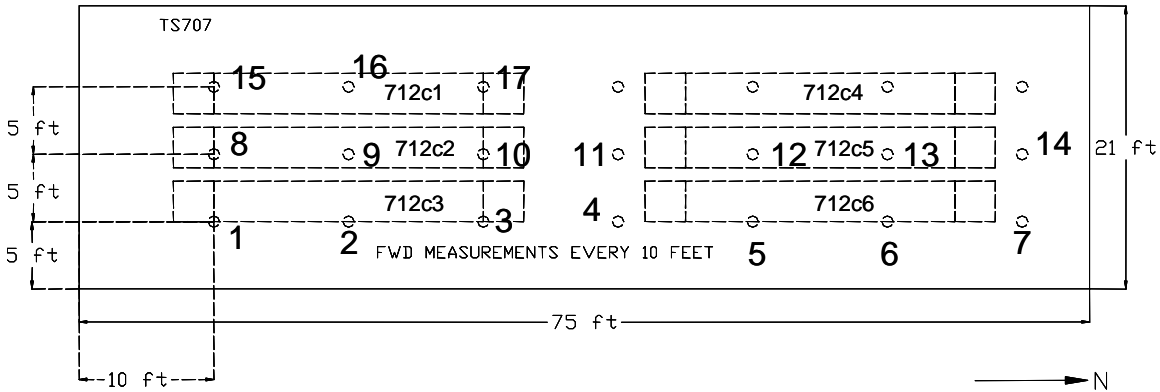
Figure F1. Location of FWD tests in Test Section 712.

Table F 1. FWD tests at 17 locations in Test Section 712.

	Sensor	W1	W2	W3	W4	W5	W6	W7
Radial Distance	(m)	0	0.3	0.61	0.91	1.22	1.52	1.83
	(in.)	0	12	24	36	48	60	72
Station	Load	Deflection (mil)						
1	14481	41.8	21.3	8.8	5.0	3.7	2.9	2.3
2	14448	44.4	21.4	8.1	4.7	3.6	2.8	2.2
3	14503	40.2	23.1	9.0	4.5	3.3	2.7	2.1
4	14512	37.2	20.5	8.3	4.5	3.4	2.7	2.2
5	14412	35.9	19.9	9.0	5.0	3.6	2.9	2.3
6	14391	37.7	21.0	8.9	4.8	3.5	2.8	2.2
7	14386	35.4	20.6	9.8	5.1	3.6	2.8	2.2
8	14229	45.7	23.5	9.2	5.0	3.8	3.1	2.5
9	14322	44.4	23.0	9.3	4.9	3.6	2.9	2.3
10	14331	37.6	21.4	9.1	4.8	3.4	2.8	2.2
11	14257	35.3	18.6	7.7	4.3	3.2	2.6	2.1
12	14205	34.0	19.1	8.6	4.7	3.5	2.8	2.3
13	14226	38.2	20.7	8.8	4.9	3.6	2.8	2.3
14	14245	37.5	21.9	9.6	4.9	3.5	2.8	2.3
15	14193	41.1	21.1	8.6	5.1	3.8	2.9	2.3
16	14186	37.8	20.1	8.7	4.8	3.5	2.6	2.1
17	14209	32.2	18.2	8.2	4.6	3.4	2.6	2.1

Test parameters:
Plate radius……………………………….5.95 in (151 mm)
Air and pavement temperature……………. 68 ºF (20 ºC)